4-27-2017

AKAP7γ Regulation of PKA Substrate Phosphorylation

Marc J. Rigatti
Uconn Health Center, MRigatti@uchc.edu

AKAP7γ Regulation of PKA Substrate Phosphorylation

Marc Joseph Rigatti, MD PhD

University of Connecticut, 2017

In the cell, cAMP-protein kinase A (PKA) signaling is compartmentalized. Two different receptor types, both utilizing cAMP and PKA as second messenger and signal effector, are able to convey separate signals that result in phosphorylation of distinct substrates. Signal compartmentation is possible primarily because of A Kinase Anchoring Proteins (AKAPs) that bind both PKA and a target substrate, effectively co-localizing them. AKAPs are also capable of binding to other necessary signaling components like adenylate cyclase and phosphodiesterase, thus enabling AKAPs to coordinate a signaling microdomain containing many of necessary components. In this thesis I present multiple lines of evidence demonstrating how AKAP7γ is able to regulate PKA phosphorylation. First, I show that AKAP7γ is able to self-associate, forming dimers and possibly higher order oligomers. I predict via computational modeling that this behavior will increase both the speed and magnitude of PKA signaling. Next, I demonstrate that AKAP7γ participates in a highly dynamic phosphorylation-state dependent interaction with phospholamban (PLB), and predict via computational modeling that this allows low concentrations of AKAP7γ to regulate phosphorylation of much higher concentrations of substrate. Finally I demonstrate via computational modeling that contrary to the widely accepted hypothesis of AKAP signaling, the

catalytic subunit of PKA is likely retained within the AKAP-PKA complex during signaling events. I further show that the structure of the complex is an important determinant of substrate phosphorylation. This work offers new insight into the function of AKAPs and offers an update to the AKAP signaling hypothesis.

AKAP7γ Regulation of PKA Substrate Phosphorylation

Marc Joseph Rigatti

B.S./B.S., Eastern Connecticut State University, **2007**

M.S., University of Connecticut, **2010**

A Dissertation

Submitted in Partial Fulfillment of the

Requirements for the Degree of

Doctor of Philosophy

at the

University of Connecticut

2017

APPROVAL PAGE

Doctor of Philosophy Dissertation

AKAP7γ Regulation of PKA Substrate Phosphorylation

Presented by
Marc Rigatti, B.S., M.S.

Major Advisor _____
Kimberly L. Dodge-Kafka

Major Advisor_____
Ion I. Moraru

Associate Advisor _____
Ann Cowan

Associate Advisor _____
John Carson

Associate Advisor _____
Yi Wu

University of Connecticut
2017

Acknowledgements

This work is dedicated to my beautiful wife and daughter. My life has been forever changed for the better because of you.

First, I would like to acknowledge my PI's Kim Dodge-Kafka and Ion Moraru. Kim, thank you for believing in me and for allowing me to pursue work that has been so far outside of your expertise. Your support and encouragement is greatly appreciated. Ion, thank you for the many times you have provided me with ideas or inspiration that have saved my models. You are perhaps the busiest person I have ever met and at times can be near impossible get a hold of, but somehow you manage to come through when I absolutely need your help. As a biochemist with little training in math, I never would have imagined that I would become a computational biologist, but somehow here I am and I thank you both for providing me with the opportunity and support.

I would like to thank my committee, Ann Cowan, John Carson, and Yi Wu. Ann and John, thank you for sticking with me during the entire year I spent pursuing FCS/PCH. Your help allowed me pull off what I thought at time was nearly impossible. To all of you, thank you for being so accommodating of my random unscheduled visits to your office with all of my questions. The accessibility of CAM faculty is something that makes this department a very special place to be and has made me feel like I really had the support to pursue so many things that were outside of my comfort zone.

To the entire Virtual Cell Team: without all of you, my success in computational modeling would not have been possible. Jim, thank you for the many hours you have spent with me, discussing all things engineering, physics, chemistry, programming, biology etc. You have provided me with enough help and guidance through these past few years that you probably should have been my third co-PI. To Ed, thank you for all your help re-writing Paul's software to suit my needs, for assisting me in learning how to program, and for offering so many helpful suggestions that have allowed me to hack my way to functional scripts. To Jeff, thank you for not having a heart attack when I occupy 80% of the cluster space and generate 4TB of data in a single weekend! To Frank, Dan, and Gerard, thank you for all of your help. It's really amazing that I have had such easy access to you all. I can't imagine what it would have been like to deal with the occasional quirks of VCell on my own. Thank you everyone, for being so kind and supportive. I know I am not officially part of the VCell team, but I feel like I am.

To Ji Yu and Dmo, thank you for providing me with the training and equipment necessary to pursue single particle tracking of PKA. The project may not have gone far, but it has provided me with a lot of inspiration for other ideas and enough data to get them started. Dmo, thank you so much for all of the time you

have spent training me on the TIRF scope, for the many hours you have spent analyzing my data, and for all of the thoughtful discussion. Ji, thank you for all the advice, especially on the analysis of my Langevin dynamic simulations.

To all of my former lab mates, John, Andrew and Arpita: thank you for all of your hard work in laying the foundations of my work. Our time together in lab was short, but I'm glad to know you all. Thank you for all of your support and helpful discussion, and for being available to help me finish some of the work that you started.

To my family: thank you for all of your support, encouragement, and unconditional love. Dad, thanks for sharing your love of science, and for never really growing up. I will always remember the many projects we have built together; the rockets, CO_2 powered cannons, and the neighbors destroyed lawn chair. Mom, thanks for always being there for me and for sacrificing so much to allow me to do what I have done. There is no way I would have been able accomplish half of what I have in life without you. Thank you to both of you for supporting me on this extremely long journey.

Last but not least, I'd like to thank my wife. I can't imagine a better person to share this long journey with. There are few people that could possibly understand what this is like, but you do. Thank you for all of the discussions of all things science, for your love and support, and for having such confidence in me.

Table of Contents

Table of Figures

Abbreviations

AMPA – α-amino-3-5-methyl-4-isoxazole propionic acid
AKAP – A Kinase Anchoring Protein
AKAR – A-kinase activity reporter
AC – Adenylate cyclase
C – Catalytic subunit of PKA
cAMP – Cyclic adenine mononucleotide phosphate
Co-IP – Co-immunoprecipitation
CTB – Characteristic time of binding
CTP – Characteristic time of phosphorylation
ENaC – Epithelial Na^+ channel
FRET – Forster resonance energy transfer
GFP – Green fluorescence protein
LD – Langevin Dynamics
LTCC – L-type Ca^{2+} channel
MAP – Mitogen-activated protein
MBP – Maltose binding protein
PCH – Photon counting histogram
PDE – Phosphodiesterase
PKA – cAMP-dependent protein kinase A
PGE_1 – Prostaglandin E1
PLB – Phospholamban
PKI – Protein kinase inhibitor
R – Regulatory subunit of PKA
RyR – Ryanodine receptor
SERCA2a – Sarcoplasmic endoplasmic reticular Ca^{2+} ATPase
SPR – Surface plasmon resonance
TnI – Troponin I
VSNC – Voltage sensitive Na^+ channel

Chapter 1

Introduction

cAMP Signaling

In 1958, Earl Sutherland and Ted Rall reported the isolation of an unusual adenine ribonucleotide formed by liver in the presence of ATP, Mg^{2+}, and epinephrine or glucagon (*1*). This unusual ribonucleotide that stimulated the formation of liver phosphorylase in response to epinephrine or glucagon was called 3,5-AMP, now known as cyclic AMP (cAMP) (*2*). Since their initial discovery, the cAMP signaling pathway has become one of the most well characterized signal transduction systems due to its ubiquitous presence in all cell types. It is now widely appreciated that many hormones and neurotransmitters exert their physiological functions via activation of the cAMP pathway and its downstream effectors. Hormone binding to seven trans-membrane domain G protein-coupled receptors at the cell surface results in the activation and release of the Gαs subunit. Subsequent activation of adenylate cyclase (AC) by Gαs stimulates increased production of cAMP and activation of downstream effectors including cAMP-dependent protein kinase A (PKA), the guanine nucleotide exchange factor Epac, and cyclic nucleotide-gated ion channels. Following activation of these downstream effectors, cAMP levels are returned to baseline via degradation by phosphodiesterases (PDEs).

A decade after the discovery of cAMP, Kuo and Greengard advanced the idea that ubiquitous cAMP dependent protein kinases mediate most, if not all effects of cAMP in eukaryotes (*3*). According to their hypothesis, the ability of a hormone to produce the appropriate response depends upon expression of the

appropriate AC-linked receptor and PKA substrates. Thus, receptor expression determines the sensitivity of a cell type to a particular hormone, and the presence of specific substrates determines the response. According to Rall, this hypothesis presented “the unsatisfying picture of the catalytic subunit of protein kinase swimming about, happily phosphorylating a variety of cellular constituents whether they need it or not” (*4*). At the time, activation of AC by hormone binding at the cell surface was thought to result in uniform increases in cAMP concentration across the cell due to the high diffusion coefficient of cAMP. Such increases in cAMP would lead to cell wide activation of PKA and phosphorylation of all PKA substrates. For cell types that express multiple receptors with separate downstream targets, this hypothesis did not provide a means for preventing cross-talk among multiple signaling pathways. Rall’s criticism regarding the apparent lack of substrate specificity of PKA phosphorylation is even more pertinent in light of recent evidence demonstrating that a single cell type may contain over 100 PKA substrates (*5*).

In the late 1970’s evidence began to accumulate that activation of a single receptor type did not lead to global substrate phosphorylation, rather it caused phosphorylation of a specific subset of PKA substrates. The work of Keely demonstrated that while prostaglandin E1 (PGE_1) and epinephrine both produce increases in cAMP and activation of PKA in the rat heart, only epinephrine caused a significant increase in glycogen phosphorylase activity (*6*). Similar work in adipose tissue by Honeyman and Levy demonstrated that while epinephrine,

isoproterenol, and glucagon produced parallel activation of glycogen phosphorylase and lipolysis, serotonin activated glycogen phosphorylase but failed to induce lipolysis (*7*). Hayes and Brunton demonstrated further, that different receptor types are not only capable of producing separate down stream effects, they also may not share the same pool of cAMP and PKA (*8*). Isoproterenol and PGE_1 were each found to increase both production of cAMP and activation of PKA in the rat heart, yet isoproterenol activated glycogen phosphorylase and induced increased contractility while PGE_1 did not. Importantly, stimulation with both agents had an additive effect on the production of cAMP and activation of PKA, but did not produce an increase in either glycogen phosphorylase activity or contractility compared to isoproterenol alone. These findings formed the basis of the idea of compartmentation, in which it was hypothesized that each hormone activates a discrete pool of PKA. This hypothesis is supported by the findings of Corbin *et al,* who demonstrated that specific isozymes of PKA are distributed within distinct cellular compartments (*9*), thus providing a potential mechanism for compartmentation. By associating with a specific PKA isozyme, a receptor may target only the substrates associated with the compartment of the given isozyme. While Hayes and Brunton were largely correct, the mechanism that enabled anchoring of specific PKA isozymes to distinct compartments remained unknown. This role is fulfilled by A-Kinase anchoring proteins (AKAPs).

A-Kinase Anchoring Proteins

Protein kinase A is a broad specificity serine/threonine kinase consisting of a regulatory subunit (R) dimer and two catalytic subunits (C). The binding of two molecules of cAMP to each regulatory subunit induces a conformational shift that releases the active C subunits (*10*). Although each of the two subunits comprising the PKA heterotetramer has several isoforms, their diversity is limited in comparison to the number of receptors utilizing the cAMP-PKA signaling pathway. There are four isoforms of the regulatory subunit (RIα, RIβ, RIIα and RIIβ) and three isoforms of the catalytic subunit (Cα, Cβ, and Cγ), while the total number of GPCRs in the human genome has recently been estimated at over 800 receptors (*11*). Several years after the compartmentation hypothesis was suggested, a previously unknown protein was identified by Sarkar *et al* as a contaminant that co-purified with RII following cAMP-sepharose affinity chromatography (*12*). This protein, now known as an A-kinase anchoring protein (AKAP), provided the molecular mechanism for cAMP-PKA signal compartmentation (*13*).

AKAPs are a diverse family of proteins that share little sequence homology and are defined only by their ability to bind PKA. The total number of AKAPs is estimated to be >70, resulting from alternative splicing of mRNAs encoded by 43 different genes (*14*). While the majority of AKAPs interact only with RII, a few dual specificity AKAPs have been identified that bind both RI and RII, though the affinity for RI is typically several fold less (*15*, *16*). AKAPs interact

with the N-terminal dimerization/docking domain of the R subunit dimer through a 14-18 amino acid amphipathic helix sequence (*17*). By simultaneously binding to both PKA and a given substrate, AKAPs direct PKA phosphorylation to a specific substrate or set of substrates (Fig 1.1).

The functional significance of AKAPs has been well established by disrupting AKAP-PKA binding (*18*). Disruption of PKA anchoring by AKAP is most commonly achieved using Ht31(493-515) peptide, a fragment of an AKAP cloned from human thyroid. This fragment represents the minimum necessary region for PKA binding to the AKAP and is generally referred to simply as Ht31 (*19*). In hippocampal neurons, Ht31 has been shown to uncouple PKA from a-amino-3-5-methyl-4-isoxazole propionic acid (AMPA)-type glutamate receptors, resulting in attenuated postsynaptic AMPA currents (*20*). Disruption of PKA anchoring in the pancreatic β-cell line RINm5F has been demonstrated to block cAMP responsive insulin secretion and to suppress cAMP mediated intracellular calcium elevation (*21*). Similar disruption of normal function by interfering with PKA anchoring in sperm has been observed as well, with Ht31 inhibiting cAMP dependent motility in a time and concentration dependent manner (*22*). Additionally, it has been demonstrated that disrupting PKA anchoring in rat heart cells redistributes RII, with loss of the typical striated pattern. Importantly, disruption reduces phosphorylation of several key PKA substrates including phospholamban (PLB), Ryanodine receptor (RyR), and Troponin I (TnI) after stimulation with isoproterenol, and also produces changes in cardiac contractile

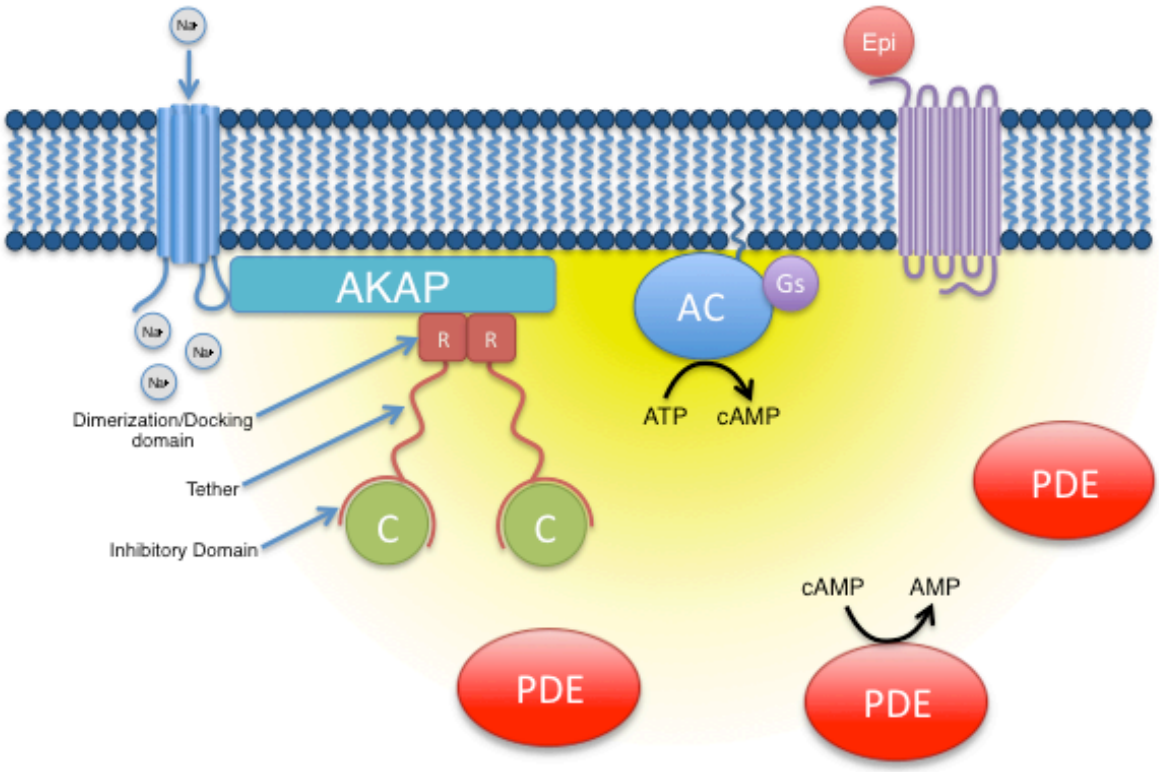

Figure 1.1 AKAP compartmentalizes PKA signaling by anchoring PKA to specific substrates. PKA binds to AKAP through its regulatory subunit dimer (R), which associates with AKAP through the dimerization/docking domain. In the inactive conformation, the catalytic subunit (C) is bound to the complex via the inhibitory domain of the regulatory subunit. Activation of a GPCR leads to cAMP production by AC. The increase in cAMP causes local activation and release of the PKA catalytic subunit resulting in phosphorylation of the AKAP bound substrate, which in this example is a Na^+ channel. The increase in cAMP is confined to the local area and returned to baseline via PDE. The diffusion of cAMP away from AC and its degradation by PDE is represented by the yellow gradient.

parameters (*23*, *24*). Together, these examples clearly show the importance of PKA anchoring for regulation of substrate phosphorylation, leading to changes in cellular physiology.

The ability of AKAPs to focus the catalytic activity of PKA on a particular substrate results from simultaneously associating with both the kinase and substrate. This has been demonstrated using the uni-molecular Förster resonance energy transfer (FRET) sensor of PKA activity, A-kinase activity reporter 2 (AKAR2) (*25*). By modifying AKAR2 to include a C-terminal RII binding site, Dodge-Kafka *et al* were able to show that PKA anchoring to substrate (AKAR2) augmented both the speed and magnitude of the AKAR2 reporter response (*26*). Similar results have been obtained in a more physiologically relevant context by preventing the association of AKAP with a specific PKA substrate in cells. β-adrenergic stimulation of cardiac myocytes leads to phosphorylation of PLB, producing changes in Ca^{2+} handling and contractility. Disruption of the AKAP7δ-PLB interaction in rat heart cells using a competitive peptide inhibitor attenuated isoproterenol induced PLB phosphorylation by up to 50% (*27*).

Although the primary role of AKAPs is most often considered to be compartmentation of cAMP-PKA signaling, AKAPs are able to assemble multimolecular signaling complexes that can include almost any type of regulatory enzyme (*14*). The ability of AKAPs to act as scaffolds for enzymes other than PKA was first discovered in 1995 by Coghlan et al (*28*). This work

demonstrated that AKAP79 interacts with and inhibits the actions of protein phosphatase 2B (PP2B). A ternary complex of PKA, AKAP, and PP2B was isolated from bovine brain, and colocalization of these components was established in cultured hippocampal neurites. This result suggests that AKAPs could coordinate regulation of the phosphorylation state of neuronal substrates. As the diversity of regulatory enzymes found to interact with AKAPs has expanded, the idea of cAMP-PKA signal compartmentation has evolved accordingly. The ability of many AKAPs to form multi-molecular complexes including AC, PDE, PKA, and a specific PKA substrate allows AKAPs to coordinate a cAMP microdomain in which all components necessary for signaling are colocalized (*29*). Although numerous AKAPs are capable of coordinating signaling microdomains, the work presented within is focused upon AKAP7 specifically.

AKAP7 (AKAP18)

In 1997 Gray *et al* reported the discovery of a 15kD protein associated with the L-type Ca^{2+} channel (LTCC) that physically links PKA to the channel, thus facilitating regulation of voltage-dependent potentiation (*30*). Consistent with the current AKAP naming scheme, this protein was called AKAP15. Soon after, an 18kD AKAP was identified that similarly associated with the LTCC (*31*). While it was suggested that AKAP18 was likely a homologue of AKAP15, cloning of AKAP18 related cDNAs revealed that AKAP15 and AKAP18 were, in fact, the

same (*32*). Additional isoforms of AKAP18 that arise from the same gene (AKAP7) but are differentially localized were also discovered. AKAP15/18, now referred to as AKAP18α, is the shortest of the isoforms and is targeted to lateral plasma membrane by a C-terminal (residues 1-16) lipid modification region that is both myristoylated (G1) and palmitoylated (C4, C5) (*31*). AKAP18β, a slightly longer AKAP containing a 23 amino acid insertion between the C-terminal lipid modification region and the RII binding region, localizes to both lateral and apical plasma membrane. AKAP18γ, a larger 37kD isoform lacking the lipid modification sites, localizes both to cytosol and to plasma membrane via direct protein-protein association. AKAP18δ, the largest of the AKAP18 isoforms, is highly similar to AKAP18γ in both structure and localization with an additional 27 amino acid segment at the N-terminus (Fig 1.2) (*33*).

The most well studied isoform of AKAP18 is AKAP18α, which functions primarily to regulate PKA phosphorylation of various ion channels including the LTCC (*30*, *31*, *34*), the K^+ channel complex KvLQT1/Isk (*35*), and voltage-sensitive Na+ channels (VSNC) (*36-38*). Association of AKAP18α with LTCCs and VSNCs requires both lipid modification of the N-terminus and direct binding to the channel through a leucine zipper motif positioned distal to the RII binding site (amino acids 42-49) (*31*, *34*, *38*, *39*). Functionally, AKAP18α has been demonstrated necessary for PKA dependent modulation of current through all of the channels mentioned above. Disruption of AKAP18α membrane targeting has

A

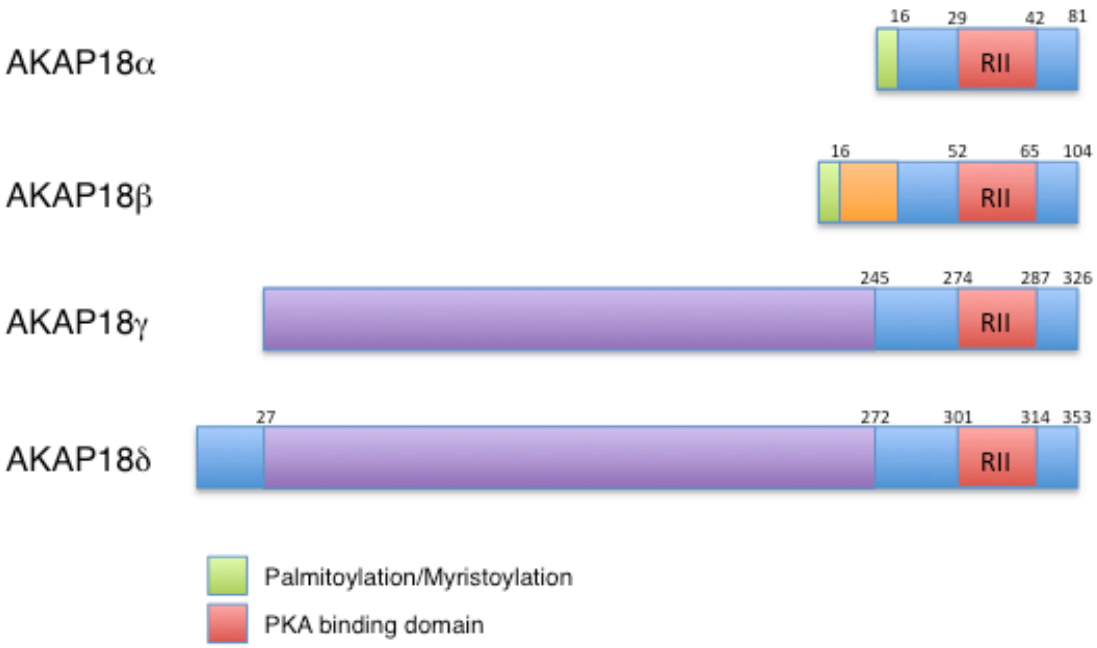

B

Isoform	Cellular Location	Substrates
AKAP18α	PM	LTCC, KvLQT1/Isk, VSNC, ENaC
AKAP18β	Vesicles	unknown
AKAP18γ	PM, Nucleus, Cytosol	PLB, AQP2, I-1, PP1
AKAP18δ	PM, Nucleus, Cytosol, Vesicles	PLB, AQP2

Figure 1.2 AKAP18 isoforms**.** A) Structure of each of the isoforms. AKAP18α and AKAP18β represent the short isoforms, which contain a membrane targeting sequence. The genes for the short isoforms are identical with the exception of an insertion in AKAP18β (orange region). AKAP18γ and AKAP18δ represent the long isoforms of AKAP18 and do not contain a membrane-targeting region although they do both associate with membranes via protein-protein interaction. These isoforms are identical except for the first 27 amino acids of AKAP18δ. B) Cellular location and known substrates of each AKAP18 isoform.

been shown to reduce Ca^{2+} current and to blunt GLP-1 mediated insulin secretion in RINm5F pancreatic β-cells (*31*). In the heart, AKAP18α anchoring of PKA to the $Ca_V1.2$ channel was found necessary for β-adrenergic regulation of cardiac contraction with similar reductions in Ca^{2+} current produced upon disruption of AKAP18α-Cav1.2 binding (*39*). Permanent disruption of this interaction in mice, by knocking out the C-terminal region of the Cav1.2 channel (LTCC), leads to the development of heart failure (*40*). The K_VLQT1/Isk complex, a component of the delayed rectifier K+ current that functions to repolarize cardiac myocytes, is also regulated by AKAP18α. Phosphorylation of KVLQT1 has been shown to increase current amplitude, increase the characteristic deactivation time of the channel, and to negatively shift its activation curve (*35*). In neuronal cells, dopamine stimulated PKA phosphorylation of $Na_V1.2$ channels reduces peak Na+ current by 20-50% (*41*). Disruption of AKAP18a interaction with Nav1.2 channels with a competitive inhibitory peptide resulted in a 20% reduction in dopamine induced peak Na+ currents (*38*).

In comparison to AKAP18α, relatively little is known about the β, δ, and γ isoforms of AKAP18. Since it's discovery in 1999 by Trotter et al, nothing has been published on AKAP18β. The longest isoform of AKAP7, AKAP18δ, was discovered in 2001 by Klussman and Rosenthal (*42*). In the kidney, activation of the vasopressin V2 receptor on the basolateral surface of principal cells in the collecting duct leads to translocation of aquaporin 2 (AQP2) to the apical membrane surface, thus facilitating water reabsorption. Translocation of AQP2

containing vesicles to the apical surface is a PKA dependent process, which AKAP18δ was demonstrated to regulate (*42*). Interestingly, while AKAP18δ has been shown to translocate with AQP2 to the apical surface of principal cells, it appears that RII dissociates following cAMP stimulation and does not translocate with AKAP18δ to the apical surface (*33*). In the mouse heart, AKAP18δ localizes PKA to the phospholamban (PLB)-sarcoplasmic/endoplasmic reticulum Ca^{2+} ATPase (SERCA) complex at the sarcoplasmic reticulum (SR) via direct interaction of AKAP18δ with PLB (*27*). The interaction of PLB with SERCA prevents translocation of Ca^{2+} from the cytosol into the SR (*43*). Phosphorylation of PLB at S16 by PKA dissociates PLB from SERCA, thereby restoring its activity. Disruption of AKAP18δ-PLB binding with Ht31 significantly diminished PLB phosphorylation, demonstrating that AKAP18δ is necessary for PLB phosphorylation (*27*). It is important to note that AKAP18γ replaces AKAP18δ in human myocytes, so one may consider AKAP18γ homologous to AKAP18δ in the regulation of PLB (*44*). Like AKAP18β, AKAP18γ was identified by Trotter *et al* in 1999 as a novel long isoform of AKAP18 (*32*). AKAP18γ was shown to partition equally between cytosolic and particulate fractions and was hypothesized to associate with membranes via direct protein-protein interaction due to the lack of a lipid anchor. While AKAP18γ contains a consensus nuclear localization sequence, the scaffold is not consistently localized to nuclei. The initial description of AKAP18γ localization did not note its presence in nuclei, though it

was later described as localizing RI to the nuclear membrane in mouse oocytes(*45*).

Similar to other AKAPs, AKAP18 is capable of binding enzymes other than PKA, which may serve regulatory functions within the AKAP complex. Co-expression of the epithelial Na^+ channel (ENaC) and AKAP18α has been demonstrated to reduce Na^+ conductance by 80-90%, however the reduction in channel activity was found to be unaffected by either PKA activation or inhibition (*46*). Reduced ENaC activity was instead determined to result from the activity of PKCa, which was shown to interact with AKAP18α. This interaction has been shown not only for AKAP18α, but also for AKAP18γ (*47*). Scaffolding of PKCα by AKAP18 has been demonstrated to increase the activity of PKC, amplifying both the rate and magnitude of phosphorylation while also insulating PKC from the effects of inhibitors (*48*). AKAP18γ has also been shown to interact with protein phosphatase 1 (PP1) as well as its inhibitor I-1 (*49*). Phosphorylation of I-1 by AKAP18γ-linked PKA is known to result in inhibition of PP1 activity and is suggested to act as a feed-forward mechanism that would potentiate phosphorylation of AKAP18γ bound PKA substrates like PLB.

Coordination of PKA phosphorylation by AKAPs

The functional and physiological consequences of PKA scaffolding by AKAPs are well known. This class of proteins not only functions to compartmentalize signaling by directing PKA phosphorylation to a particular

substrate, it also augments PKA kinetics, increasing both the rate and magnitude of phosphorylation (*26*). However, precisely how AKAPs confer specificity to the actions of PKA remains unclear. The established mechanism of PKA activation appears to necessitate the release of the catalytic from its regulatory subunit, effectively negating the tethering actions of AKAP (*10*). The most commonly cited hypothesis is that AKAPs act to increase the local concentration of PKA, thus upon activation a large pool of active PKA is available to phosphorylate substrate. This hypothesis is unsatisfying given that the local concentration of PKA will quickly diminish with the rapid diffusion of PKA away from its point of release.

Much of the accumulated evidence suggesting that the catalytic subunit must be released from its regulatory subunit to phosphorylate substrate comes from *in vitro* experiments. The possibility that PKA is not released *in vivo* remains, and there has been some evidence to suggest that this is the case. In a series of fluorescence anisotropy experiments with PKA containing a fluorescently labeled catalytic subunit, Yang et al demonstrated that fluorescence anisotropy did not increase upon addition of cAMP as was expected, suggesting that the catalytic subunit was not released (*50*). They also showed that the un-dissociated complex retained full catalytic activity. According to Martin *et al*, the release of the catalytic subunit is dependent upon auto-phosphorylation of the regulatory subunit (*51*). Cell expressing PKA with mutant RII subunits that are unable to be autophosphorylated do not release the catalytic subunit in response to cAMP

stimulation. More recently, Smith *et al* were able to demonstrate that the catalytic subunit of PKA is retained within the AKAP complex following stimulation of PKA activity(*52*).

The work presented here focuses upon the regulation of PKA phosphorylation by AKAP18γ. In chapter 2, I present evidence of AKAP7γ dimerization and show via computational modeling how dimerization could potentially increase the magnitude of substrate phosphorylation. In chapter 3, I demonstrate that the interaction of AKAP7γ with PLB is dependent on the phosphorylation state of PLB, and show that this state-dependent interaction may allow small quantities of AKAP18γ to coordinate phosphorylation of large quantities of PLB. Finally, in chapter 4, I demonstrate via Langevin Dynamic simulation of the AKAP-PKA complex that the length and flexibility of the unstructured tether region of the regulatory subunit potentially modulates the catalytic rate of PKA. I further demonstrate by modeling that release of the catalytic subunit from the complex does not result in efficient phosphorylation of AKAP bound substrate, suggesting that the increased local concentration hypothesis for compartmentation by AKAPs is incorrect. Instead, my work suggests that AKAPs work by affecting the efficiency of phosphorylation reactions. In sum, the work presented here changes our model of AKAP signaling, demonstrating a new mechanism of PKA regulation by the AKAP7γ complex.

Chapter 2

AKAP7γ Oligomerization augments PKA signaling

Arpita Singh*, Marc Rigatti*, Andrew V. Le, Cathrine R. Carlson, Ion I. Moraru, Kimberly L. Dodge-Kafka

*These authors contributed equally to this work

This chapter was submitted for publication in *Journal of Signal Transduction* in its present form

Author Contributions

A.S. and M.R. contributed equally to the writing of this manuscript. A.S. performed all of the biochemical work including protein production and purification, immunoprecipitation, and pulldowns. M.R. performed the fluorescence correlation spectroscopy (PCH) and computational modeling. A.V.L. performed the SPR experiments. C.R.C. performed the peptide array study.

Abstract

A-kinase anchoring proteins constitute a family of scaffolding proteins that contribute to spatiotemporal regulation of phosphorylation events mediated by cAMP-dependent protein kinase A (PKA). In particular, AKAP7 is a family of alternatively spliced proteins that participates in cardiac calcium dynamics. Here, we demonstrate via pull-down from transfected HEK-293 cells and by direct protein-protein association that AKAP7γ self-associates. Self-association appears to be an isoform specific phenomenon, as AKAP7α did not associate with itself or with AKAP7γ. Surface plasmon resonance suggests that the AKAP7γ self-association occurs via two high affinity binding sites with K_D values in the low nanomolar range. Mapping of the binding sites by peptide array reveals that AKAP7γ interacts with itself through two regions of the protein. Photon counting histogram analysis (PCH) of AKAP7γ-EGFP expressed in HEK-293 cells confirmed that AKAP7γ-EGFP self-associates in the cell as well. Lastly, computational modeling of PKA dynamics within AKAP7γ complexes suggests that oligomerization may augment phosphorylation of scaffolded PKA substrates. In conclusion, our study reveals AKAP7γ self-associates to form a homo-dimer and possibly higher-order oligomers and that this phenomenon could be an important step in mediating effective substrate phosphorylation in cellular microdomains.

Introduction

Phosphorylation of target proteins is a key mechanism utilized by the cell to induce changes in physiology and function. Numerous kinase-substrate interactions have been defined, yet the mechanism through which specificity of these phosphorylation events is achieved is still unclear. Recent work has suggested that the subcellular localization of signaling enzymes to discrete locations in the cell confers spatiotemporal control over phosphorylation events (*53*). This is facilitated by scaffolding proteins, which tether the kinase to the same signaling complex as its substrates, allowing for increased speed and amplification of phosphorylation events (*54*). While the physiological significance of many kinase-binding scaffolds has been investigated, the influence of the molecular architecture of the complex on cellular processes is presently unclear.

Oligomerization of signaling enzymes is an important mechanism for the transduction of cellular signals (*55*, *56*). Whether forming a hetero or homo oligomer, this process often begins at the level of the receptor as a first step in transducing a signal from outside the cell to the intracellular environment (*57*). Oligomer formation is not limited to upstream signaling events. A few recent studies have demonstrated that scaffolding proteins can oligomerize, influencing their signaling functions. For example, the yeast scaffold Ste5, which initiates the mitogen-activated protein (MAP) kinase cascade in the *Saccharomyces cerevisiae* pheromone response pathway, dimerizes upon pheromone treatment, to enhance MAP kinase signaling in the cell (*58*). Similarly, oligomerization of β-

arrestin1 sequesters the scaffold in the cytoplasm, inhibiting its nuclear actions (*59*). Importantly, these examples demonstrate that oligomerization greatly impacts the function of the scaffold.

For cAMP signaling, A-kinase anchoring proteins (AKAPs) focus the actions of the cAMP-dependent protein kinase (PKA) to specific targets, allowing for microdomains of kinase activity (*54*). It is becoming evident that AKAPs have a more profound effect on the regulation of substrate phosphorylation than simply binding PKA. Many AKAPs have been shown to bind to phosphodiesterases, protein phosphatases, and adenylyl cyclases as well, allowing for localized control of cAMP concentration (*60-62*). Thus, AKAPs are able to coordinate all components necessary for PKA signaling, lending support to the concept of holistic substrate phosphorylation regulation by AKAPs.

Our recent investigations focused on defining AKAP7-orchestrated cAMP microdomains. AKAP7 is a family of alternatively spliced isoforms that are known to play a role in cardiac calcium dynamics (*27*, *63*). Here, we reveal that AKAP7γ oligomerizes, as demonstrated both *in vitro* and in a cellular context, and we predict via computational modeling that this may result in enhancement of PKA substrate phosphorylation. This self-interaction is limited to the large isoforms of AKAP7, correlating with previous findings that AKAP7α and AKAP7γ are differentially targeted in the cell and display unique functions (*32*). Using peptide array to define the sites on AKAP7γ that mediate binding found several domains involved in the oligomerization. In agreement with this finding, surface

plasmon resonance analysis confirms that AKAP7γ interacts with itself via several high-affinity binding sites. Using photon counting histogram (PCH) analysis we are able to detect dimerization of AKAP7γ in live cells. In order to investigate the functional significance of oligomerization on substrate phosphorylation, we developed a mathematical model using the Virtual Cell Software (http://www.vcell.org). Computational analysis suggests that formation of dimeric complexes enhances the magnitude of substrate phosphorylation. Collectively, our work demonstrates that oligomerization of AKAP7γ impacts phosphorylation events orchestrated by the AKAP and suggests that these findings may be applied to other AKAP complexes.

Materials and Methods

Antibodies

For western blot analyses, the following antibodies were used: mouse monoclonal anti-GFP (Santa Cruz, 1:1000), goat polyclonal anti-dsRED (Santa Cruz, 1:1000), rabbit anti-His tag (Millipore, 1:10,000), rabbit anti-mCherry (BioVision, 1:5000) and mouse anti-GST tag (Santa Cruz, 1:10,000). To immunoprecipitate EGFP-tagged proteins, rabbit anti-GFP (Santa Cruz 3 μg) was used.

Construct design

AKAP7γ-pET32a, AKAP7α-EGFP-N1 and AKAP7γ-EGFP-N1 were used as previously described (*31*, *32*, *49*). AKAP7γ 1-150-EGFP and AKAP7γ 150-end-EGFP were constructed by PCR amplification and sub-cloning into the EcoRI-BamHI sites of pEGFP-N1 (Clontech). AKAP7γ-pMAL was constructed by PCR amplification and sub-cloning into the BamHI-EcoRI sites of pMal-c5E (NEB). AKAP7γ-mCherry was constructed by PCR amplification and sub-cloning into the EcoRI-BamHI sites of pmCherry-C1 (Clontech). Monomeric EGFP and tandem EGFP used for PCH analysis were obtained from the lab of Dr. Kathy Herrick-Davis.

Recombinant Protein Purification

For purification of recombinant AKAP7γ-His/S-tag, bacteria were grown to OD_{595} 0.8 then induced with IPTG (1mM final concentration) for 3hrs. After centrifugation, the bacteria were lysed in binding buffer (20mM HEPES (pH 7.4), 0.5M NaCl, 5mM imidazole along with 0.5% triton-X, 0.25mg/ml lysozyme, 1mM DTT, 1mM EDTA, and Protease Inhibitor Cocktail) for 2hrs. Following centrifugation, protein was purified from supernatant by Ni-NTA agarose pulldown overnight (0.5mL of 50% slurry; Ni-NTA solution, Qiagen). Ni-NTA agarose was washed 3x in binding buffer and protein was eluted with binding buffer + 800mM imidizole. Protein was concentrated with Amicon Ultra centrifugal filters (Millipore). Elution buffer was slowly exchanged with PBS while

concentrating the protein in the centrifugal tubes. Protein concentration was determined by comparison to BSA standards via image densitometry of coomassie stained SDS-PAGE gels. Image densitometry was performed with Image J software (NIH).

A similar protocol was followed for AKAP7γ-maltose binding protein (MBP) purification. The MBP tagged protein was lysed in buffer containing protease inhibitor cocktail (20mM Tris-HCl (pH 7.4), 200mM NaCl, 1mM each of EDTA, Na Azide, and DTT). Separated cell lysate was passed through amylose resin packed column, followed by 5 washes with lysis buffer. The protein was eluted with lysis buffer containing 10mM maltose. The protein was concentrated and analyzed as described above.

Cell transfection

For analysis of AKAP7γ binding to itself, HEK-293 cells at 50% confluency were transfected using calcium phosphate precipitation with pEGFP-AKAP7γ and either mCherry-AKAP7γ or mCherry control (10μg) overnight under 5% CO_2 at 37°C. Cells were harvested 18hrs later for cell extract.

For PCH, HEK-293 cells were grown on uncoated glass coverslips to 70% confluency and transfected with 300ng plasmid DNA (EGFP, tandem EGFP or AKAP7γ-EGFP) in Opti-MEM (Invitrogen) serum free medium using 6μl PLUS reagent and 4μl lipofectamine. After 2hrs, transfection media was replaced with

serum supplemented DMEM (10%FBS). Cells were used for photon counting histogram analysis 12-24hrs post-transfection.

Pull-down Assays

In-vitro: Purified His/S tagged AKAP7γ (5μg) was incubated with either AKAP7γ-MBP (5μg) or MBP (5μg), and rocked overnight at 4°C. The next day, the amylose resin was added for 4hrs to isolate the complex. The amylose beads were washed 4x in lysis buffer (as described in maltose tagged protein purification above) for 10-15min while rocking. The components of the complex were then separated via SDS-PAGE and analyzed by western blot.

From cell supernatant: Lysates prepared from AKAP7γ-EGFP transfected HEK-293 cells were incubated with either 5μg purified recombinant AKAP7α-His/S-tag pre-loaded on S-agarose beads (Novagen), or with purified 5μg AKAP7γ-MBP pre-loaded on amylose agarose beads (Novagen). For control groups, either unrelated His/S-tag protein or isolated MBP was used. The pull-downs were rocked overnight at 4°C, followed by 4 washes with their respective buffers for 10-15min while rocking. The isolated complex was then subjected to separation via SDS-PAGE followed by western blot analysis.

SPR Analysis

SPR analysis was performed using the BIAcore T100 platform. Purified recombinant AKAP7γ or AKAP7α were covalently immobilized to the surface of a sensor chip (BIAcore type CM5) using NHS (*N*-hydroxysuccinamide) and EDC [1-ethyl-3-(3-dimethylaminopropyl)-carbodiimide] (Biacore amine coupling kit). The amount of ligand bound was 150RU (resonance units). Protein analytes (AKAP7γ or AKAP7α) were diluted over a range of concentrations (12.5-200nM) in HBS buffer (10mM Hepes (pH 7.4), 150mM NaCl and 0.005% Surfactant P20) and were injected over the sensor surface at a flow rate of 30μl/min for 300s. Post injection phase, dissociation was monitored in HBS buffer for 300s at the same flow rate. The surface was regenerated between injections using 10mM NaCl at a flow rate of 50μl/min for 30s. Sensorgrams were analyzed by BIAcore T100 evaluation software using the appropriate biophysical models.

Peptide array membrane synthesis and S-tagged AKAP7γ overlay

Human AKAP7γ peptides were synthesized as 20-mer peptides with three amino acid offsets on membranes using a Multipep automated peptide synthesizer (INTAVIS Bioanalytical Instruments AG, Koeln, Germany). The peptide array membranes were blocked for 2 hours in 1% casein in TBST (tris-buffered saline with 1% tween) before incubation with 2 μg/ml recombinant human S-tagged AKAP7γ in 1% casein (in TBST) overnight at 4°C. Thereafter the membranes were washed five times in TBST for 5 min before incubation with HRP-conjugated

anti-S tag antibody (Abcam, ab18589, 1:2500) for 1 hour at room temperature. Binding was detected using ECL Prime (RPN 2232, GE HealthCare) and chemiluminescence signals were detected by Las 1000 (Fujifilm, Tokyo, Japan).

Photon Counting Histogram Analysis

Photon counting in live HEK-293 cells was performed with a Zeiss LSM 510 ConFocor3 confocal microscope mounted on an AxioVert 200M. Excitation was achieved at 488nm with a 30mW Argon laser at 50% power with attenuation set to 0.5. Fluorescence emission was collected with a 40X 1.2NA water immersion objective (Zeiss C-Apochromat 1.2W Korr UV-Vis-IR). Detection was performed with an avalanche photodiode (Zeiss). For each cell, five 10s measurements were made from five different locations within a given cell. Photon-counting histograms (PCH) were generated using LSM-FCS software with a bin time of 10μs. Global analysis of measurements with count rates ranging from 20-100 kHz was performed for each construct. Monomeric and dimeric (tandem) EGFP histograms were fit using a single component model, while AKAP7γ-EGFP histograms were fit using a two-component model with the brightness values constrained to those derived from the fit of the monomeric and dimeric EGFP. Measurements exhibiting photo-bleaching or other anomalies producing instability of the fluctuation trace were excluded from analysis. A single-photon three-dimensional Gaussian model was assumed for the excitation volume.

Computational Modeling

A compartmental deterministic model of scaffold oligomerization was implemented using the Virtual Cell modeling software (http://www.vcell.org). The model is composed of 18 species, three compartments (plasma membrane, cytosol, and endoplasmic reticular membrane), and 11 reactions. The reaction network can be considered as being composed of four general modules: 1) production and degradation of cAMP, 2) the dynamic interactions of regulatory subunit, catalytic subunit and cAMP in the cytosol, 3) the dynamics of these same proteins and cAMP scaffolded on the ER membrane by AKAP, and 4) phosphorylation/dephosphorylation of target protein X on the ER membrane. A diagram of the reaction network and table of the kinetic parameters is shown in figure 1. For each oligomeric state of the scaffold represented in the different versions of the model, the concentration of each species is initialized with a value near steady state in unstimulated conditions. Each simulation is allowed to run for 200s allowing each species to reach its equilibrium constant for each oligomer before stimulation. Stimulation of PKA activity is achieved by increasing the amount of AC present on the plasma membrane from $5/\mu m^2$ to $50/\mu m^2$ for a period of 100s, simulating the increase in Gs-associated AC during β-adrenergic stimulation. The resulting increase in cAMP leads to activation of scaffolded PKA and phosphorylation of the target protein X. Active PKA is then inactivated by interacting with PKI. The ability of PKA to self-regulate via autophosphorylation has been shown previously (*51*). We hypothesized that if a single catalytic

subunit were to be activated within an AKAP complex, this may subsequently lead to activation of the remaining population of PKA within the complex. This hypothesis was implemented via the following equation (eq. 1). This equation adjusts for the probability of all catalytic subunits within the oligomeric complex becoming active following activation of a single catalytic subunit in the complex, where n represents the oligomeric state of the scaffold (ex. 1 = monomer, 2 = dimer):

(1) $(Total\ AKAP\ bound\ PKA)\left(1-\left(\frac{Inactive}{Total}\right)^{n}\right)*n$

The result of eq. 1 represents the amount of catalytic subunit available to phosphorylate its target, X, and is substituted for [E] in the Henri-Michaelis Menten irreversible reaction step for phosphorylation of X (eq 2).

(2) $V=\frac{[E]\cdot k_{cat}\cdot[X]}{K_m+[X]}$

Simulations of all oligomeric states have the same amount of active AKAP-scaffolded PKA both at equilibrium and during stimulation. The behavior of the AKAP-scaffolded PKA is altered by eq. 1&2 to reflect the hypothesized behavior in each oligomeric state.

A

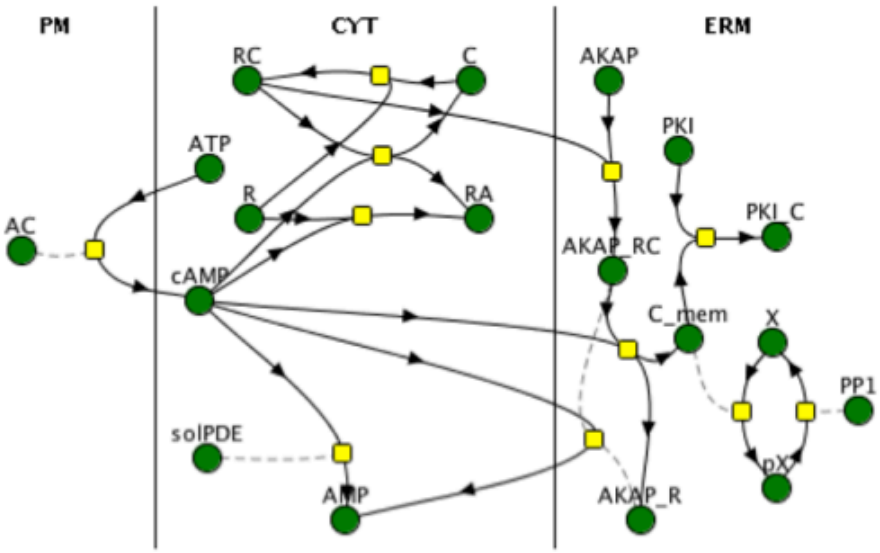

B

Reaction	Kinetics	kcat	Km	Kf	Kr	Reference
ATP --> cAMP	Henri-Michaelis-Menten	12 s^{-1}	11 µm			BRENDA Database
X --> pX	General	22.6 s^{-1}	65.2 molecules/$µm^2$			Masterson et. Al 2011
pX --> X	Henri-Michaelis-Menten	2.4 s^{-1}	65.0 molecules/$µm^2$			BRENDA Database
cAMP --> AMP (cyt)	Henri-Michaelis-Menten	2.0 s^{-1}	5.5 µm			BRENDA Database
cAMP --> AMP (mem)	Henri-Michaelis-Menten	0.098 s^{-1}	5.5 µm			
R + cAMP --> RA	Mass Action			100 $µm^{-1}s^{-1}$	2 s^{-1}	
C + R --> RC	Mass Action			0.31 $µm^{-1}s^{-1}$	0.00023 s^{-1}	Diskar 2010
RC + cAMP --> C + RA	Mass Action			1 $µm^{-1}s^{-1}$	0.177 $µm^{-1}s^{-1}$	Diskar 2010
AKAP_RC + cAMP --> AKAP_R + C_mem	Mass Action			1 $µm^{-1}s^{-1}$	0.177 $µm^{-1}s^{-1}$	Diskar 2010
AKAP + RC --> AKAP_RC	Mass Action			1 $µm^{-1}s^{-1}$	0.005 s^{-1}	Herberg et. al. 2000
PKI + C_mem --> PKI_C	Mass Action			1 $µm^{-1}s^{-1}$	0.01 s^{-1}	

Figure 2.1 Computational Model of AKAP oligomerization **A)** Network diagram **B)** Reaction kinetic parameters

Results

Direct cellular association of AKAP7γ with itself

In order to understand the molecular architecture of the AKAP7γ signaling complex and to determine if the AKAP can be the basis for higher order structures, we first looked to see if purified, recombinant AKAP7γ could pulldown an AKAP7γ complex when transiently expressed in cells. Lysate prepared from HEK-293 cells transfected with AKAP7γ-EGFP was incubated with amylose beads charged with either AKAP7γ-maltose binding protein (MBP) or MBP alone. The protein stain of the nitrocellulose before western blot analysis showing AKAP7γ-MBP (lanes 1 and 2) or MBP alone (lanes 3 and 4) is shown in Figure 2.2A, lower panel. Input lysate (20μl) from cells expressing AKAP7γ-EGFP is shown in lane 5. Importantly, AKAP7γ-MBP was able to pulldown AKAP7γ-EGFP from the transfected cell lysate (Figure 2.2A, upper panel, lanes 1 and 2), suggesting the AKAP7γ signaling complex may contain multiple AKAP7γ molecules. As a control, beads charged with purified MBP alone did not pulldown AKAP7γ-EGFP (Figure 2.2A, upper panel, lanes 3 and 4). To verify the existence of such complexes in cells, we co-expressed AKAP7γ-mCherry with either AKAP7γ-EGFP or EGFP alone in HEK-293 cells. AKAP7γ-mCherry input (20 μL) for each immunoprecipitation is shown in Figure 2.2B, lower panel. Immunoprecipitates from these cells isolated with an anti-GFP antibody demonstrate that AKAP7γ-mCherry and AKAP7γ-EGFP associate in cells (Figure 2.2B, upper panel, lanes 3 and 4), while EGFP control does not co-precipitate

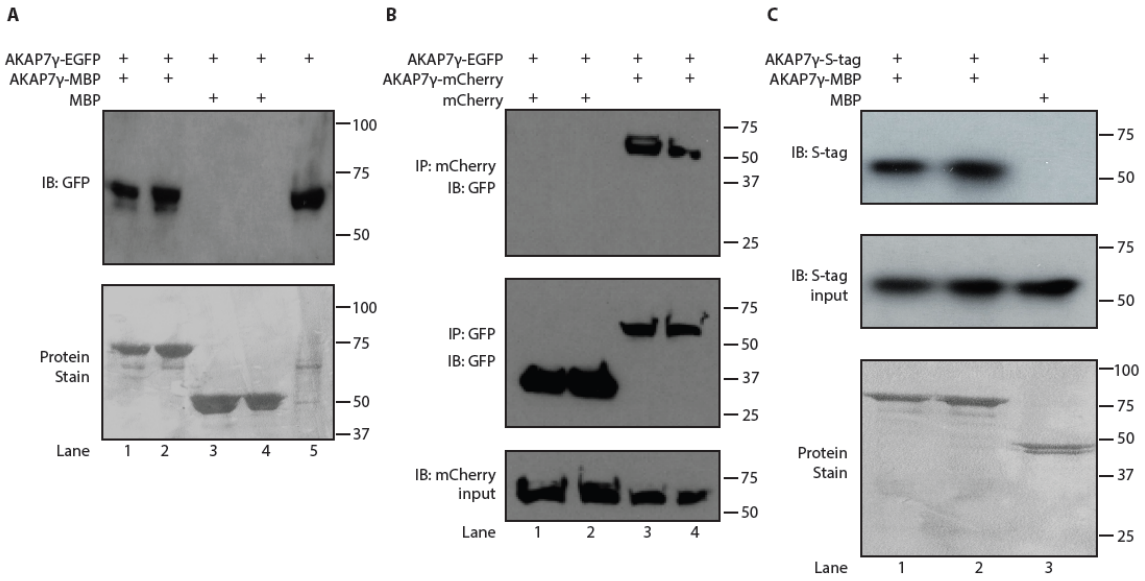

Figure 2.2 Direct cellular association of AKAP7γ with itself.
A) Lysates from AKAP7γ-EGFP transfected HEK-293 cells were subjected to pulldown assays using bacterially purified AKAP7γ-MBP (maltose binding protein) pre-charged on amylose agarose resin (lanes 1 and 2) or Maltose pre-charged on amylose agarose resin (lanes 3 and 4). Input from the transfected cells (20μl) is shown in lane 5. Anti-GFP antibody was used for detecting protein interactions by Western blot analysis (upper panel) while the protein stain of the nitrocellulose before western blot analysis is shown in the lower panel. n=3. B) Western blot analysis of anti-GFP immunoprecipitates isolated from HEK-293 cells co-transfected with AKAP7γ-mCherry and either EGFP alone, or AKAP7γ-EGFP (upper panel). To confirm immunoprecipitation of both EGFP and AKAP7γ-EGFP, the nitrocellulose membranes were stripped and reprobed for GFP using a monoclonal anti-GFP antibody (middle panel). Lower panel depicts mCherry western blot analysis of the input from each condition. n=3. C) *In vitro* pulldown of purified S-tagged AKAP7γ incubated with AKAP7γ-MBP precharged on amylose agarose resin (lanes 1 and 2) or control MBP (lane 3). Anti-His antibody was used to detect the interaction (upper panel). Equal amounts of S-tagged AKAP7γ were used in each condition, as shown by analysis of the input used in each experiment (middle panel). Lower panel shows the protein stain of the nitrocellulose before western blot analysis to demonstrate equal amounts of MBP-tagged proteins. n=3.

AKAP7γ-mCherry (lanes 1 and 2). As a control, both the EGFP (lanes 1 and 2) and AKAP7γ-EGFP (lanes 3 and 4) immunoprecipitates were probed with anti-GFP to demonstrate the immunoprecipitation of both proteins (Figure 2.2B, middle panel). This co-precipitation could be due to multiple binding sites on other common binding partners within the AKAP complex. To determine if AKAP7γ can directly associate with itself, we conducted a pulldown assay using amylose beads charged with either bacterially expressed AKAP7γ-MBP (lanes 1 and 2) or MBP alone (lane 3) incubated with bacterially expressed S-tagged AKAP7γ. The protein stain of the nitrocellulose membrane before western blot analysis displaying the MPB tagged proteins used is shown in Figure 2.2C, lower panel. S-tagged AKAP7γ input for each experiment is shown in the middle panel. Importantly, we detect a direct association between S-tagged AKAP7γ and AKAP7γ-MBP (lanes 1 and 2, upper panel), but not S-tagged AKAP7γ and MBP (lane 3, upper panel). Based on these experiments, we conclude AKAP7γ can stably associate with itself.

Isoform specificity and binding affinity of AKAP7γ oligomers

The *AKAP7* gene encodes at least 4 alternatively spliced isoforms: α, β, γ, and δ (*32*). The smaller isoforms (α & β) are lipid modified in their N-terminal domain, directing their location to the plasma membrane (*31*). However, the larger isoforms (γ & δ) require additional protein-protein interactions for their intracellular targeting (*32*). We investigated whether the shorter isoforms could

also associate with themselves or other isoforms. To address this question, lysate was prepared from HEK-293 cells transfected with AKAP7γ-EGFP and incubated with purified recombinant S-tagged AKAP7α or AKAP7γ bound to S-protein beads. The protein stain of the nitrocellulose before western blot analysis demonstrating the beads are charged with AKAP7α (lanes 2 and 3) or AKAPγ (lanes 4 and 5) is shown in Figure 2.3A, lower panel. Input lysate (20 μl) from cells expressing AKAP7γ-EGFP is shown in lane 1. Importantly, S-tagged AKAP7γ was able to pulldown AKAP7γ-EGFP specifically from the transfected cell lysate (Figure 2.3A, upper panel, lanes 4 and 5). However, we did not detect the presence of AKAP7γ-EGFP with AKAP7α pulldowns (Figure 2.3A, upper panel, lanes 2 and 3), suggesting there is no cross isoform interaction. To further confirm this observation, we conducted the inverse experiment. Lysate collected from HEK-293 cells transfected with AKAP7α-EGFP was incubated with S-beads charged with S-tagged AKAP7α (lanes 2 and 3) or AKAP7γ (lanes 4 and 5). As expected, we did not detect any interaction between the two isoforms (Figure 2.3B, upper panel).

To further increase our understanding of this interaction, the detailed binding kinetics of the AKAP7γ interaction were analyzed by surface plasmon resonance (SPR). AKAP7γ and AKAP7α were chemically conjugated to separate flow chambers of a CM5 sensor chip. A range of concentrations of either AKAP7γ (*black*) or AKAP7α (*red*) (25nM to 200nM) was injected, and the

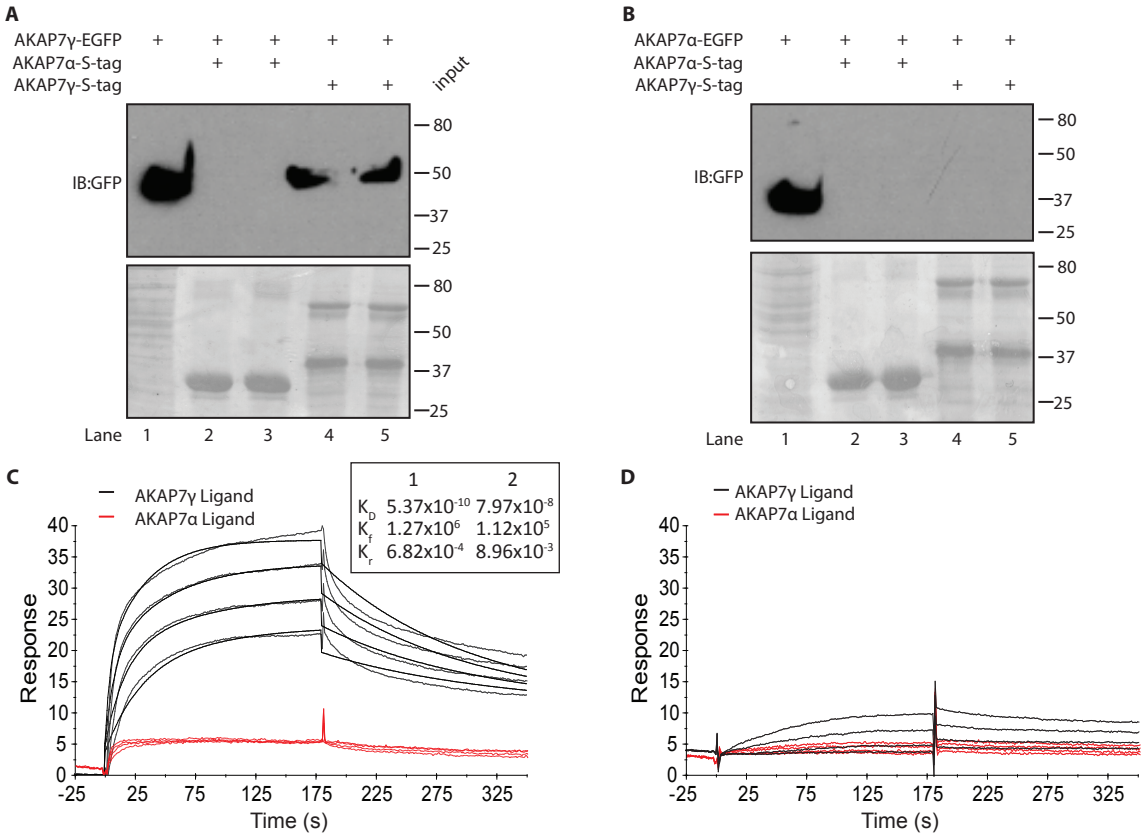

Figure 2.3 AKAP7γ forms homo-oligomers displaying high affinity interactions. **A)** Lysates from AKAP7γ-EGFP transfected HEK-293 cells were subjected to pulldown assays using bacterially purified S-tagged AKAP7α (lanes 2 and 3) or AKAP7γ (lanes 4 and 5) precharged on S-protein resin. Anti-GFP antibody was used for detecting protein interactions by western blot analysis (upper panel). Protein stain of the nitrocellulose membrane before western blot analysis is shown in the lower panel. Input from the transfected cells (20μl) is shown in lane 1. n=3. **B)** Lysates from AKAP7α-EGFP transfected HEK-293 cells were subjected to pulldown assays using bacterially purified S-tagged AKAP7α (lanes 2 and 3) or AKAP7γ (lanes 4 and 5) precharged on S-protein resin. Anti-GFP antibody was used for detecting protein interactions by western blot analysis (upper panel). Protein stain of the nitrocellulose membrane before western blot analysis is shown in the lower panel. Input from the transfected cells (20μl) is shown in lane 1. n=3. **C)** SPR was performed by immobilizing 150RU of AKAP7γ (black) and AKAP7α (red) in separate flow cells on a CM-5 chip and measuring the response when passing over a range of concentrations (25-200nM) of either AKAP7α (D) or AKAP7γ (C). The sensorgram was best fit with a heterogeneous ligand model suggesting the presence of two binding sites on AKAP7γ. The affinities of the two binding sites were 0.537nM and 79.7nM (χ^2 = 1.33), as determined by the BIAcore T100 evaluation software.

binding dissociation constant (K_D) was determined from the fit of the sensorgrams. We detected a high affinity interaction between AKAP7γ and itself that is best fit with a heterogeneous ligand model, suggesting at least two sites of interaction that display binding affinities of 0.537nM and 79.7nM (χ^2 = 1.33) (Fig. 2.3C). However, no significant binding between AKAP7α and AKAP7γ was detected. This was confirmed in reciprocal experiments, where we chemically conjugated AKAP7α to the sensor. No binding between AKAP7α and AKAP7γ or itself was detected (Fig. 2.3D). These results support the hypothesis that AKAP7γ forms only homo-associations.

Mapping the sites in AKAP7γ responsible for homo-association.

The SPR results suggest that multiple sites of interaction may exist between AKAP7γ and itself. To determine the number and location of binding sites, a series of AKAP7γ fragments were created (Figure 2.4A) and incubated with lysate from HEK-293 cells transfected with AKAP7γ-EGFP (Fig 2.4B). The protein stain of S-protein beads charged with the different AKAP7 proteins used in the experiment is shown in Figure 2.4A, lower panel. Input lysate (20μl) from cells expressing AKAP7γ-EGFP is shown in the designated lane. In confirmation of our previous results, recombinant purified full-length AKAP7γ, but not AKAP7α, was able to pulldown AKAP7γ-EGFP from transfected cell lysate (Figure 2.4B, upper panel). Additionally, both halves of AKAP7γ, AKAP7γ(1-150) and AKAP7γ(150-323), were able to pulldown AKAP7γ-EGFP from transfected cell

lysate, revealing that each half of the protein participates in the homo-association of AKAP7γ (Fig 2.4A).

To further refine the location of the binding sites, the human AKAP7γ sequence was synthesized as 20-mer peptides with three amino acid offsets on membranes using a Multipep automated peptide synthesizer, and then subjected to overlay with bacterially purified, full length, S-tagged AKAP7γ (Figure 2.4C, upper panel). Using an HRP-conjugated anti-S tag antibody, binding was observed to two regions; amino acids 43-98 and amino acids 202-296. Importantly, the HRP-conjugated anti-S tag antibody did not detect any spots in the absence of overlay with purified AKAP7γ (Figure 2.4C, lower panel). This data offers further confirmation that there are two regions of interaction between AKAP7γ and itself.

Dimerization of AKAP7γ can be detected in cells

The existence of two sites of interaction of AKAP7γ with itself suggests the potential to form multimeric structures. This possibility was investigated via photon counting histogram (PCH) analysis of AKAP7γ-EGFP expressed in live HEK-293 cells. Photon counting histogram analysis is a method of fluorescence correlation spectroscopy that allows for determination of the size (brightness, ε) and concentration (number, n) of a given oligomer from fluctuations in signal intensity. This technique uses standard confocal optics to create a measurement volume on the order of 0.5fL. As fluorescent particles diffuse through the

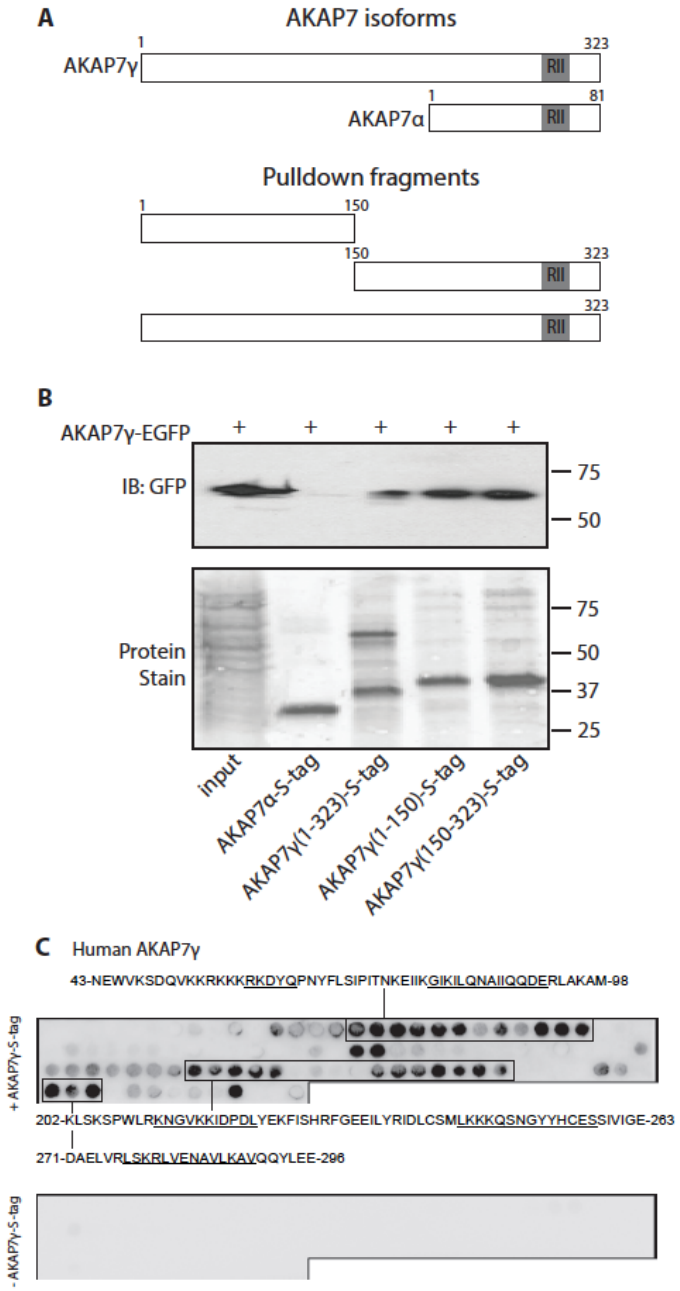

Figure 2.4 Mapping the sites in AKAP7γ responsible for oligomerization. **A)** Schematic depicting AKAP7γ fragments used for pulldown experiments. **B)** Lysates from AKAP7γ-EGFP transfected HEK-293 cells were subjected to pulldown assays using bacterially purified S-tagged AKAP7 deletion fragments precharged on S-protein resin; AKAP7γ-150-323, AKAP7γ-1-150, full-length AKAP7γ or AKAP7α. Anti-GFP antibody was used for detecting protein interactions by western blot analysis (upper panel). Protein stain of the nitrocellulose membrane before western blot analysis is shown in the lower panel. Input from the transfected cells (20μl) is shown in the last lane. n=3. **C)** The full length AKAP7γ sequence was spotted as overlapping 20-mer peptides with 3 amino acid shifts on cellulose membranes and subjected to overlay using S-tagged AKAP7γ. Binding was detected by chemiluminescence using an HRP-conjugated S-protein antibody (upper panel). The antibody did not detect any binding in the absence of S-tagged AKAP7γ overlay (lower panel). n=4.

measurement volume, their signal is detected by a highly sensitive detector such as an avalanche photodiode. The change in signal intensity is dependent upon the average number of particles within the volume (n) and the brightness of a given particle (ε). At low average particle concentrations, the change in fluorescence intensity resulting from a single particle entering or leaving the volume is readily detected, while at high concentrations this change is less detectable. Detection of the change in intensity over time yields a fluctuation trace. The fluctuation trace (Figure 2.5A) is divided into small increments of time (bins) and the signal intensity (counts) is averaged within each increment. The average signal for each bin is then plotted as frequency vs. counts/bin to yield the photon counting histogram (Figure 2.5A), which can be fit to determine the brightness and concentration of the fluorescent particles present. Cells expressing low yet detectable amounts of AKAP7γ-EGFP were selected for analysis due to the dependence of signal variance on the inverse of the number of particles present in the confocal volume. For each cell chosen, five regions were selected from within the cytoplasm for analysis. Each region was measured 5 times for 10s per measurement. The data for each construct was fit globally with either a single component model (EGFP monomer and dimer) or two component model (AKAP7γ-EGFP) yielding a brightness value (ε) and concentration for either one or two species respectively. This type of fitting allows for the derivation of a single brightness value based upon the aggregate data

A

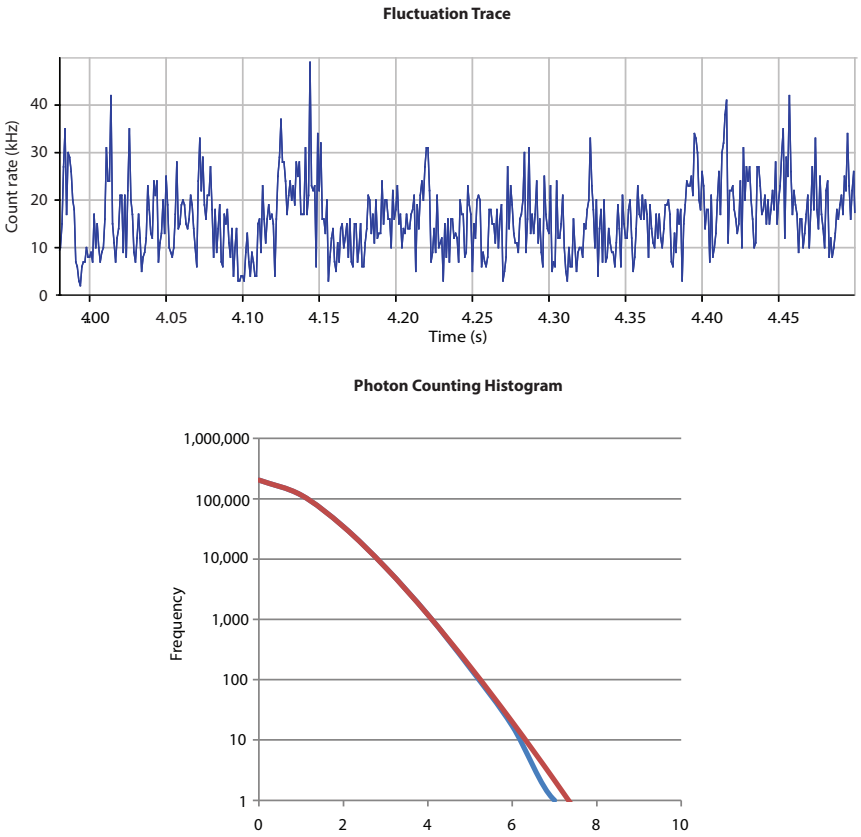

B

	Cells (measurements)	$\varepsilon_{Monomer}$	ε_{Dimer}	χ^2_{global}
Monomer	4(91)	9468 ± 72	-	1.10
Dimer	4(55)	-	16967 ± 100	1.14
AKAP7γ-EGFP	5(75)	9500	17000	1.04

	Total Measurements	Dimer Present	Dimer >10% Total	Avg. [Monomer] (nM)*	Avg. [Dimer] (nM)*	Avg. [Dimer]/[Total]*
AKAP7γ-EGFP	75	52	42	19.81 ± 2.40	3.99 ± 0.06	0.200 ± 0.003

Figure 2.5 Photon counting histogram detects dimerization of AKAP7γ in live cells. **A)** A representative section of the fluctuation trace (above). The fluctuation trace is divided into 10ms bins and plotted as a histogram of frequency vs. counts/bin (below). Fitting of the histogram yields the concentration (number, n) and brightness (e) of the fluorescent particles. **B)** Data summary. HEK-293 cells were transfected with monomeric EGFP, dimeric EGFP, or AKAP7γ-EGFP. Selected cells were measured 5 times at 5 different positions within the cytosol for 10s per measurement. Measurements exhibiting bleaching or other instabilities in fluorescence intensity were excluded from analysis. Global fitting of the data produced near ideal fits (χ^2_{global} of 1.0 is ideal). Monomeric and dimeric EGFP were fit using a single component model, while AKAP7γ was fit using a 2-component model allowing for the detection of both monomeric and dimeric AKAP7γ-EGFP. *Average concentrations and [Dimer]/[Total] were determined from the 52 measurement in which the presence of dimer was detected.

from all measurements of a given fluorescent construct, rather than averaging individual values derived from each individual measurement. Global-fitting of the EGFP monomer and dimer yielded brightness values of 9468 ± 72 ($\chi^2_{reduced}$ = 1.10) and 16967 ± 100 ($\chi^2_{reduced}$ = 1.14) respectively (Figure 2.5B). For AKAP7γ-EGFP 75 total measurements from 5 cells were best fit using a two component model with brightness values constrained to 9500 and 17000 representing monomer and dimer respectively (χ^2 = 1.04). Of 75 total measurements included in the analysis, dimer was detected in 52 measurements and in 42 measurements >10% of the total particles detected represent dimer (Figure 2.4B). Among the 52 measurements that detect dimer, the average concentration of monomer is 19.81±2.40nM and the average concentration of dimer is 3.99±0.06nM. On average, 20±0.3% of the particles detected is dimer, indicating that 28.7% of AKAP7γ-EGFP is in the dimeric form. Based upon the concentrations of monomer and dimer, the apparent Kd of dimerization falls in the range from 78.8-126nM with an average of 98.4nM. This apparent Kd is consistent with the kinetic data from SPR. Attempts to detect higher order oligomeric structures by fitting AKAP7γ-EGFP data with larger brightness values were unsuccessful. However, this does not exclude the possibility that higher order AKAP7γ oligomers exist. The concentrations of higher order oligomers was likely insufficient either for detection, or for discrimination from the population of monomers and dimers. This evidence offers further confirmation that self-association of AKAP7γ occurs in live cells.

Oligomerization of AKAP7γ functions to increase target phosphorylation

Our finding that AKAP7γ is able to form homo-dimers is interesting and leads us to question the functional role of oligomerization. The two large regions of interaction make it exceedingly difficult to disrupt AKAP7γ oligomerization. Thus, we decided to test the possible functional significance of AKAP7γ oligomerization *in silico*. We created a compartmental deterministic model that simulates the dynamics of the PKA regulatory (RIIα) and catalytic subunits (Cα) in response to cAMP, both in the cytosol and on the endoplasmic reticulum (ER) membrane. We chose to model the dynamics of AKAP7γ at the ER due to recent work demonstrating localization of the scaffold at the ER in cardiac myocytes (*27*). Included in the model is autophosphorylation of RIIα, as this is documented as a key component for activation of Cα when complexed with RIIα (*10*, *51*, *64*). In our model, it is assumed that the probability of activation of all Cα subunits within an oligomer increases as the total number of activated Cα subunits increases (Equation 1, methods). Active Cα subunits were modeled to participate in the phosphorylation of a generic target protein X (X → pX) existing on the ER membrane (Equation 2, methods). The time course of formation of pX is shown for separate simulations that compare oligomeric states from monomer to tetramer (Figure 2.6A). Upon stimulation of PKA activity, the amount of pX increases in all cases. When the monomeric state (n=1) is simulated, phosphorylation of our target protein occurs as it would if the feed-forward assumption is not made. Removal of the stimulus leads to

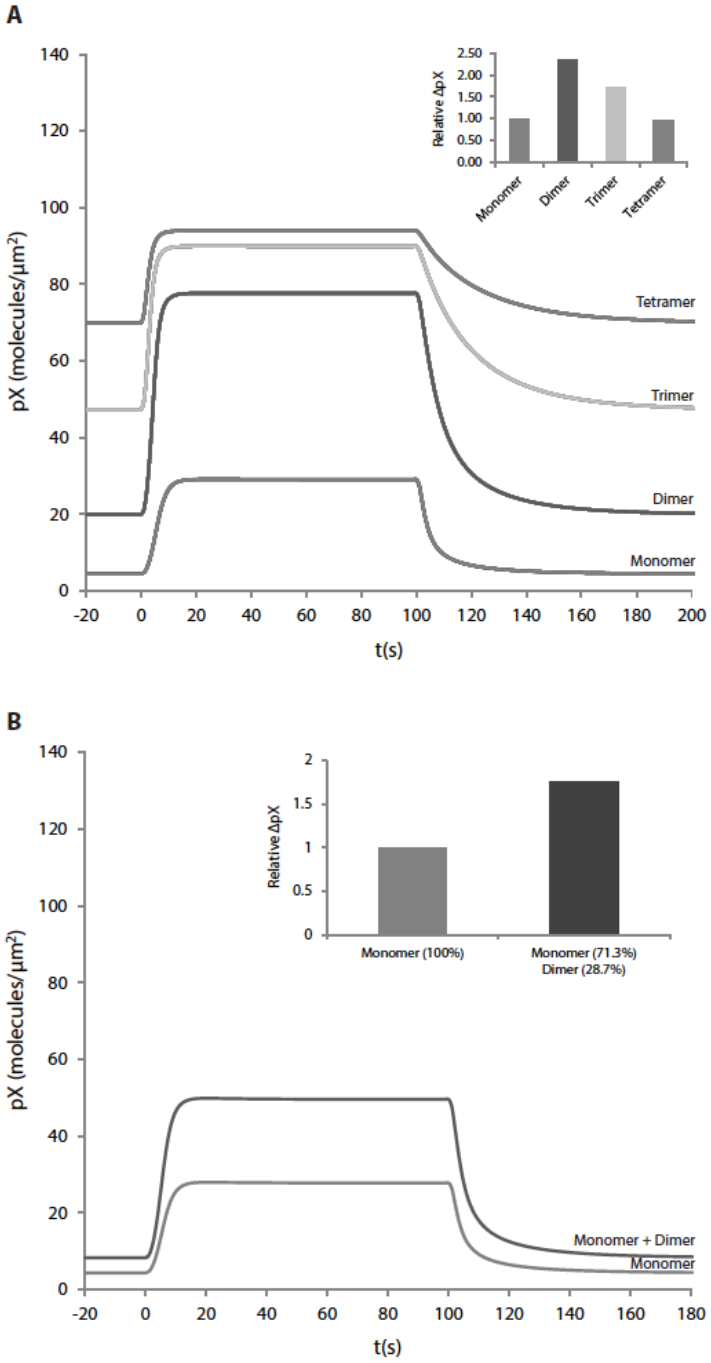

Figure 2.6 Oligomerization of AKAP7γ functions to increase target phosphorylation. **A)** Time course of target protein X phosphorylation for each oligomeric state. An increase in cAMP production is simulated from 0-100s resulting in activation of AKAP bound PKA and phosphorylation of target protein X. The inset shows the change in [pX] from baseline to maximal phosphorylation relative to the change in phosphorylation produced by the monomeric state. **B)** Time course of target X phosphorylation for a mixture of monomer and dimer as measured via PCH. The concentration of monomeric and dimeric AKAP complexes were adjusted so that 71.3% of the total AKAP exists as monomer and 28.7% exists as dimer. An increase in cAMP production was simulated as above. The inset shows the change in [pX] from baseline to maximal phosphorylation relative to 100% monomer.

dephosphorylation of pX and return to baseline. Oligomerization of AKAP7γ affects the baseline, magnitude, and speed of phosphorylation of protein X (Fig. 2.6A & 2.6B). The largest magnitude change of pX occurred in the dimeric state, with larger order AKAP7γ oligomers exhibiting decreased magnitude change in pX (Figure 2.6B). When the active scaffolded PKA population was adjusted to reflect a mixture of monomeric and dimeric states according to our PCH data, the baseline phosphorylation level remains low (8.26 molecules/μm^2) while the magnitude change in pX increases by 76% in comparison to monomer only (Figure 2.6A & 2.6B). This analysis demonstrates the possible impact of AKAP7γ oligomerization on the rate of PKA substrate phosphorylation.

Discussion

Significant work has demonstrated the impact of scaffolding on the organization of signaling proteins into discrete focal points of subcellular enzyme activity (*65*). However, information regarding the molecular architecture of scaffolds and their influence on phosphorylation events is currently lacking. Here, through the use of a combination of protein biochemistry, fluorescence correlation spectroscopy and computational modeling, we deciphered that the scaffolding protein AKAP7γ dimerizes *in vitro* and in cells. Our ability to detect dimerization via PCH indicates that dimerization is occurring in live cells. Importantly, computational modeling suggests that dimerization may act to increase target phosphorylation. These findings represent a previously

unappreciated mechanism involved in the configuration of AKAP complexes and the regulation of protein phosphorylation.

Oligomeric proteins, composed of two or more polypeptide chains, represent a major fraction of total cellular proteins (*55*). Interestingly, a search of the BRENDA enzyme database (http://www.brenda.uni-koeln.de/) reveals that of the total 452 human enzymes with known subunit composition, over 300 exist in multimeric states. Oligomerization of signaling proteins is a common phenomenon that occurs in many signal transduction networks. This is especially true at the level of the receptor, in which numerous examples of oligomerization exist (*57*, *66*). Recent evidence suggests intracellular scaffolding proteins also oligomerize (*67*, *68*). Several recent reports have demonstrated homo-oligomerization of AKAP5, AKAP12 and AKAP-Lbc (*69-71*). Dimer formation of these AKAPs is mediated by direct protein-protein interactions. A leucine zipper motif in the N-terminus of AKAP-Lbc dictates the interaction while multiple domains of AKAP5 are required for dimerization (*69*, *71*). As we have shown, AKAP7γ dimerization also occurs via direct interaction. Determination of the binding kinetics via SPR reveals that AKAP7γ forms a dimer via high-affinity interaction that occurs at two sites. We were able to detect dimerization of AKAP7γ in cells via PCH and estimate the affinity of interaction from the concentrations of monomer and dimer. The estimated Kd based on our PCH result is approximately 98nM, which is remarkably similar to the Kd of site-two (79.7nM) from the fit of our SPR data. Although the affinity of site-one from the

SPR analysis is much higher, it is possible that interaction of AKAP7γ with endogenous binding partners in the cell alters the affinity of this site, or that binding simply cannot occur due to steric hindrance. Our efforts to map the sites of binding confirm that two major regions of interaction exist. Interestingly, the crystal structure of the common central domain contained in the long AKAP7 isoforms (amino acids 76-292 of AKAP7δ) does not indicate oligomerization of the AKAP (*72*). This structure lacks the N-terminus of AKAP7γ, which is predicted to exist in an unordered arrangement, according to FOLDindex©. Several AKAPs have a natively disorganized, unfolded configuration that is hypothesized to aid in the docking of a multitude of binding partners (*69*, *70*, *72*). However, this unstructured flexibility also significantly hinders conventional structural analysis. Hence, this N-terminal domain of AKAP7γ may contribute significantly to its oligomerization. In fact, our peptide array analysis demonstrates that the majority of the interacting sequence from 43-98 is not contained in the original crystal structure. Other possible mechanisms include post-translational modification driven interactions, and coiled-coil interactions (*73-75*). Analysis of the AKAP7γ sequence using the PredictProtein web site as well as both MARCOIL and LOGICOIL web resources support these possibilities for AKAP7γ. Testing these potential mechanisms for oligomerization will help in delineating the means of AKAP7γ complex formation.

Signaling proteins utilize oligomerization to enhance their known cellular functions. One of the better-studied examples is the receptor tyrosine kinase

(RTK). Dimerization of RTKs results in activation and autophosphorylation of tyrosine residues on the intracellular domain of the receptor (*76*, *77*). This step initiates the recruitment of other signaling proteins and propagation of signals from the receptor to intracellular targets. Though often thought to function in a monomeric state, a number of G-protein coupled receptors (GPCRs) have been shown to form both homo- and hetero-dimers, often resulting in enhanced activity (*57*).

The consequences of AKAP oligomerization are still unclear, but may affect multiple processes. Mass spectrometry analysis of the AKAP5 complex suggests that upon dimerization, AKAP5 associates with four calcineurin phosphatase heterodimers, and two calmodulin molecules (*69*). By increasing the concentration of the phosphatase in a localized area, it is suggested that AKAP5 can generate specific pools of second messenger-mediated events at the plasma membrane. How this change in stoichiometry affects substrate dephosphorylation or kinetics of enzyme activation has not been investigated. However, other studies of the native AKAP5 complex in hippocampal neurons suggest this increase in stoichiometry is an *in vitro* artifact, as no increase in stoichiometry was detected *in vivo* (*78*). Oligomerization may also affect regulation of intrinsic enzymatic activity of an AKAP. AKAP-Lbc is a guanine nucleotide exchange factor (GEF) for RhoA (*79*). Disruption of AKAP-Lbc dimerization dramatically increased its GEF activity, suggesting that oligomer formation acts to limit the basal activity of the AKAP (*71*). However, AKAP7γ

does not display any known intrinsic enzymatic activity, suggesting this mechanism is not applicable.

To explore the possible functional significance of AKAP7γ oligomerization, we created a computational model of PKA scaffolding. Significant work has demonstrated that release of active Ca subunit from the PKA holoenzyme requires not only cAMP binding to the RIIα subunit, but also autophosphorylation of RIIα *(16-18)*. This leads us to hypothesize that in the context of an AKAP7γ oligomer, release of a single Cα subunit can potentiate the release of additional Cα via phosphorylation of RIIα present in the oligomer. In the monomeric state, a single Cα can stimulate release of only one extra Cα subunit, but, in a dimeric or oligomeric state, release of additional Cα subunits is possible. This double negative feedback loop ultimately increases substrate phosphorylation due to the increased probability of phosphorylation resulting from increased Cα release (Figure 2.7). This is simulated by defining activation of PKA in the AKAP7γ complex as a probability function in which the chance of activating all Cα subunits increases as the number of active Cα subunits within the complex increases (Eq. 1). The model suggests that the physiologic consequence of AKAP7γ oligomerization could be increased baseline phosphorylation, increased magnitude of phosphorylation in comparison to the monomeric state, and increased speed of phosphorylation. For the distribution of monomeric and dimeric AKAP7γ derived from our PCH experiment, the model predicts a 1.91 fold increase in baseline phosphorylation and a 1.77 fold increase in magnitude of

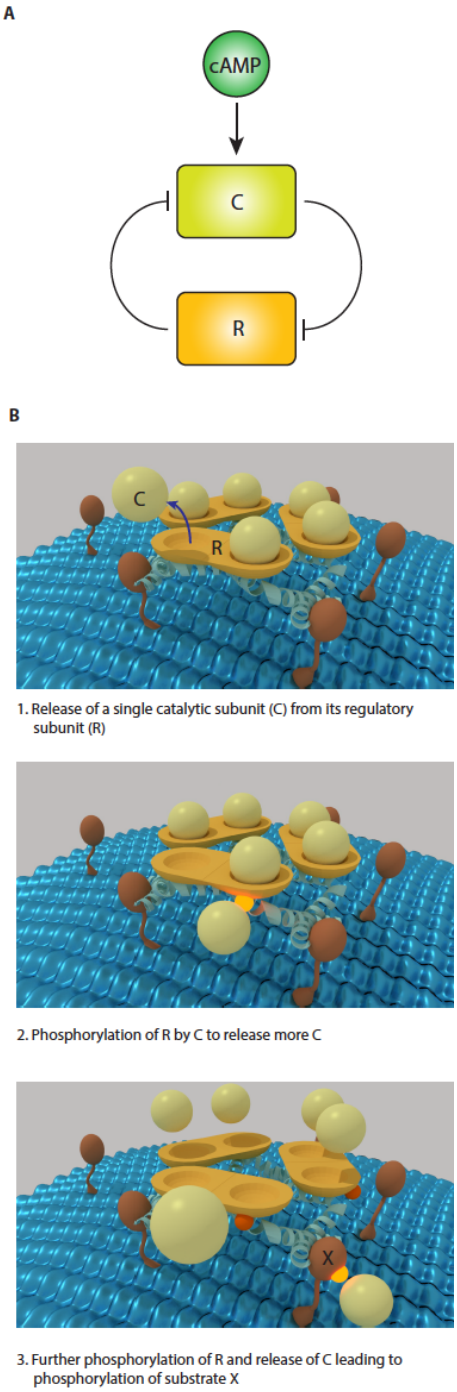

Figure 2.7 Double negative feedback model of PKA activation **A)** Double negative feedback loop. In the resting state, Cα is inhibited by RIIα. However, once Cα is activated by cAMP it is able to phosphorylate RIIα at Ser-99, which prevents RIIα from inhibiting Cα. **B)** Illustration of the double negative feedback mechanism occurring within a hypothetical trimeric AKAP complex. AKAP (light blue helix) recruits PKA (R homodimer, orange; C, light yellow) to a membrane (blue) associated target X (red). In the context of this AKAP oligomer, activation of a single Cα is likely to phosphorylate RIIα within the complex leading the release of further Cα. This process feeds forward, increasing the probability that all Cα within the complex will become active as each additional Cα is activated. The increased amount of active Cα also increases the probability of target phosphorylation.

phosphorylation in comparison to monomer only. It is important to note that our finding does not result from an increase in AKAP7γ or PKA concentrations at the ER membrane, it reflects the consequence of oligomerization on PKA activity. In all simulations the total amount of PKA scaffolded to the membrane by AKAP7γ remains the same. The double negative feedback behavior of Cα activation has the potential for interesting consequence when considered in a spatial context. The free diffusion of active Cα may permit its interaction with AKAP7γ complexes that exist beyond the location of its complex of origin. This could enable the spatial spread of PKA activation and target phosphorylation similar to that of a calcium spark. Spatial spread of the PKA signal in this manner would depend upon many factors including: the diffusion coefficient of Cα, the density of AKAP complexes, the ability of Cα to re-associate with RIIα, and the spatiotemporal fluctuation in cAMP concentration.

We have discovered an additional component of the AKAP7γ signaling complex and demonstrated that dimerization of AKAP may impact phosphorylation of PKA substrates. As several PKA targets of AKAP7γ have been identified, including PDE4D, the PP1 inhibitor I-1 and the cardiac calcium regulatory protein phospholamban, AKAP7γ oligomerization has the possibility of effecting phosphorylation of these endogenous substrates.

Chapter 3

Phosphorylation-state dependent interaction between AKAP7δ/γ and phospholamban increases phospholamban phosphorylation

Marc Rigatti, Andrew V. Le, Claire Gerber, Ion I. Moraru and

Kimberly L. Dodge-Kafka

This chapter has been accepted for publication in its present form in *Cellular Signaling*

Author Contributions

M.R. designed and analyzed the computational model and wrote the manuscript. A.V.L. performed the Biacore experiments and analyzed data. C.G. performed the in vitro kinase assays. K.L.D. performed the IP.

Abstract

Changes in heart rate and contractility in response to sympathetic stimulation occur via activation of cAMP dependent protein kinase A (PKA), leading to phosphorylation of numerous substrates that alter Ca^{2+} cycling. Phosphorylation of these substrates is coordinated by A-kinase anchoring proteins (AKAPs), which recruit PKA to specific substrates (*29*). Phosphorylation of the PKA substrate phospholamban (PLB) is a critical determinant of Ca^{2+} re-entry into the sarcoplasmic reticulum and is coordinated by AKAP7δ/γ (*27*, *43*). Here, we further these findings by showing that phosphorylation of PLB requires interaction with AKAP7δ/γ and that this interaction occurs only when PLB is unphosphorylated. Additionally, we find that two mutants of PLB (R9C and Δ14), which are associated with dilated cardiomyopathy in humans, prevent association with AKAP7δ/γ and display reduced phosphorylation *in vitro*. This finding implicates the AKAP7δ/γ-PLB interaction in the pathology of the disease phenotype. Further exploration of the AKAP7δ/γ-PLB association demonstrated a phosphorylation state-dependence of the interaction. Computational modeling revealed that this mode of interaction allows for low concentrations of AKAP and PKA (100-200nM) to regulate the phosphorylation of high concentratins of PLB (50μM). Our results confirm that AKAP7δ/γ binding to PLB is important for phosphorylation of PLB, and describe a novel phosphorylation state-dependent binding mechanism that explains how phosphorylation of highly abundant PKA

substrates can be regulated by AKAPs present at ~100-200 fold lower concentrations.

Introduction

The heart responds to an increase in sympathetic stimulation via activation of the cAMP-dependent protein kinase PKA, leading to phosphorylation of several key substrates. These substrates mediate Ca^{2+} entry, release, and uptake into intracellular stores. Phosphorylation therefore allows the heart to increase the force contraction and the rate of relaxation by changing the kinetics of the Ca^{2+} transients that underlie these physiological events. Importantly, several key studies have demonstrated that PKA must be compartmentalized with its substrate in the heart in order for phosphorylation to occur (*80*). This is accomplished via A-kinase anchoring proteins (AKAPs), a class of scaffolding proteins that compartmentalize PKA with its substrates, thereby forming a microdomain of PKA activity. Importantly, disruption of PKA anchoring using global AKAP/PKA disrupting peptides greatly impacts the contractile response of the myocyte to sympathetic stimulation, demonstrating the importance of AKAPs for regulation of cardiac Ca^{2+} dynamics (*23*, *81*).

A key AKAP that plays a role in the regulation of cardiac Ca^{2+} dynamics is AKAP7 (*82*). This AKAP has four splice variants (α, β, γ and δ), with a range of molecular weights from 18 to 50 kDa (*32*). AKAP7δ/γ plays an important role in the rate of relaxation of the heart via mediating the phosphorylation of the cardiac protein phospholamban (PLB) (*27*). In its unphosphorylated state, PLB binds to the Sarcoplasmic Reticulum Ca^{2+}-ATPase (SERCA2) pump and decreases pump action, thus providing a rate-limiting step in the cardiac contraction/relaxation

cycle. Phosphorylation of PLB disrupts the PLB/SERCA2 interaction, thereby accelerating Ca^{2+} re-uptake into cardiac stores and allowing for an increase in the rate of relaxation. Importantly, peptide-based disruption of the AKAP7δ-PLB interaction in the rat myocyte significantly attenuates the sympathetic-promoted phosphorylation of the protein and the increase in Ca^{2+} re-uptake associated with stimulation (*27*). It is important to note that AKAP7δ is replaced by AKAP7γ in the human and mouse myocyte (*44*). Hence, it has been suggested that this interaction could be used as a potential drug target in heart failure patients (*83*).

A number of AKAP7δ/γ binding partners with the capacity to influence PLB phosphorylation have been identified including protein kinase C (PKC), protein phosphatase-1, inhibitor-1 (I-1), and phosphodiesterase 3A (PDE3A) (*49*, *84*, *85*). This evidence provides us with the key elements of the AKAP7δ/γ signaling microdomain, which may control PLB phosphorylation. However, one particularly critical question exists: how does a low abundance protein like AKAP7δ/γ regulate phosphorylation of a very high abundance protein like PLB? This question was eloquently posed by Don Bers in his 2002 review of cardiac-excitation contraction coupling, commenting *"…it is less clear how targeting would practically work for phospholamban and troponin I phosphorylation (as compared with I_{Ca} or RyR). This would require very high amounts of the various anchoring and signaling proteins because troponin I and phospholamban are present at 50μM or higher concentrations and are dispersed widely in the cell* (*86*)*."*

The implied assumption of AKAP microdomain signaling is that AKAPs remain bound to their respective PKA substrates regardless of the state of the complex. If true, such a mechanism would require high concentrations of both AKAP and its binding partners that is similar to that of the PKA substrates – but the cellular concentration of PKA is not nearly as high as PLB, nor are the concentrations of AKAP7δ/γ or its other binding partners (Protein phosphatase 1, Inhibitor-1 and Phosphodiesterase4D3) (*47*, *49*, *87-89*). However, it is clear that the AKAP plays an important role in the phosphorylation of PLB (*90*). Here, we confirm that binding of PKA to AKAP7δ/γ is required for PLB phosphorylation and that deletion of the PKA binding domain on the AKAP7 results in a significant reduction in PLB phosphorylation. Importantly, several human mutants of PLB, which are known to exhibit decreased phosphorylation and are associated with dilated cardiomyopathy, do not interact with AKAP7δ/γ, suggesting that the PLB-AKAP7δ/γ interaction is necessary for phosphorylation. Therefore, the question remains: how are these AKAP-binding requirements compatible with the efficient phosphorylation of large amounts of PLB? We hypothesized that this could be explained by our newly observed phosphorylation state-dependent binding of AKAP7δ/γ to PLB. Here, we show that the high affinity association between AKAP7δ/γ and PLB is lost upon phosphorylation of PLB. A computation model of the detailed biochemical kinetics of the pathway showed that if state-dependent binding is included in the reaction network, phosphorylation of high concentrations of PLB is possible at low concentrations of both AKAP7δ/γ and

PKA, consistent with the observed results (*90*). Importantly, our experimental findings and kinetic analysis provide a mechanistic hypothesis of AKAP7δ/γ complex signaling in cardiac myocytes that reconciles the problem with disparity of complex component concentrations.

Experimental Methods

Antibodies

The following primary antibodies were used for immunoblotting: mouse monoclonal Phospholamban (Millipore; 1:1000 dilution), polyclonal phosphor-phospholaman serine 16 (Millipore; 1:500), mouse monoclonal GFP (Santa Cruz Biotechnology; 1:500 dilution), polyclonal mCherry (Thermo Scientific Pierce; 1:3000 dilution), monoclonal PKA RIIα subunit (Santa Cruz Biotechnology; 1:500). Immunoprecipitations were carried out using the following antibodies: polyclonal AKAP7 (Sigma; 5μg), mouse monoclonal GFP (Santa Cruz Biotechnology; 5μg), mouse monoclonal Phospholamban (Millipore; 3μg)

Expression constructs

The human phospholamban construct was obtained from Origene and amended with EcoRI/BamHI restriction sites using PCR, and subcloned into the peGFP-N1 vector. Mutant phospholamban constructions were made by site directed mutagenesis.

Cell Transfection and Immunoprecipitation

HEK293 cells were transfected at 50-70% confluency in 60mm plates using the calcium phosphate method with 6 μg of each plasmid DNA. Cells were treated with various drugs for the time specified, and cell lysate was collected in 0.5ml HSE buffer (HEPES, pH 7.4, 150mM NaCl, 5mM EDTA, 1% Triton X-100 and protease inhibitors). Supernatants were incubated overnight at 4°C with the indicated antibody and 15ml of prewashed protein A-or G-agarose. Following extensive washing, captured proteins were solubilized in 2X sample buffer and analyzed by immunoblot.

Rat heart extract was prepared as previously described (*26*, *91*). Immunoprecipitating antibodies were added to 500μl of extract along with 13μl protein agarose. After an overnight incubation followed by extensive washing, captured proteins were analyzed by immunoblot.

In vitro Phospholamban phosphorylation assays

Various PLB peptides (1μg) were incubated in kinase buffer (50mM Tris-HCL pH 7.5, 5mM $MgCl_2$) containing 100mM ATP, 5mM [γ^{-32}]ATP and 800 units of purified PKA catalytic subunit (NEB). After a 15 minute incubation at 30°C, the reaction mixture was spotted onto phosphocellulose strips and washed five times in 75mM phosphoric acid. Filters were air dried and counted.

Rat neonatal myocyte culture

Myocytes were prepared from 2 day old Sprague-Dawley rats, as previously described. Cell were plated in Dulbecco's Modified Eagle medium (DMEM)with 17% Media 199, 1% penicillin/streptomycin solution, 10% horse serum and 5% fetal bovine serum (FBS) at 125,000 per cm^2. After an overnight incubation in plating medium, the myocytes were maintained in culture for up to one week in maintenance medium (79% DMEM, 20% Media 199, and antibiotic). Cells were stimulated with the various drugs as described.

Surface Plasmon Resonance

SPR analysis was performed using a BIAcore T100. Biotinylated-Phospholamban peptide (Chi Scientific) was covalently immobilized using NHS (N-hydroxysuccinamide) and EDC [1-ethyl-3-(3-(dimethylamino)propyl)carbodiimide] (Biacore amine coupling kit) to the surface of a sensor chip (BIAcore type CM5). The amount of ligand bound (in resonance units, RUs) was 300 RU. AKAP7γ protein analyte was diluted at increasing concentrations (25–100 nM) in HBS buffer (10 mM HEPES (pH 7.4), 150 mM NaCl, and 0.005% Surfactant P20) and injected over the sensor surface at a flow rate of 30 µL/min for 300 seconds. Post injection phase, dissociation was monitored in HBS buffer for 300 seconds at the same flow rate. The surface was regenerated between injections using 10 mM NaCl at a flow rate of 50 µL/min for 30 seconds. Sensorgrams were all processed by BIAcore T100 evaluation software.

GST-RII pulldown assay

Beads charged with RIIα-GST fusion protein were incubated with isolated cell lysate transfected as described above. After an overnight incubation at 4C with shaking, beads were washed extensively and captured proteins were solubilized in 2X sample buffer and analyzed by immunoblot.

Computational Modeling of the AKAP7-Phospholamban complex.

An ordinary differential equation (ODE) model of PLB phosphorylation by AKAP7δ/γ bound PKA was implemented using the Virtual Cell modeling software. The reaction network is composed two basic modules; 1) cAMP production and PKA activation and 2) AKAP7δ/γ binding and phosphorylation of PLB with a total of 18 species and 14 reactions (Table 1, Fig S1). Activation of AC via association with Gs in module 1 results in the production of cAMP that binds PKA (R2C2) resulting in sequential dissociation of each of two catalytic subunits (C). Free C is able to phosphorylate Gs within the GsAc complex resulting in the inhibition of cAMP production and, in conjunction with the activity of PDE, the return of cAMP levels to baseline. Due to the high affinity interaction of cAMP with the PKA regulatory subunit (R), C does not reassociate with R to form PKA (R2C2) following cAMP stimulation. In order to return PKA activity to baseline following stimulation we allowed cAMP bound R (R2_cAMP) to be stripped of cAMP by PDE (reference). In the second module of the reaction network PLB associates with AKAP to form a complex (AKAP_PLB) followed by phosphorylation of PLB

(AKAP_pPLB). All AKAP is bound to PKA derived from the total pool of PKA in module 1. Since AKAP bound PKA activity represents only a fraction of the total PKA activity, the total AKAP-PKA activity is defined by the following equation:

$$[E] = 2 * AKAP\_PLB * \left(\frac{C}{2 * R2C2 + R2C1 + C}\right)$$

where E represents the total amount of enzyme (active PKA) from the AKAP bound pool of PKA that is available to participate in the phosphorylation of PLB which, is defined by standard Michaelis-Menten kinetics:

$$[pPLB] = \frac{[E] * k_{cat} * [AKAP\_PLB]}{(Km + [AKAP\_PLB])}$$

To simulate the difference between phosphorylation state-dependent (AKAP does not bind pPLB) and phosphorylation state-independent (AKAP binds both PLB and pPLB) the reverse rate for the interaction of AKAP and pPLB was modulated so that AKAP bound pPLB with either equal or lower affinity than PLB. For state-independent binding, the affinity of AKAP for pPLB is the same as in the non-phosphorylated state and for state-dependent binding the forward rate was increased. For state-dependent binding to PLB the reverse rate of the AKAP-pPLB interaction was increased by a factor of 1000, changing the affinity from 13.3nm to 13.3μM. The model is available in the public biomodels folder of the Virtual Cell software.

Results

AKAP7γ directly binds to phospholamban

Due to conflicting evidence demonstrating the importance of AKAP7δ/γ for phospholamban (PLB) phosphorylation (*27*, *90*), we investigated the dynamics of AKAP7δ/γ binding to PLB as a possible regulatory function of phosphorylation. To begin with, we confirmed previous findings that AKAP7δ/γ binds directly to PLB (*27*). As shown in Figure 3.1A, PLB co-immunoprecipitated with AKAP7δ/γ from isolated rat heart extract, but not with control IgG, demonstrating that these two proteins form a complex in cardiac myocytes. Next, we investigated if this interaction was specific for the cardiac myocyte, or if association could be detected in a heterologous system. HEK293 cells were transfected with plasmids expressing mCherry-AKAP7γ in the presence and absence of GFP-phospholabman. GFP was immunoprecipitated and the association of AKAP7γ was determined by Western blot analysis (Figure 3.1B). Importantly, co-precipitation of mCherry-AKAP7γ was only seen in cells expressing GFP-PLB, demonstrating the specificity of the interaction. To further these findings and examine the kinetic properties of the interaction, we performed surface plasmon resonance (SPR). As the domain on phosholamban for binding to AKAP7γ is maintained in the first 21 amino acids, we immobilized a peptide mimicking this domain on a CM5 sensor chip. Varying concentrations of purified AKAP7γ were used to determine the dynamics of the interaction. As shown in Figure 3.1C, we confirmed a direct interaction between phospholamban and AKAP7γ with an

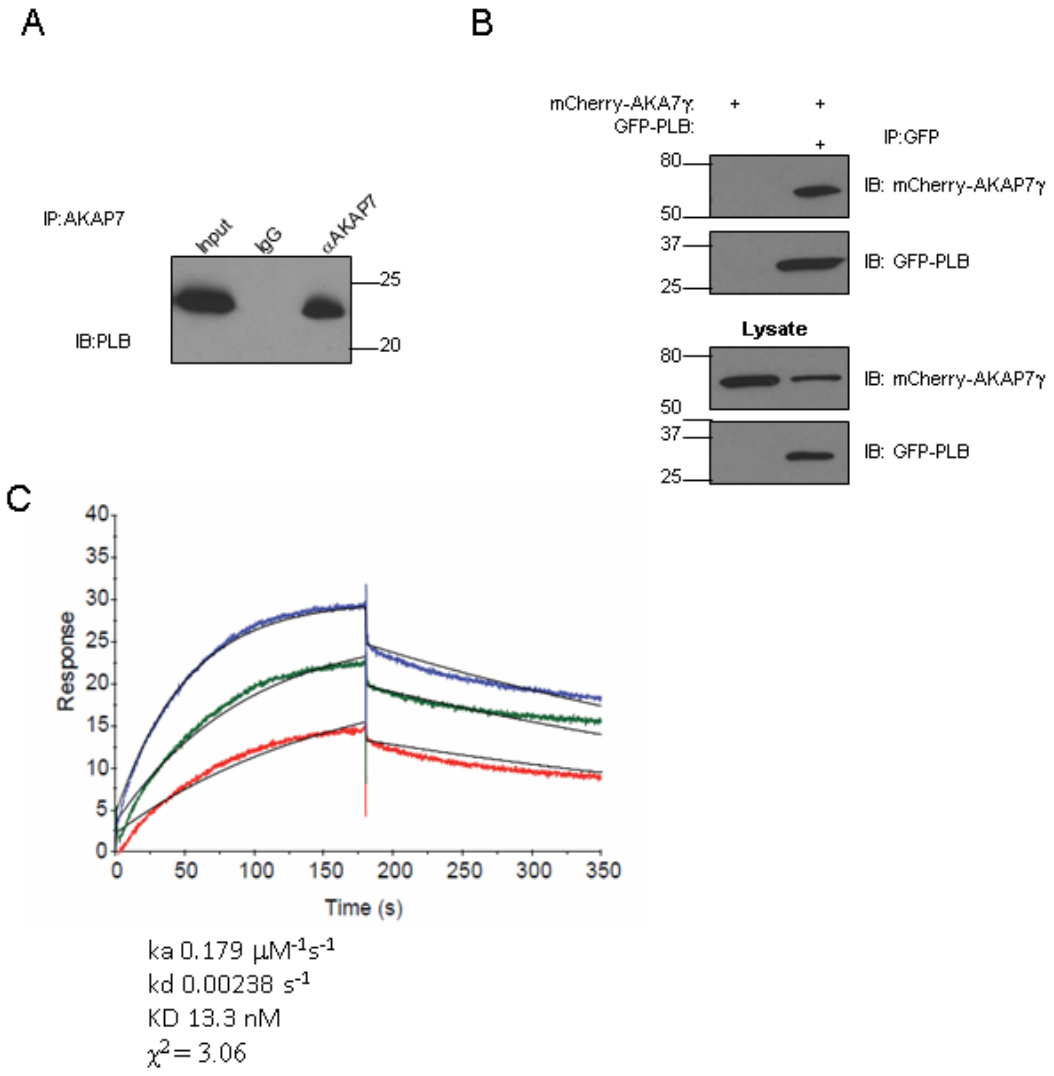

Figure 3.1 Direct cellular interaction between AKAP7δ/γ and phospholamban.
A) AKAP7γ was immunoprecipitated from rat heart extract and association of PLB was determined by Western Blot. n=3. **B)** mCherry Western blot analysis of anti-GFP immunoprecipitates isolated from HEK-293 cells co-transfected with mCherry-AKAP7γ in the presence and absences of GFP-PLB (upper panels). To confirm immunoprecipitation of equal amounts of GFP-PLB, the nitrocellulose membranes were also probed for GFP using a monoclonal anti-GFP antibody (middle panel). Lower panels depict mCherry and GFP Western blot analysis of the input (20μL) from each condition. n=3. **C)** SPR was performed by immobilizing a peptide containing the first 21 amino acids of PLB (150RUs) on a CM-5 chip and measuring the response when passing over a range of concentrations (25-100nM) of AKAP7γ. Forward and reverse rates of binding and binding affinity were determined by fitting of the sensorgram with BIAcore T100 evaluation software.

affinity of 13.3nM. Analysis of the fit of the interaction suggests one site of interaction. Taken together, these data confirm the original observation demonstrating a direct association of AKAP7γ with phospholamban that can be isolated from cardiac myocytes.

PKA bound to AKAP7δ/γ is responsible for phosphorylation of phospholamban

The primary purpose of AKAPs is to co-localize PKA and its substrate via formation of a multi-component signaling complex, resulting in enhanced substrate phosphorylation. Therefore, we next examined the necessity of PKA binding to AKAP7δ/γ for PLB phosphorylation. To investigate this association in an endogenous tissue, PLB was immunoprecipitated from rat heart lysate, and association with PKA was determined in the presence or absence of the AKAP/PKA disrupting peptide AKAP-IS (Figure 3.2A) (*15*). Disruption of PKA anchoring using the AKAP-IS peptide decreased association of the PKA RII subunit with PLB. Importantly, incubation of a control peptide did not significantly affect PKA/PLB interaction, demonstrating that PKA associates with PLB via interaction with AKAP. To determine the role of AKAP7γ in mediating this association, HEK293 cells were transfected with GFP-PLB and either wild-type mCherry-AKAP7γ, or one lacking the PKA binding domain (mCherry-DPKA-AKAP7γ). Lysate isolated from these cells was subjected to pulldown analysis using GST-tagged PKA RIIα subunit. This is a common technique used to isolate AKAP complexes from various tissues, as the RII subunit will pulldown the AKAP and all AKAP-associated proteins (*49*, *69*). As shown in Figure 3.2B,

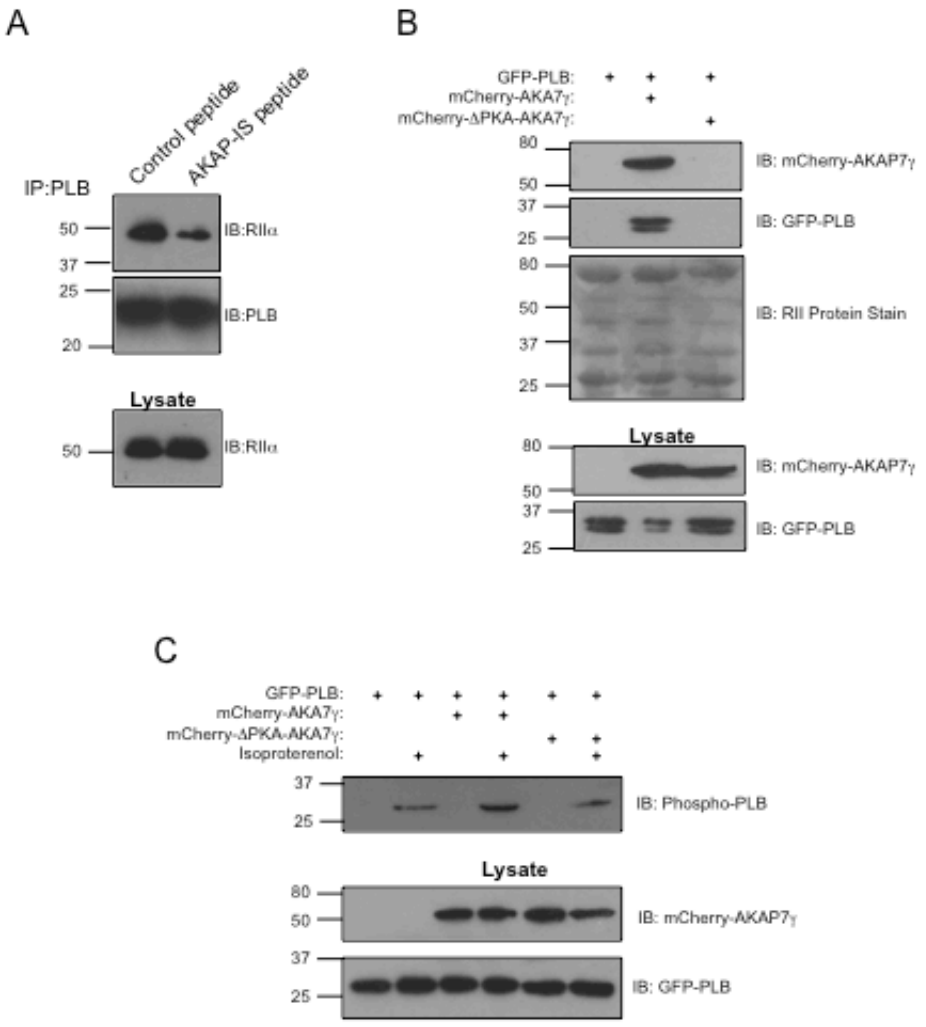

Figure 3.2 AKAP7δ/γ anchors PKA to the phospholamban complex to enhance phosphorylation. **A)** PLB was immunoprecipitated from rat heart lysate. Following extensive washing, the immunoprecipitates were incubated with the AKAP/PKA disrupting peptide AKAP-IS (10μM) or control peptide (10μM) for 30 minutes while rocking. After another round of washing, association of the regulatory subunit of PKA was determined by Western blot. **B)** HEK-293 were transfected with GFP-PLB and either wild-type mCherry-AKAP7γ, or one deficient in the PKA binding domain (mCherry-ΔPKA-AKAP7γ). Isolated lysates were subjected to pulldown assays using bacterially purified GST-tagged PKA RII subunit precharged on Glutatione-agarose; Both GFP and mCherry antibodies were used for detecting PLB and AKAP7γ interactions, respectively (upper panel). Protein stain of the nitrocellulose membrane before Western blot analysis is shown in the middle panel. Input from the transfected cells (20μl) is shown in the bottom panels. n=3. **C)** HEK-293 were transfected with GFP-PLB and either wild-type mCherry-AKAP7γ, or one deficient in the PKA binding domain (mCherry-ΔPKA-AKAP7γ). Cells were stimulated with 100μM Isoproterenol for 5 minutes before cell lystate was isolated and loaded onto and SDS-PAGE gel. Phosphorylation of PLB at Serine 16 was determined using a phospho-specific antibody (upper panel). Total expression of the proteins is shown in the lower panels using both GFP and mCherry antibodies to detect PLB and AKAP7γ, respectively. n=3

GFP-PLB only associated with the PKA subunit in the presence of full-length AKAP7γ. However, when the PKA binding domain was deleted from the AKAP, GST-RIIα could no longer pulldown PLB, demonstrating the importance of PKA anchoring to AKAP7γ. Taken together, these results implicate AKAP7γ for linking the kinase to the PLB complex.

Next, we investigated the functional significance of this interaction for regulation of PLB phosphorylation. We first performed analogous experiments to those outlined in Figure 3.2B, and looked at the role of AKAP7γ-bound PKA on PLB phosphorylation. As shown in Figure 3.2C, expression of the anchoring protein dramatically heightened PLB phosphorylation. However, when the PKA binding domain was deleted from the AKAP, this enhancement was lost, suggesting that the kinase must be attached to the AKAP for this effect.

Described human mutations of phospholamban contained in the AKAP7δ/γ binding domain decrease complex formation, thereby reducing phosphorylation

Multiple mutations of PLB have been identified and linked to familial dilated cardiomyopathy. At least two of these mutations are found in the AKAP7δ/γ binding domain, suggesting these mutation may affect the ability of PLB to bind to the AKAP7δ/γ (Schematic diagram shown in Fig 3.3A). Mutation of Arginine 9 to Cystine (PLB-R9C) displays a dose-dependent inhibition of SERCA2a and significantly decreased phospho-PLB (*92*). The other mutation found in the AKAP7δ/γ binding region is a deletion of Arginine 14 (PLB-Δ14),

which exhibits super-inhibition of SERCA2a activity, correlating with decreased PLB phosphorylation (*93*). To test the importance of AKAP7δ/γ binding to PLB for the phosphorylation of PLB, we utilized these mutations to block association. We investigated whether or not these mutations affect the ability of the complex to form in a cellular environment. AKAP7γ was coexpressed in HEK293 with wild-type PLB-GFP, or one of the mutated isoforms (PLB-R9C-GFP or PLB-Δ14-GFP). The PLB-GFP complex was isolated and association of AKAP7γ-mCherry was determined by Western Blot. As shown in Figure 3.3B, both mutations significantly decreased the co-precipitation of AKAP7γ, suggesting that a decrease in the AKAP7γ binding affinity measured in these mutants results in decreased association of AKAP7γ with the protein in a cellular context.

Importantly, the decrease in complex formation seen with the PLB mutants should reduce the concentration of PKA found in the PLB complex. To test this hypothesis, AKAP7γ was coexpressed in HEK293 with wild-type PLB-GFP, or one of the mutated isoforms (PLB-R9C-GFP or PLB-Δ14-GFP). Cell lysate was subjected to GST-RII pulldown, and association of GFP-PLB was measured. In confirmation of our findings, wild-type PLB associates with the PKA subunit when co-expressed with AKAP7γ (Figure 3.3C). However, both PLB mutations showed decreased association with the GST-RII, suggesting mutation of PLB in the AKAP7δ/γ binding domain decreases complex formation and reduces PKA association with PLB. As our hypothesis states that AKAP7δ/γ anchored PKA mediates the phosphorylation of PLB, the decrease in complex

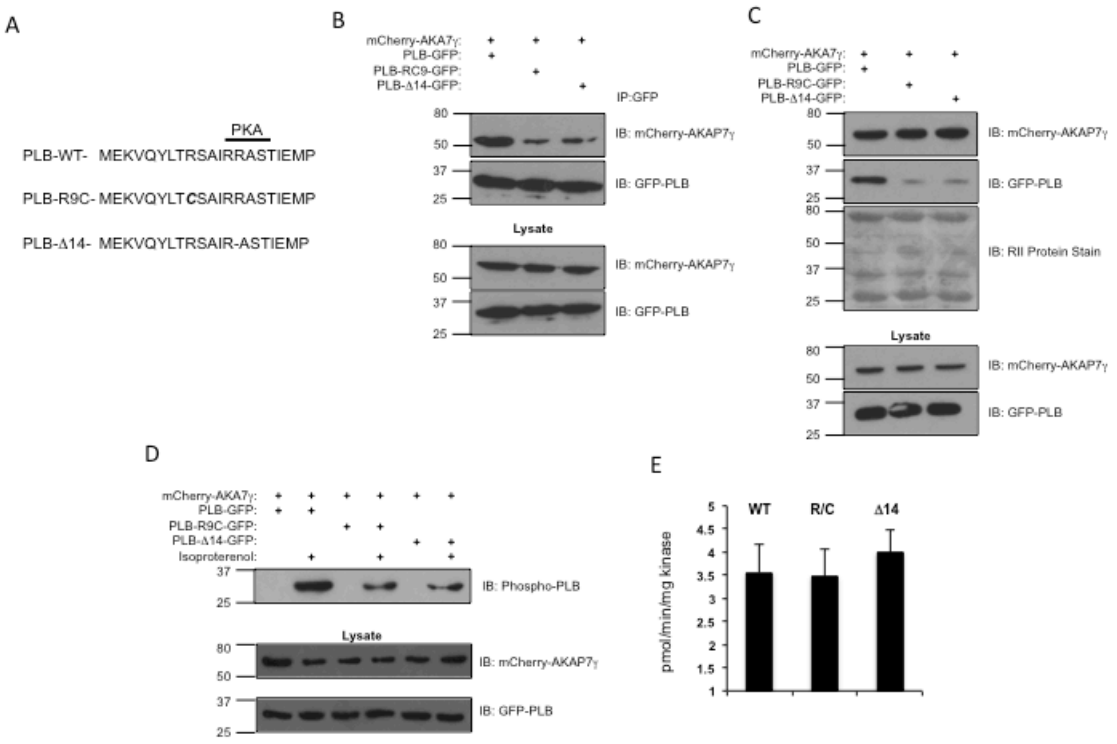

Figure 3.3 Described human mutations of phospholamban disrupt AKAP7γ binding
A) Schematic depiction of the mutations found in phospholamban that are found in the AKAP7δ/γ binding domain. **B)** mCherry Western blot analysis of anti-GFP immunoprecipitates isolated from HEK-293 cells co-transfected with mCherry-AKAP7γ and either wild-type GFP-PLB, or one of the mutated isoforms (PLB-RC9-GFP, or PLB-Δ14-GFP, upper panels). To confirm immunoprecipitation of equal amounts of GFP-PLB, the nitrocellulose membrane was also probed for GFP using a monoclonal anti-GFP antibody (middle panel). Lower panels depict mCherry and GFP Western blot analysis of the input (20μL) from each condition. n=3. **C)** HEK-293 were transfected with mCherry-AKAP7γ and either wild-type GFP-PLB, or one of the mutated isoforms (PLB-RC9-GFP, or PLB-Δ14-GFP, upper panels). Isolated lysates were subjected to pulldown assays using bacterially purified GST-tagged PKA RII subunit precharged on Glutatione-agarose; Both GFP and mCherry antibodies were used for detecting PLB and AKAP7γ interactions, respectively (upper panel). Protein stain of the nitrocellulose membrane before Western blot analysis is shown in the middle panel. Input from the transfected cells (20μl) is shown in the bottom panels. n=3. **D)** HEK-293 were transfected with mCherry-AKAP7γ and either wild-type GFP-PLB, or one of the mutated isoforms (PLB-RC9-GFP, or PLB-Δ14-GFP. Cells were stimulated with 100μM Isoproterenol for 5 minutes before cell lystate was isolated and loaded onto and SDS-PAGE gel. Phosphorylation of PLB at Serine 16 was determined using a phospho-specific antibody (upper panel). Total expression of the proteins is shown in the lower panels using both GFP and mCherry antibodies to detect PLB and AKAP7γ, respectively. n=3 **E)** PLB peptides (1μg) were incubated in kinase buffer (50 mM Tris-HCL pH 7.5, 5 mM $MgCl_2$) containing 100 mM ATP, 5 mM [γ^{-32}]ATP and 800 units of purified PKA catalytic subunit (NEB). After a 15 inute incubation at 30°C, the reaction mixture was spotted onto phosphocellulose strips and washed five times in 75 mM phosphoric acid. Filters were air dried and counted.

formation seen with the mutated isoforms of PLB should therefore result in a decrease in phosphorylation of the protein. To test this hypothesis, AKAP7δ/γ was coexpressed in HEK293 with wild-type PLB-GFP, or one of the mutated isoforms (PLB-R9C-GFP or PLB-Δ14-GFP). Cells were stimulated with 100nM Isoproterenol for 5 minutes, and phosphorylation of PLB was determined by Western Blot analysis (Figure 3.3D). In conjunction with those results seen in both transgenic animals and human patients (*92*, *93*), less phosphorylation was seen with the mutated isoforms of PLB. This finding correlates with the decreased PKA association within the mutant complexes due to deceased affinities for AKAP7γ, suggesting that one mechanism for the attenuation of phosphorylation of the mutant PLB isoforms is a significant decrease in the localization of the kinase to the complex. However, it is plausible that this effect may result from a decreased ability of these mutated isoforms to be phosphorylated by the kinase and not a disruption in the localization of the kinase to the PLB complex. To test this, peptides mimicking the first 21 amino acids of wild-type PLB, PLB-R9C or PLB-Δ14 were subjected to an in vitro kinase assay. As shown in Figure 3.3E, all peptides were able to be phosphorylated by the kinase to a similar extent, suggesting the decrease in phosphorylation of the mutated PLB isoforms seen in the exogenous system is not due to a lack of ability of the kinase to phosphorylate the mutated isoforms. Taken together, the data shown in Figure 3.3 supports the hypothesis that by linking the kinase to its substrate PLB, AKAP7δ/γ mediates phosphorylation of PLB.

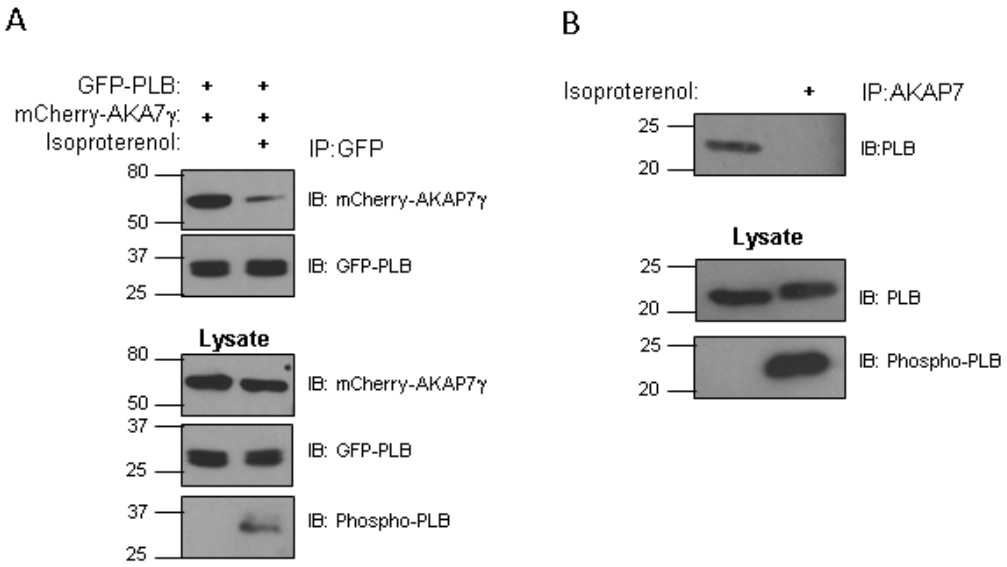

Figure 3.4 Phosphorylation of PLB significantly decreases the affinity for AKAP7δ/γ. **A)** HEK-293 were transfected with GFP-PLB and mCherry-AKAP7γ. Cells were stimulated with 100μM Isoproterenol for 5 minutes and the PLB complex was isolated by immunoprecipitation using anti-GFP. Association of AKAP7γ was determined by Western blot using anti-mCherry (upper panels). To confirm immunoprecipitation of equal amounts of GFP-PLB, the nitrocellulose membrane was also probed for GFP using a monoclonal anti-GFP antibody (middle panel). Total expression of the proteins is shown in the lower panels using both GFP and mCherry antibodies to detect PLB and AKAP7γ, respectively. Phosphorylation of PLB at Serine 16 in total lysate was determined using a phospho-specific antibody (upper panel). n=3 **B)** Rat neonatal cardiac myocytes were stimulated with 10μM Isoproterenol for 5 minutes and the PLB complex was isolated by immunoprecipitation. Association of AKAP7δ/γ was determined by Western blot (upper panel). Total expression of the proteins is shown in the lower panels. Phosphorylation of PLB at Serine 16 in total lysate was determined using a phospho-specific antibody (upper panel). n=3

Phosphorylation of phospholamban decreases the affinity for AKAP7δ/γ binding

Contained in the AKAP7δ/γ binding domain on PLB is the PKA phosphorylation site. We therefore proposed that phosphorylation of PLB would decrease the ability of the AKAP to interact with the protein. To test this hypothesis, we began by defining the change in affinity between phosphorylated PLB and non-phosphorylated PLB using SPR. We immobilized a peptide mimicking the first 21 amino acids of either wild-type PLB, or one that is permanently phosphorylated at Serine 16 to a CM5 sensor chip, and then determined the kinetic strength of the two interactions using varying concentrations of purified AKAP7γ. As shown in Figure 3.4A, when phosphorylated, the affinity of AKAP7γ and PLB is below the limit of detection, suggesting a low affinity binding. To confirm this finding in a cellular context, HEK293 cells were transfected with plasmids expressing mCherry-AKAP7γ and GFP-PLB. After a 15 minute stimulation with 100nM Isoproterenol, GFP was immunoprecipitated and the association of AKAP7γ was determined by Western blot analysis (Figure 3.4B). Importantly, co-precipitation of mCherry-AKAP7γ was dramatically decreased under conditions that result in phosphorylation of PLB. These findings were confirmed in an endogenous setting. Rat neonatal myocytes were stimulated with 10μM Isoproterenol for 15 minutes followed by immunoprecipitation of phospholamban and blotting for AKAP7γ. Association of AKAP7γ with PLB was not detected following isoproterenol stimulation. Taken

together, these findings suggest that the AKAP7δ/γ interaction with PLB is dispersed upon activation of PKA and phosphorylation of PLB.

Phosphorylation state specific binding of AKAP7δ/γ increases phospholamban phosphorylation

Our finding that the AKAP7δ/γ-PLB interaction is phosphorylation state specific is interesting given that the purpose of this interaction is to direct PKA phosphorylation to PLB. Such state selective binding suggests that AKAP7δ/γ likely binds, phosphorylates, and then unbinds PLB in a dynamic process. Thus state-selective binding has the potential to increase PLB phosphorylation in comparison to non-state-specific binding.

To investigate the potential consequence of state specific binding of AKAP7δ/γ to PLB, we created an ordinary differential equation model that simulates phosphorylation of PLB by AKAP7δ/γ bound PKA at baseline steady state and during cAMP stimulation. For all iterations of the model parameters, the simulation was run for 15000s prior to initiating our stimulation protocol, thus ensuring that all species reach a baseline steady state. At baseline steady state, the level of cAMP is 244nm and 2.4% of the total PKA is in an active state. Following initiation of our stimulation protocol, the levels of cAMP rise to 5.6mM activating 94.1% of the total PKA in 90s and decaying back to baseline in roughly 500-600s (Figure 3.5A). To test the effect of state specific binding, we compared the levels of phospho-PLB with either equal affinity of AKAP for PLB and

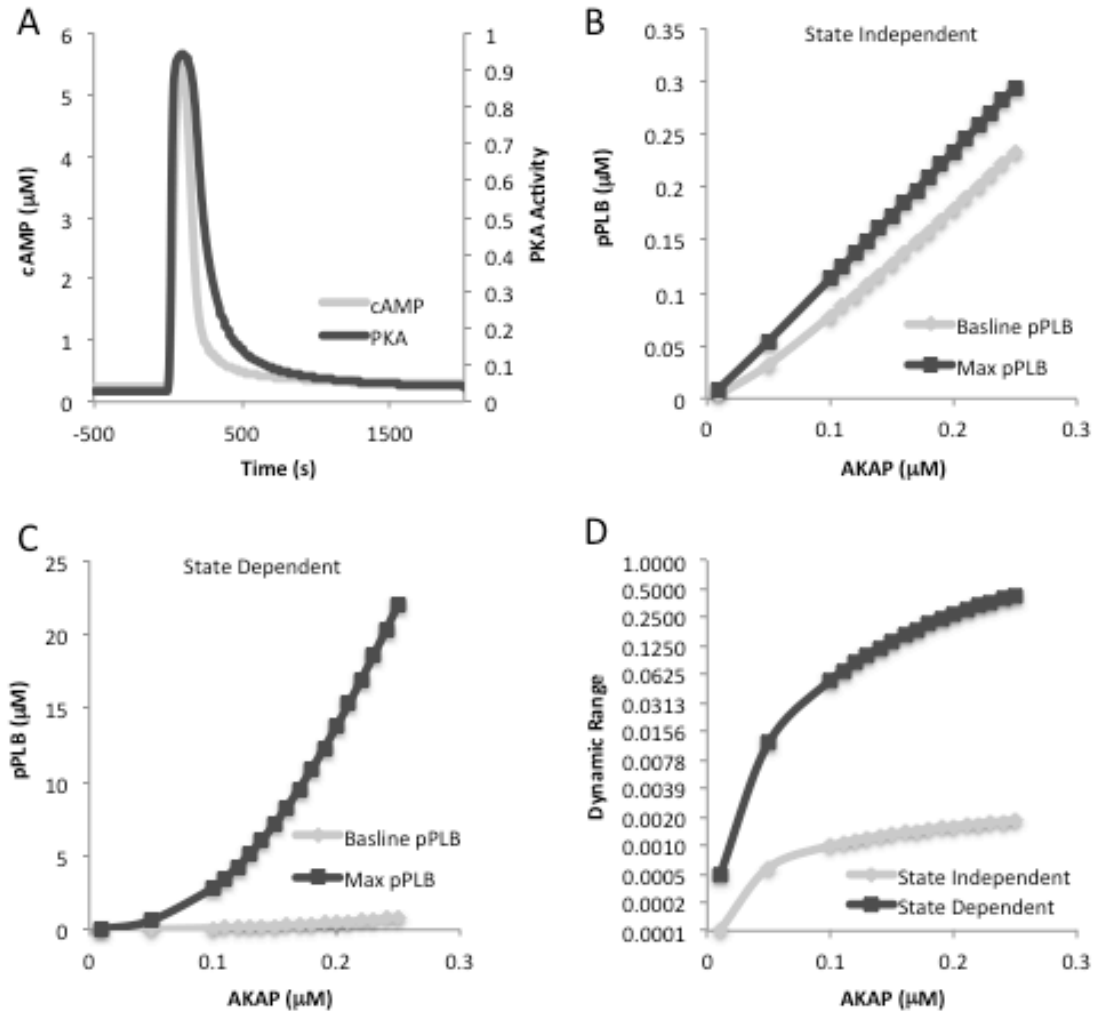

Figure 3.5 State dependent binding of AKAP to PLB dramatically increases PLB phosphorylation upon stimulation. **A)** cAMP concentration and PKA activity over the time-course of the simulations. All species in the model are at steady state prior to stimulation (t = 0s), which was achieved via activation of additional AC. **B)** pPLB concentration at baseline and maximum following stimulation for state independent binding of AKAP and PLB. **C)** pPLB concentration at baseline and maximum following stimulation for state dependent binding of AKAP and PLB. **D)** Dynamic range ($Dynamic\ Range = \frac{(Max\ pPLB - Min\ pPLB)}{Total\ PLB}$) of PLB phosphorylation for both state dependent and state independent binding of AKAP to PLB. The y-axis is on a $\log_2$ scale to enable viewing of both trends on the same graph.

phospho-PLB (state-independent), or 1000-fold lower affinity for pPLB (state-dependent). We tested AKAP concentrations ranging from 1-250nM for both state-independent binding and state-dependent binding. Unpublished analysis from our lab suggests that the level of AKAP7δ/γ present in cardiac myocytes is roughly 100nm. The total amount of PLB present in these simulations is 50μM (*86*). In the range of AKAP concentrations tested, state-independent binding of AKAP to PLB provides minimal capacity for PLB phosphorylation, with very low levels of phosphorylation at baseline and minimal response to stimulation (Figure 3.5B). We quantified the response to stimulation by calculating the dynamic range, defined as the change in concentration of phospho-PLB from baseline to maximum, divided by the total concentration of PLB. The dynamic range for state-independent binding ranges from 0.01% to 0.17% (Figure 3.5C). State-dependent binding of AKAP to PLB however, allows for maintenance of low baseline levels of PLB phosphorylation and dramatic responses to stimulation (Figure 3.5B). With state-dependent binding, the dynamic range varies from 0.05% to 42.3% (Figure 3.5D). It is important to note that while the primary determinants of the dynamic range of PLB phosphorylation are the affinity of AKAP for phospho-PLB and the AKAP concentration, the dynamic range is also modified significantly by baseline cAMP concentration and the amount of phosphatase present in the system. Higher baseline concentrations of cAMP (622nm) contribute to increased baseline activity of PKA and hence higher concentrations of phospho-PLB (Figures 3.6A and 3.6B). With the same level of

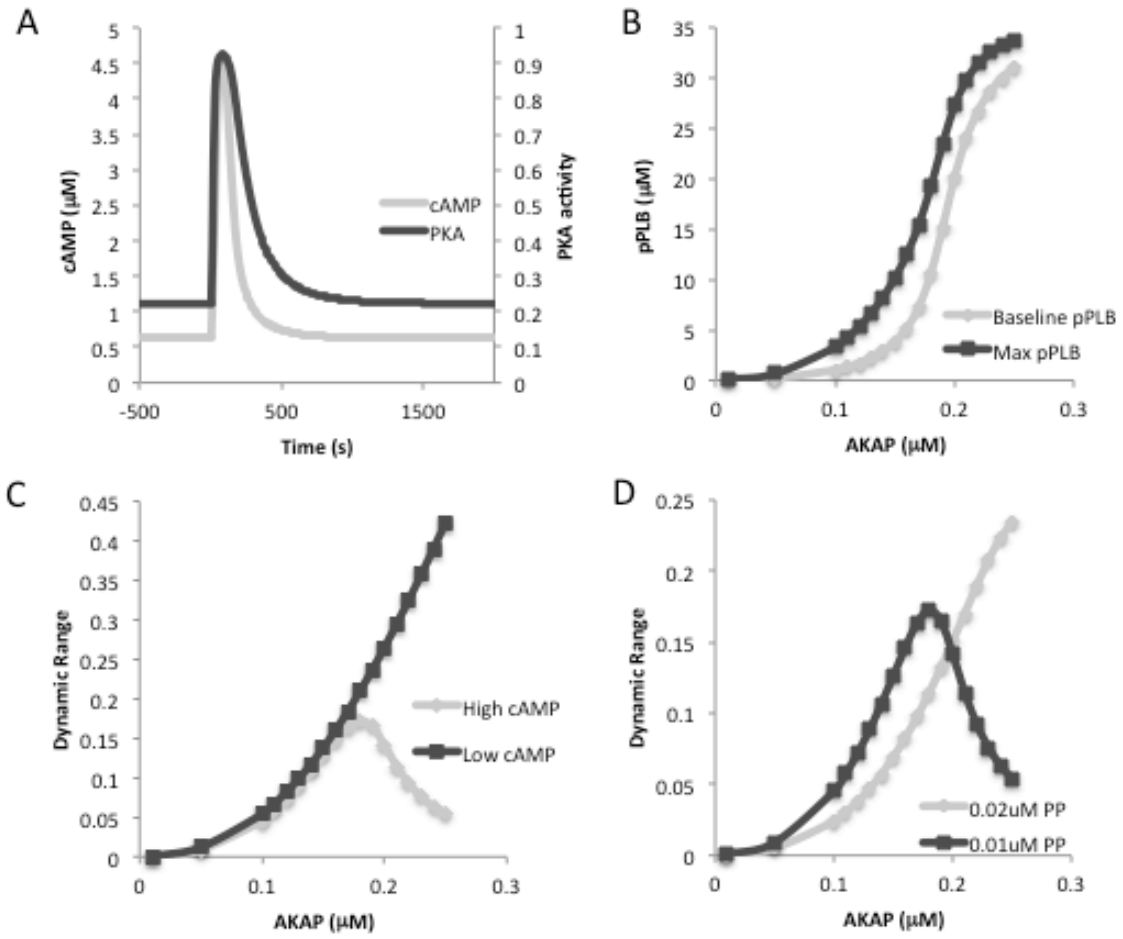

Figure 3.6 Increased baseline cAMP reduces dynamic range of PLB phosphorylation
A) cAMP concentration and PKA activity over the time-course of the simulations as in figure 5. The concentrations of AC and PDE have been adjusted to increase the baseline level of cAMP from 244nm to 622nm. **B)** pPLB concentration at baseline and maximum following stimulation for state dependent binding of AKAP and PLB. **C)** Dynamic range of PLB phosphorylation for state dependent phosphorylation at low (244nM) and high (622nM) baseline cAMP levels given AKAP concentrations ranging from 1nM to 250nM. **D)** Dynamic range of PLB phosphorylation with high baseline levels of cAMP and normal or increased protein phosphatase (PP).

stimulation, this results in a decreased dynamic range (Figure 3.6C). Additionally, it was noted that at higher baseline cAMP concentrations, increasing the AKAP concentration past 0.15mM resulted in dramatic increases in baseline phospho-PLB. While this threshold effect of AKAP concentration on baseline phospho-PLB will occur in the simulations with lower baseline cAMP concentrations, it requires higher concentrations of AKAP than we would expect to see *in vivo*. We determined that this is primarily due to a shift in the balance of PKA and phosphatase activity. Increasing the amount of phosphatase in the simulations allowed for maintenance of lower baseline phospho-PLB concentrations for AKAP concentrations at the top of our range, and slightly reduced maximal phospho-PLB for all AKAP concentrations. This resulted in a reduced dynamic range at lower AKAP concentrations, yet increased the dynamic range at higher AKAP concentrations in comparison to simulations with a lower phosphatase concentration (Figure 3.6D). The model demonstrates that phosphorylation state-dependent binding of AKAP7δ/γ to PLB could allow low concentrations of AKAP7δ/γ to phosphorylate much higher concentrations of PLB. Additionally, the data suggests that the significant increase in dynamic range seen with state-dependent binding is stable over a range of baseline cAMP and phosphatase concentrations, perhaps allowing for fine-tuning of AKAP7δ/γ complex signaling.

Discussion

The importance of AKAP7δ/γ to PLB phosphorylation and cardiac calcium dynamics has recently been called into question by the work of Jones *et al* (*90*). Their AKAP7 PKA binding domain knockout mouse displayed no obvious phenotype, nor any defect in PLB phosphorylation or Ca2+ handling in response to sympathetic stimulation. Hence, the authors suggest that AKAP7 is not responsible for anchoring PKA to PLB, and suggest that another AKAP likely performs this function. Their deletion construct is expected to ablate only the PKA and $Ca_v1.2$ binding domains of all AKAP7 isoforms, although no effect on L-type calcium current was seen. It is concerning that the authors did not demonstrate that the truncated protein products do not associate with PKA. Additionally, it is noteworthy that previous work by this group found that complete ablation of AKAP5 in mice does not show an obvious phenotype, while specific ablation of the PKA binding domain does (*94*). It is possible that deletion of exon 7 behaves more like a full length AKAP7-knockout, which is consistent with the lack of detection of all isoforms of the AKAP in this model. Additionally, if a truncated version of AKAP7δ/γ is still expressed in the mouse, it would still bind all the other components of the complex and perhaps the balance of phosphorylation to dephosphorylation is changed. Further investigation of this mouse model is warranted before concluding that AKAP7δ/γ anchoring to PKA is not important.However, the data shown here clearly demonstrates the role of AKAP7δ/γ in mediating phosphorylation of PLB. AKAP7δ/γ was first identified as

the AKAP that directs PKA mediated phosphorylation of PLB by Lygren *et al* in 2007. This work showed that disruption of the AKAP7δ-PKA interaction results in a reduction in PLB phosphorylation by approximately 50% and that this has a significant effect on Ca^{2+} dynamics (*27*). Our work confirms this finding by showing that disrupting PKA binding to the complex, or decreasing the affinity for AKAP7δ/γ and PLB reduces PKA phosphorylation of PLB. Hence, AKAP7δ/γ should be a key player in the calcium dynamics of the heart.

Several human PLB mutations have been discovered that are associated with dilated cardiomyopathy. Two PLB mutants in particular, PLB-R9C and PLB-Δ14, display hypo-phosphorylation, yet the mechanism of the decrease in phosphorylation is unclear at present (*92*, *93*). We examined the ability of these PLB mutants to associate with AKAP7γ and found a significant reduction in PKA association with the complex and a reduction in phosphorylation of the mutant proteins when compared to wild-type PLB in cells. Together, these findings suggest that hypo-phosphorylation associated with the human PLB mutants is most likely due to impaired interaction with AKAP7δ/γ. Given the clinically significant phenotype associated with these mutants, our findings indicate that the AKAP7δ/γ-PLB interaction is critically important for maintaining PLB phosphorylation and normal cardiac function in humans.

Phosphorylation of PLB by PKA occurs at S16, which is located within the region of the AKAP7δ/γ binding site. The location of this phosphorylation site suggests that it may affect AKAP7δ/γ binding to PLB. Our attempts to detect

AKAP7δ/γ-pPLB binding indicated a lack of association in both transfected cells and stimulated rat neonatal myocytes. This finding is very interesting, and suggests that the AKAP7δ/γ-PLB interaction may be very dynamic. Given the phosphorylation dependence of this binding interaction, AKAP7γ may work by essentially shuttling PKA from one PLB molecule to the next as it binds, directs phosphorylation, and then unbinds to find its next unphosphorylated target. This sort of interaction has the potential to greatly amplify PLB phosphorylation.

To confirm whether the new finding of phosphorylation state binding dependency on PLB phosphorylation could in fact have such an amplification effect, we created an ordinary differential equation model of the complex dynamics. For AKAP-PLB interactions that are phosphorylation state-independent, the ability to achieve complete PLB phosphorylation would require at least an equimolar ratio of AKAP to PLB, since each PLB molecule would need an associated AKAP-PKA complex. In the range of AKAP concentrations tested, our model suggests that state-independent binding of AKAP to PLB cannot achieve levels of PLB phosphorylation that would allow for effective modulation of SERCA2a activity. Furthermore, the results suggested that state-independent binding would be insensitive to stimulation given that the dynamic range of phosphorylation with the maximum amount of AKAP tested is only ~0.2% of the total PLB concentration. However, state-dependent binding of AKAP to PLB enables low concentrations of AKAP7γ to direct phosphorylation of much higher concentrations of PLB. While the concentration of PLB is suggested to be 50μM

or greater in cardiac myocytes, only 10-20% of the total PLB is in the monomeric form that can interact with and inhibit SERCA2a (*43*, *86*). Our simulations show that at physiologically relevant concentrations of AKAP7δ/γ a dynamic range of PLB phosphorylation can be achieved such that complete phosphorylation of monomeric PLB is possible. Thus, phosphorylation state-specific binding could explain the ability of low concentration proteins like AKAP7γ to regulate phosphorylation of high concentration proteins like PLB and troponin.

Data from our model also highlights the importance of the balance between AC and PDE activity, as well as PKA and phosphatase activity. The level of cAMP present in a given AKAP domain clearly defines the maximum dynamic range possible, as increased baseline cAMP results in higher baseline PKA activity resulting in a narrowed dynamic range of phosphorylation. While the increased baseline phosphorylation may be tempered by increased phosphatase activity, this too results in a slight decrease in the dynamic range of phosphorylation. Importantly, the significant increase in dynamic range seen with state-dependent binding, in comparison to state-independent binding, still exists with variation in baseline cAMP and phosphatase concentration.

This also raises a particularly intriguing hypothesis that such a mechanism may allow the cell to adapt to fluctuations in baseline cAMP concentration. As cAMP concentrations rise, additional phosphatase could restore baseline levels of phosphorylated substrate while still allowing for a sufficient dynamic range to provide a detectable signal. This important role of phosphatase in the dynamic of

PLB phosphorylation is consistent with several published results demonstrating the importance of phosphatase inhibition for PLB phosphorylation, lending further credence to these findings (*95-97*).

Our findings reaffirm the importance of AKAP7δ/γ in directing phosphorylation of PLB and present a novel mechanism that can explain the decrease in PLB phosphorylation associated with human PLB mutants. The state-dependent binding of AKAP7δ/γ also explains how it may be possible that low concentrations of AKAP and PKA could regulate phosphorylation of high concentrations of substrate, as is the case for PLB and troponin. These findings require us to consider that AKAP complexes in general may be much more dynamic than previously thought. Further investigation of the AKAP7γ-PLB complex kinetics is warranted, as well as careful examination of other AKAP complexes that may also exhibit similar state-dependent interactions.

Chapter 4

Langevin Dynamic Simulation of AKAP-PKA Complex: Re-envisioning the local concentration mechanism for directing PKA phosphorylation

Marc Rigatti, Paul J. Michalski, Kimberly L. Dodge-Kafka, Ion I. Moraru

Author Contributions

M.R. wrote the manuscript and performed the computational modeling and data analysis. P.J.M. wrote the Langdyn software and methods section and assisted the computational modeling and data analysis.

Abstract

The second messenger cAMP and its effector cAMP-dependent protein kinase A (PKA) constitute a ubiquitous cell signaling system. In its inactive state PKA is composed of two regulatory subunits that dimerize, and two catalytic subunits that are inhibited by the regulatory subunits. Activation and release of the catalytic subunits occurs upon binding of two molecules of cAMP to each regulatory subunit. Although many receptor types existing within the same cell may use this signaling system, compartmentation of signaling does occur due to A-Kinase Anchoring Proteins (AKAPs), which act to co-localize PKA with specific substrates. The molecular mechanism allowing AKAPs to direct PKA phosphorylation to a particular substrate remains unknown. This is primarily due to the large body of evidence suggesting that the catalytic subunit, which is highly diffusable, is released in response to cAMP. Recent evidence from Smith et al suggests that in the cell, the catalytic subunit may not be released from the AKAP complex (*52*). They further demonstrated that alterations in the structure of the PKA regulatory subunit tether affect substrate phosphorylation. We use novel computational software based on Langevin dynamics, Langdyn, to simulate the AKAP-PKA complex in order to determine a molecular mechanism for the changes in phosphorylation seen with alteration in tether length and flexibility, and also to demonstrate whether or not AKAPs can effectively direct PKA phosphorylation to a particular substrate upon release of the catalytic subunit from the complex. We find that short and flexible tethers contribute to a decrease

in the average characteristic time of binding, allowing the catalytic subunit to spend more time in a bound state with the substrate, which yields faster characteristic times of phosphorylation. We further demonstrate that release of the catalytic subunit from the AKAP complex abrogates the effect of tethering, with characteristic times of phosphorylation similar to non-AKAP bound PKA. The data demonstrates that AKAPs likely do not release the catalytic subunit in directing PKA phosphorylation to AKAP bound substrates. In combination with the changes in characteristic time of phosphorylation that are driven by tether structure, this work indicates that the purpose of AKAPs may be to increase the efficiency of phosphorylation of particular AKAP substrates.

Introduction

The second messenger cAMP and its effector, cAMP-dependent protein kinase A (PKA), constitute a ubiquitous cell-signaling network responsible for the phosphorylation of numerous substrates. Recent experimental methods that employ mass spectrometry identify 112 potential PKA substrates in a single cell type (*5*). The existence of such an abundance of PKA substrates in a single cell highlights the importance of signal compartmentation within the cAMP-PKA signaling pathways. Achieving phosphorylation of specific substrates in response to an extracellular stimulus is complicated by the rapid diffusion of cAMP and also by diffusion of the PKA catalytic subunit. The vast majority of evidence regarding PKA activation indicates that binding of cAMP to allosteric sites on the regulatory subunits results in the simultaneous activation and release of the catalytic subunit (*10*). The co-discoverer of cAMP, Ted Rall, once said that this scheme presents "…the unsatisfying picture of the catalytic subunit of protein kinase swimming about, happily phosphorylating a variety of cellular constituents whether they need it or not"(*98*).

However, it is clear that there is great specificity in PKA phosphorylation dynamics. It has been known since the late 1970's that cAMP-PKA signaling is actually compartmentalized. Stimulation of the β-adrenergic receptor in cardiomyocytes was shown to the activate glycogen phosphorylase, while stimulation of the PGE1 receptor did not, even though both receptors signal via cAMP and PKA (*8*). The discovery of A Kinase Anchoring Proteins (AKAPs) has

provided at least a partial explanation of signal compartmentation. This class of proteins coordinates a multi-protein signaling microdomain by co-localizing PKA with specific substrates and additional effectors like phosphodiesterase, adenylate cyclase, and phosphatase (*29*). The ability of an AKAP to coordinate such a multi-protein signal complex allows for the local production and degradation of cAMP, thereby spatially restricting PKA activation. Co-localization of PKA with its substrates in this manner is hypothesized to confer specificity of phosphorylation by increasing the local concentration of PKA. While achieving a high local concentration of PKA via anchoring to a specific substrate in a particular location is straightforward, the result of this mechanism following PKA activation and release is less obvious. Since the activated catalytic subunit is freely diffusible, it may diffuse to and phosphorylate other substrates in the same manner expected for the AKAP bound substrate. While phosphorylation of non-local substrates may be inhibited by the presence of protein kinase inhibitor (PKI), a pseudosubstrate inhibitor of PKA, it must be acknowledged that PKA will not necessarily diffuse to and phosphorylate its associated substrate even if released in close proximity of its substrate. Thus, these data call into question the mechanism of PKA scaffolding.

In contrast, recent evidence has surfaced that PKA is not released following stimulation and is able to maintain catalytic activity while bound to its regulatory subunit (*50*, *52*). The ability of PKA to phosphorylate its substrates while remaining bound to the AKAP complex would provide for a much more

convincing hypothesis regarding specificity of substrate phosphorylation. This novel mechanism of PKA activation has recently been investigated by cryo-EM using AKAP7γ as a model system. The AKAP7γ-PKA complex has been demonstrated to posses a remarkable amount of conformational flexibility owing to the intrinsically disordered tether region of the PKA regulatory subunits (*52*). This tether restricts the catalytic subunit to space within ~16nm of the AKAP-PKA interface. Truncation of the tether was shown to increase substrate phosphorylation relative to phosphorylation with the WT tether length. It was further demonstrated that following stimulation with the β-adrenergic agonist isoproterenol, the catalytic subunit remains within the AKAP complex. These results suggest that the tether physically constrains PKA to the location of the substrate during phosphorylation and that the structure of the tether is an important determinant of substrate phosphorylation. Importantly, these findings suggest that scaffolding of PKA to substrates by AKAP may not function as currently hypothesized.

Using a computational approach, we sought to provide a mechanistic explanation for the results of Smith *et al* by determining how tether length and flexibility are able to affect phosphorylation. Additionally, we aimed to investigate the effect of releasing the catalytic subunit on the rate of substrate phosphorylation in order to demonstrate whether or not the current hypothesis regarding AKAP function is reasonable. We used Langevin Dynamic (LD) simulation to explore the effect modulating the length and flexibility of the PKA

tether region on phosphorylation of AKAP complex bound substrate. Our work demonstrates that shorter and more flexible tethers allow the catalytic subunit to interact with its substrate more often, resulting in higher rates of phosphorylation. Furthermore, our simulations of catalytic release from the AKAP complex demonstrate that anchoring PKA to its substrate does not reliably direct the catalytic subunit to substrates within the complex if it is released from the complex. This suggests that to obtain the substrate specificity seen in multiple experimental models, PKA must retain its holoenzyme conformation. Our findings strongly support emerging evidence that the PKA catalytic subunit is retained within the AKAP-PKA complex. Interestingly, the same mechanism that explains substrate specificity of the AKAP complex also seems to confer high catalytic efficiency, helping to explain the observation that AKAPs increase the speed of substrate phosphorylation (*26*). This work lends new meaning to the idea of local concentration that better explains the ability of AKAPs to control substrate specificity.

Methods

Langevin Dynamic Modeling

LD simulations were carried out using *Langdyn*, novel software written by Dr. Paul Michalski. *Langdyn* is an appropriate modeling platform when the molecules in the system can be described in a coarse-grained manner as a set of biochemically distinct spherical sites connected by stiff links. The AKAP-PKA complex is well described in this manner. Models that seek to describe finer details, such as the motion of individual amino acids, are more appropriately simulated with molecular dynamics, while models with less detail will run faster with other solvers.

Molecules are constructed in the graphic user interface in a three-step process. First, the *types* of sites in the molecule are defined. For the AKAP-PKA complex, there are five types of sites: an anchor, which is necessary for linking molecules to a membrane, substrate, AKAP_R (AKAP bound to the regulatory subunit dimer), R_C (regulatory subunit bound to the catalytic subunit), and flex links that allow us to modulate flexibility of the regulatory subunit tether. Each type can possess an arbitrary number of internal states, which can be associated with a set of biochemical reactions (reactions are described below). For example, substrate is assigned two states, unphosphorylated and phosphorylated. Each type also has an associated physical size, diffusion constant, and color (for visualization purposes).

Secondly, *sites* are added to the molecule, and each site is assigned one of the previously defined types. To construct the AKAP-PKA complex we add a minimum of seven sites: an anchor, substrate, AKAP_R, two flex links, and two R_C. Physically, sites are modeled as impenetrable spheres in order to accurately capture excluded volume effects.

Lastly, *links* are added to connect the sites to each other. Each site can be linked to an arbitrary number of other sites in either two or three-dimensions. The only requirement is that sites cannot overlap. Links are stiff and thus define an inter-site distance, but are free to rotate around the sites. For example, a triangular molecule with three sites will not maintain its geometry in the simulation with only two links, but will if a third bond is added to enforce a distance between the two outer sites. Links are only used to control the distance between sites and do not occupy physical space, and both sites and other links are free to pass through a link. Excluded volume is only enforced by sites.

Geometry

Langdyn currently only supports a rectangular geometry with reflecting boundary conditions. The rectangular geometry is partitioned into an extra-cellular space, a planar membrane, and an intracellular space. The size of the membrane and the depths of the intra- and extra-cellular spaces are user defined. Future versions of Langdyn will support a wider variety of geometries.

Particle Motion: Diffusion and Constraints Due to Binding

Particle motion is influenced by two classes of forces: random forces that lead to diffusional motion, and inter-particle forces that impose the constraints from intra- and inter-molecular bonds. These forces are incorporated in the over-damped Langevin equation (1) (*99*),

$$(1) \quad \zeta \vec{v} = \vec{F}_{\text{rand}} + \vec{F}_{\text{bonds}}$$

where ζ is the coefficient of viscous friction, $\vec{v}$ is the particle velocity, and $\vec{F}_{\text{rand}}$ and $\vec{F}_{\text{bonds}}$ represent the random forces and the total force of bonds. The random forces are guaranteed to recapitulate the desired diffusion provided they are chosen from normal distribution with variance

$$(2) \quad \langle \vec{F}_{\text{rand}}(t) \cdot \vec{F}_{\text{rand}}(t') \rangle = 2 n_d D \zeta^2 \, \delta(t - t')$$

where D is the desired diffusion coefficient, n_d is the dimension of the system (here $n_d = 3$), and the delta function simply states that the random force is uncorrelated in time. The bonds are modeled as stiff springs,

$$(3) \quad \vec{F}_{\text{bonds}} = \sum_i k_i \left(r_i - r_{0,i} \right) \hat{r}_i$$

where the sum runs over all bonds, k_i is a spring constant, $\hat{r}_i$ is the unit vector pointing from the particle to the neighbor with which it shares a bond, r_i is the current inter-particle distance, and $r_{0,i}$ is the equilibrium bond distance. The exact value of the spring constant is not important, provided the spring is stiff enough to keep sites near the expected distances but not so stiff that accurate motion requires unreasonably small time steps. In Langdyn all bonds have a spring

constant that allows us to use time steps on the order of 1 to 100 ns for biologically relevant diffusion constants.

Reactions

Zeroeth-order. Langdyn supports particle creation reactions, which are often used to buffer the concentration of a species. Given a macroscopic creation rate, k_{create}, with units μM/s, a single molecule is added to the system at each time step with probability $k_{\text{create}}Vdt$, where V is either the intra- or extra-cellular volume depending on the location of the molecule.

First-order. Langdyn supports two general types of first order reactions, both of which are described by a reaction rate, r, with units s^{-1}, and which occur at each time step with probability rdt. These are: 1) Bond dissociation reactions. When a dissociation reaction occurs the bond is simply removed from the system. 2) Internal state transitions. These describe the transitions between the internal states of each site, as defined by the type of that site. The probability of these transitions can depend on the identities of binding partners or the states of other sites in the same molecule. The former dependency would be used to prevent a transition from an unphosphorylated to a phosphorylated state unless the site is bound to a kinase. The latter dependency can be used to model allosteric interactions.

Second-order. Langdyn supports binding reactions between two sites. A bond is modeled by the creation of a new link between the reacting sites. The link

modeled identically to the links which hold molecules together, except it has an associated off rate which controls molecular dissociation. Particle-based simulations often use the Smoluchowski approach (*100*) to model bimolecular reactions, but such an approach is incompatible with excluded volume. Instead, we modified the approach described in Ref. (*101*) to account for excluded volume. Each site is associated with two radii, the physical radius, ρ_i (i=1,2), which is defined in molecule construction and enforces excluded volume, and a slightly larger reaction radius, R_i. Two reactive sites undergo a binding reaction with probability $\lambda\, dt$ per time step when their reaction radii overlap. The reaction rate λ is related to the macroscopic on rate, k_{on}, with units of $\mu M^{-1}s^{-1}$, through

$$(4)\quad k_{\text{on}} = 4\pi R D\left(1 - \frac{r_0}{R}\frac{\rho\cosh\big((R-\rho)/r_0\big) + r_0\sinh\big((R-\rho)/r_0\big)}{r_0\cosh\big((R-\rho)/r_0\big) + \rho\sinh\big((R-\rho)/r_0\big)}\right)$$

where $r_0 = \sqrt{D/\lambda}$, $D = D_1 + D_2$, $\rho = \rho_1 + \rho_2$, and $R = R_1 + R_2$.

The AKAP-PKA complex model consisted of a single molecule composed of five types with a structure based on the published geometry of the complex as detailed in the results (*52*). For each model variant, a 1sec simulation of a single complex in a 50nm^3 volume was run 500 times on a high performance computing cluster. The phosphorylation state of the complex was recorded at 10ms intervals yielding 100 data points per simulation.

Data reduction and analysis

Data reduction and analysis was performed using custom scripts written in Python using the SciPy library. To determine the characteristic time of binding or phosphorylation, 500 runs of a single model were grouped into sets of 50 runs and the average for the unbound or unphosphorylated state was taken at each time point. Since there is only 1 molecule per simulation, this produces an exponential decay from 1 to 0 as the average state of the molecule transitions from completely unbound or unphosphorylated to completely bound or phosphorylated. The resulting 10 sets of averaged data produced from the 500 runs were then fit with a single exponential model (Eq. 5), where y is the average value of the state, b is the inverse of the characteristic time of binding or phosphorylation, and t is time.

$$(5)\ y = e^{-b*t}$$

The mean and standard deviation of the characteristic times for the 10 sets of averaged data are reported.

To determine the average time spent in the bound state for a given set of simulations, the total number of data points in which the complex existed in a bound state was determined for each run. The time spent in the bound state was then averaged for all 500 simulations of a particular model. The mean and standard deviation are reported for each model variation.

Analytical Prediction of Phosphorylation Rate

Expected catalytic rates for PKA were calculated using the standard Michaelis-Menten equation (Eq. 6), where V is reaction velocity (mm/s), k_{cat} is the catalytic rate (s^{-1}), Km is the Michaelis constant (mM), and [E] and [S] are the enzyme and substrate concentrations (mM) respectively.

$$(6)\ V = \frac{k_{cat}[E][S]}{Km + [S]}$$

This model of ensemble enzymatic reactions has been shown, both theoretically and experimentally, to hold for single molecule reactions (*102*, *103*). The Michaelis constant was calculated from the following equation (Eq. 7), where kcat is the catalytic rate and kf and kr are the reverse and forward rate constants for the binding of enzyme to substrate.

$$(7)\ Km = \frac{k_r + k_{cat}}{k_f}$$

Since the volume accessible to the catalytic subunit is limited by the tether length (distance from center of the AKAP_R subunit to center of RC), the concentrations of E and S were adjusted to a spherical volume with a radius equal to the tether length. Given the adjusted concentrations and known k_{cat}, k_f and k_r, we determine V (μM/s). The reaction velocity is then converted to catalytic rate by dividing through by the adjusted enzyme concentration.

Results

Modeling the AKAP-PKA complex

Simulation of substrate phosphorylation within the AKAP-PKA complex is a multifaceted task that necessitates accounting for structural details in addition to standard reaction kinetics. Such structural detail generally falls within the realm of molecular dynamics simulation; however, this method is very computationally expensive and would not be appropriate given the time-scales of the binding and phosphorylation reactions in question. Similarly, stochastic simulation of this reaction network could be accomplished using a tool like Smoldyn. Yet, this method does not account for space filling of molecules and the spatial resolution of this type of modeling would be pushed to its absolute limits. Our novel simulation software takes advantage of Langevin Dynamics (LD) to provide a meso-scale modeling platform that accounts for coarse-grained structural details and is capable of simulating the AKAP-PKA complex with the appropriate spatial resolution.

In the LD software, molecules are constructed from spheres or *sites* of a particular type and springs or *links*. Our model of the AKAP-PKA complex is constructed of 5 molecular *types*: anchor, substrate, AKAP_R, linker, and RC (Fig 4.1A). The geometry of the AKAP complex is based upon the 3D reconstruction from Smith *et al* (*52*). In order to link the molecule to the membrane it is necessary to include an anchor, which represents the membrane insertion of our target substrate. The interface of AKAP with the

A

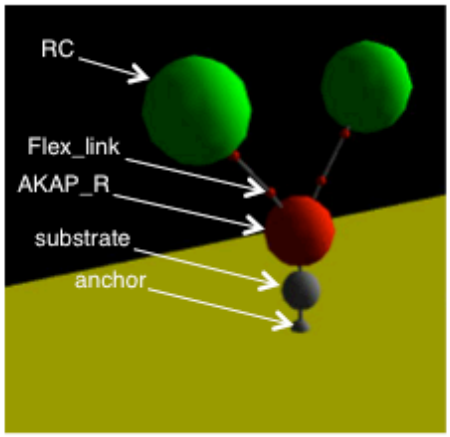

B

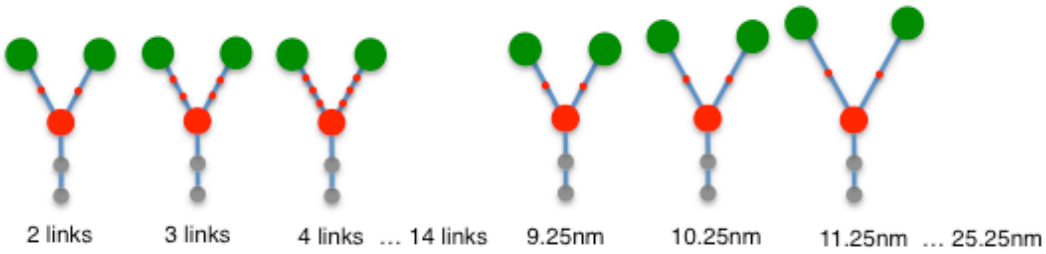

C

Type	Radius (nm)	Diffusion Coefficient (μM/s²)
Anchor	1.0	0.011
Substrate	2.0	0.011
Linker	0.1	3.0
AKAP_R	3.5	0.011
RC	4.625	3.0

Bind Only

RC + substrate ⟶ RC_substrate	kf 10mMs^{-1}	kr 0 s^{-1}

Bind No Phosphorylation

RC + substrate ⟷ RC_substrate	kf 10mMs^{-1}	kr 350 s^{-1}

Bind and Phosphorylate

RC + substrate ⟷ RC_substrate	kf 10mMs^{-1}	kr 350 s^{-1}
RC_substrate ⟶ RC_phosho_substrate	kcat 21s^{-1}	
RC_phosho_substrate ⟶ RC +phospho_substrate	kf 1000mMs^{-1}	

Figure 4.1 Langevin Dynamic Model of the AKAP-PKA complex. A) Structure of the AKAP-PKA complex with labeled site types. B) A total of 190 model variants were created that vary in both flexibility (left) and length (right). C) Model Parameters. Characteristics assigned to each site type (above) and kinetic parameters of each reaction network (below).

dimerization/docking domain of the PKA regulatory subunits is represented by AKAP_R, and the catalytic subunit bound to the inhibitory domain of the regulatory subunit is represented by RC. The diffusion rates of the molecule types are based upon standard rates for cytosolic and membrane bound proteins. The diffusion rate of GFP in chinese hamster ovary cells has been measured at 27μm^2/s (*104*). Although our diffusion coefficient for RC is roughly one order of magnitude less than that of GFP, simulations with diffusion coefficients varying from 3-15μm^2/s show no effect on the characteristic time of phosphorylation (data not shown). Diffusion rates for transmembrane proteins are generally less than 0.1μm^2/s. Since links between sites are stiff, we create flexibility in the link between AKAP_R and RC by adding dummy sites called flex links. By increasing the number of links in the tether, we are able to increase the flexibility. To simulate the effects of tether length and flexibility on the rate of substrate phosphorylation, we created a series of models in which the total length of the tether (center of AKAP_R to center of RC) is varied as well as the number of link segments (Fig 4.1B). A total of 190 model variations were created with lengths varying by increments of 1nm from 9.25m to 25.25nm, and flexibility ranging from a minimum of 2 link segments to a maximum of 14 link segments. For shorter tether lengths, the maximum number of link segments is limited by the number of flex link sites that could be fit within the tether length. The properties assigned to each site type as well as the kinetics of the simulated reactions are outlined in

figure 4.1C. The reaction kinetics are based on electronic measurements of single-molecules catalysis by PKA (*105*).

AKAP-PKA complexes with shorter more flexible tethers display faster characteristic times of enzyme-substrate binding and spend more time in the bound state on average

Phosphorylation of substrates by PKA occurs in a multi-step process involving binding of both ATP and substrate prior to catalysis. Due to the high cellular concentration of ATP, it is reasonable to model this process in two steps: 1) binding of PKA and substrate, 2) phosphorylation of substrate. Given that the catalytic rate of PKA is unlikely to be altered by the structure of the tether, we hypothesized the any changes in the apparent rate of catalysis would be driven by altered binding of the catalytic subunit with its substrate.

We first examined the characteristic time of binding (CTB), defined as the time from simulation start to the first binding event (Fig 4.2A). For this set of simulations, only the forward binding reaction was included (Fig 4.1C). CTBs varied from a minimum of 0.445ms ±0.078 to a maximum of 3.812ms ± 0.563. In general, shorter and more flexible tether lengths displayed faster CTBs. The effect of varying tether length is most dramatic for the least flexible model variations, while there is virtually no difference in the CTB with change in length for the most flexible model variations. Similar trends are seen with changes in

flexibility at the extremes of the model variations. Changes in tether flexibility affect CTB least for short tether lengths and most for longer tether lengths.

Since the catalytic rate of PKA ($21s^{-1}$) is much slower than k_r for binding of catalytic to substrate ($350s^{-1}$), binding and unbinding of the catalytic subunit and substrate is expected to occur multiple times prior to phosphorylation on average. Model variations allowing catalytic and substrate to exist in a bound state for a greater fraction of total simulation time were hypothesized to have an increased probability of substrate phosphorylation and hence faster characteristic times of phosphorylation (CTP). We determined the average fraction of time spent in the bound state (FTB) by simulating binding and unbinding of catalytic subunit and substrate without allowing substrate phosphorylation (Fig 4.1C). The average FTB ranged from 0.415 ±0.05 to 0.847 ±0.043 with variations following the same trends as for characteristic times of binding (Fig 4.2B). Since the k_f and k_r remain unchanged for all model variations, the differences in the FTB must result from a change in the apparent forward rate of binding.

Increases in apparent k_f of binding and average time spent in the bound state translate to decreases in characteristic times of phosphorylation

The variation in the CTBs and FTBs suggested that changes in the tether length and flexibility were likely to affect substrate phosphorylation. Model variations displaying an increased FTB were expected to display shorter CTPs because this should increase the probability of phosphorylation. We determined the CTP by simulating binding and unbinding of the catalytic subunit to substrate,

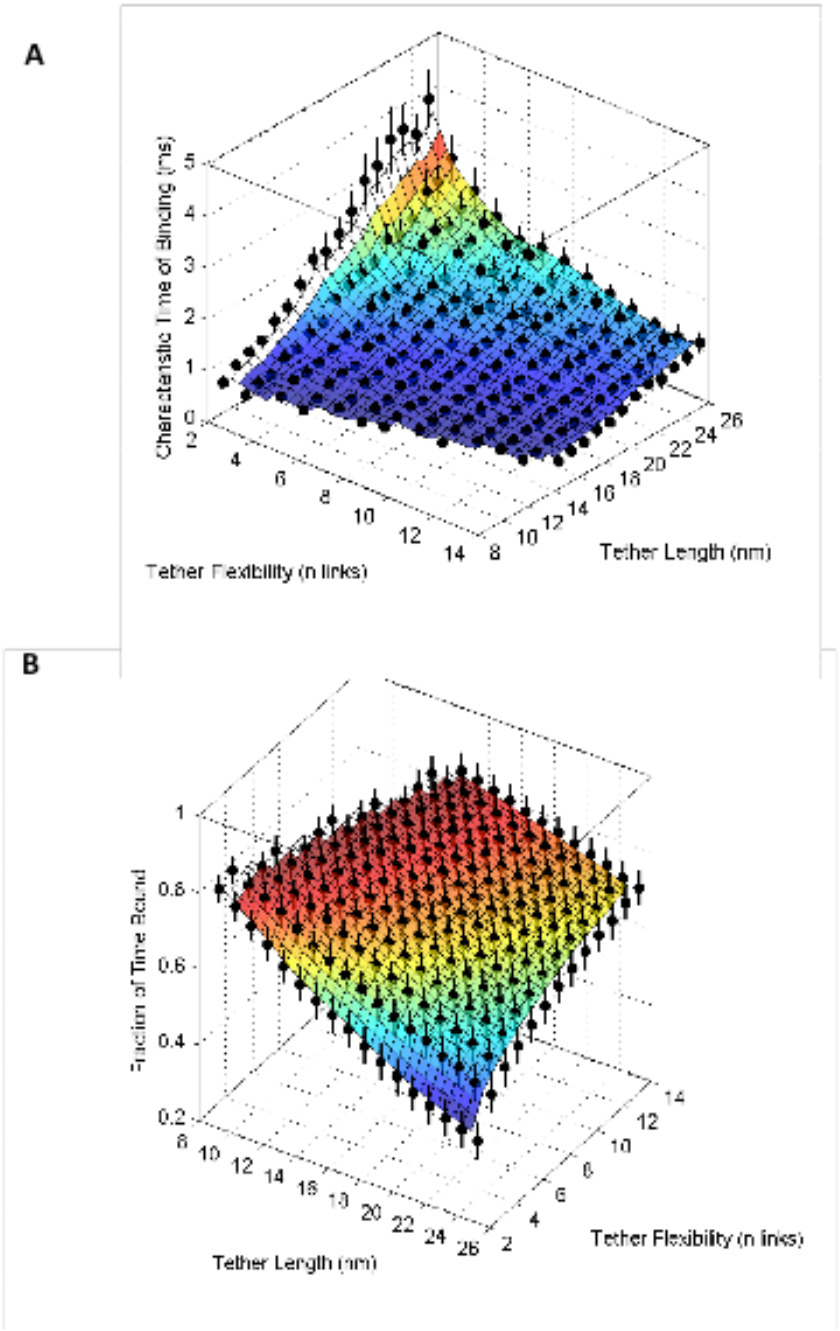

Figure 4.2 Tether length and flexibility modulate binding of the catalytic subunit to substrate. A) Characteristic times of binding with varied tether length and flexibility. Simulations were run for only the binding reaction of catalytic and substrate (no unbinding). Each data point represents the average time from simulation start to binding of catalytic and substrate for 10 sets of 50 simulations ±1SD. B) Average fraction of time that the catalytic subunit and substrate spend in the bound state. Binding and unbinding of the catalytic subunit with substrate were simulated over the course of 1s. Each data point represents the average fraction of time(s) ±1SD for 500 simulation runs.

and irreversible substrate phosphorylation (Fig 4.1C). CTPs varied from a minimum of 0.054s ±0.004 to a maximum of 0.119s ±0.012 (Fig 4.3A). As expected, the general trend was that models with shorter and more flexible tethers to displayed the fastest CTPs.

In order to verify that the CTPs predicted from the LD simulations are realistic, we used the quasi-steady state Michaelis-Menten model of enzyme kinetics to generate an analytical prediction for comparison. While the assumptions implicit in the original derivation of Michaelis-Menten kinetics are not valid for our single molecule simulations, it has been demonstrated both theoretically and experimentally that this model is a good approximation of reaction velocity even for single enzyme kinetics (*102*, *103*). In order to determine the expected CTP using the Michaelis-Menten model, we adjusted the concentrations of the catalytic subunit and substrate by considering their local concentrations to be the number of molecules within a spherical volume having a radius equal to the length of the tether. The predicted reaction velocity was then converted to a catalytic rate (inverse of CTP) by dividing by the local concentration of the catalytic subunit. The analytical predictions of CTP agree reasonably well with the LD simulation results for models with the most flexible tethers for each length (Fig 4.3B). The characteristic times of phosphorylation predicted by Michaelis-Menten kinetics are roughly twice as fast as those predicted by LD simulation. This deviation from the analytical prediction is a result of anchoring of the substrate to the membrane, which prevents its free

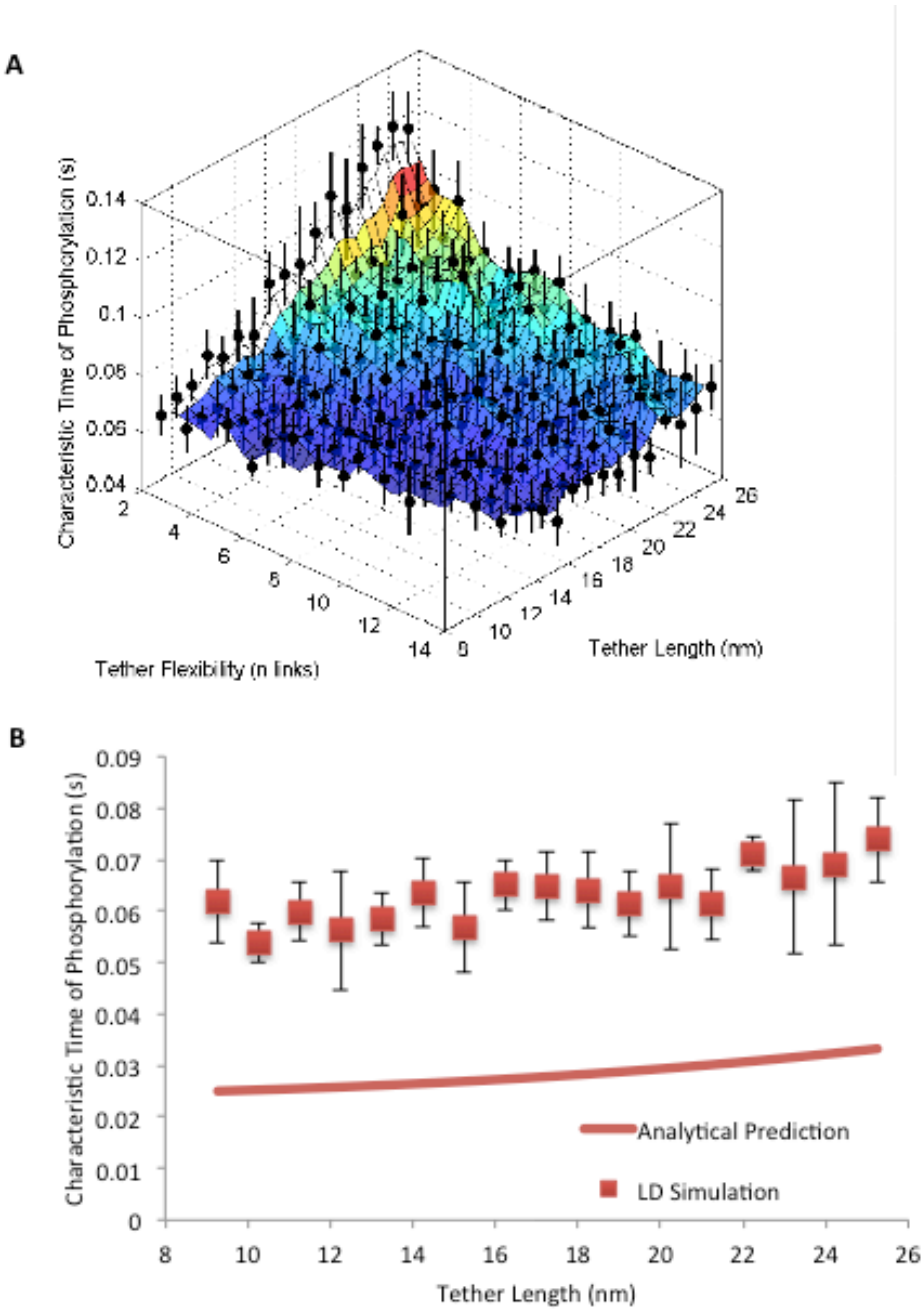

Figure 4.3 Tether length and flexibility modulate the rate substrate phosphorylation. A) Characteristic times of phosphorylation with varied tether length and flexibility. Simulations included binding and unbinding of the catalytic subunit with substrate as well as irreversible substrate phosphorylation. Each data point represents the average time from simulation start phosphorylation of substrate for 10 sets of 50 simulations ±1SD. B) Comparison of characteristic times of phosphorylation for the most flexible model variations at each length to characteristic times of phosphorylation predicted by Michaelis-Menten kinetics with adjusted concentrations of enzyme and substrate. A second set of LD simulations of the most flexible tether variations with only one catalytic subunit was run for each length for comparison to the analytical predictions.

diffusion within the same volume occupied by the catalytic subunits thereby reducing the CTP.

Release of the catalytic subunit abrogates the effect of PKA tethering for a single AKAP-PKA-substrate complex

It is well established that the primary function of AKAPs is to compartmentalize cAMP/PKA signaling. Numerous studies have demonstrated that disruption of AKAP binding to a particular substrate leads to a decrease in phosphorylation or change in the expected physiologic response (*23*, *24*, *35*). How AKAPs direct PKA phosphorylation to AKAP complex bound substrates remains unknown as the widely accepted mechanism of signaling requires the release of the catalytic subunit (*10*). In light of our findings that the structure of the regulatory subunit tether alters phosphorylation kinetics and evidence that the catalytic subunit is not released from the AKAP-PKA complex, we simulated the release of the catalytic subunit from the complex to determine its effect on substrate phosphorylation.

To simulate the effect of releasing of the catalytic subunit on phosphorylation of AKAP complex bound substrate, we removed the tether from the model and initialized the simulations with two catalytic subunits positioned within 16.25nm of AKAP_R (WT), within 5nm of the substrate (close), or randomly throughout the 50nm^3 simulation space (Fig 4.4A). Positioning of the catalytic subunits at the maximum distance from AKAP_R that could be expected for the wild type geometry lead to an average CTP of 0.193s ±0.025. Interestingly,

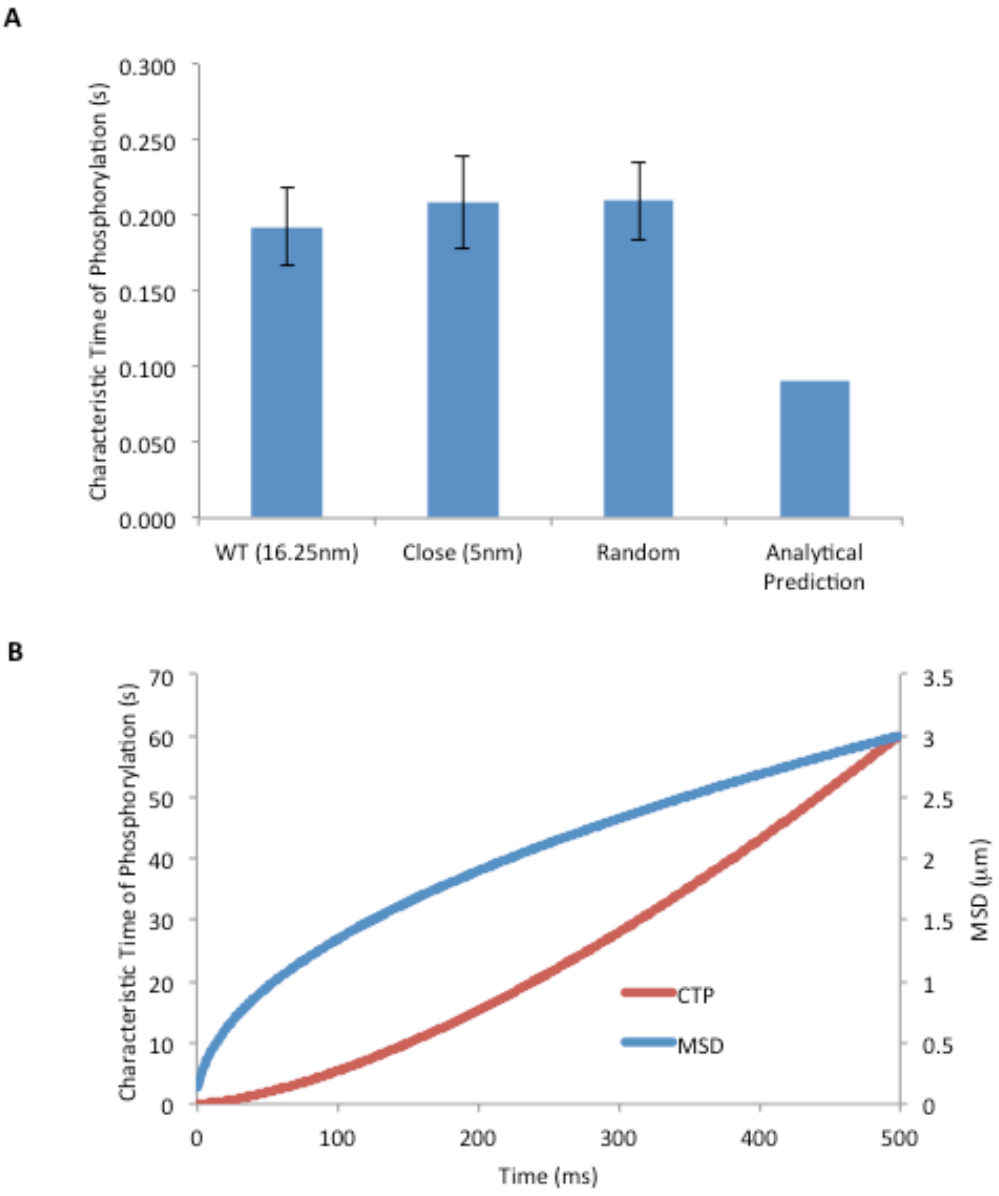

Figure 4.4 Simulation of release of the catalytic subunit from the AKAP-PKA complex. A) Release of the catalytic subunit was simulated by removing the tether from the model and initializing the simulations with the catalytic subunits positioned either 16.25nm from substrate, 5nm from substrate or randomly within the simulation space. The characteristic times of phosphorylation are compared to the analytical prediction for two catalytic subunits and a single substrate within a $50nm^3$ volume. B) Predicted change in characteristic time of phosphorylation (CTP) and mean squared distance of PKA as two catalytic subunits diffuse from their initial position within the AKAP complex.

positioning the catalytic subunits close enough to the substrate for binding to occur in the first time step of the simulation did not improve the CTP (0.208s ±0.031). Positioning the catalytic subunits within the space available to tethered PKA also did not improve the CTP compared to random positioning of the two catalytic subunits within the simulation space (0.210s ±0.026). These results suggest that anchoring of PKA to substrates by AKAP is not an effective method of directing PKA phosphorylation to the bound substrate if the catalytic subunit must be released in order for phosphorylation to occur. Regardless of how close the catalytic subunits are positioned upon release, the CTP does not differ from that of randomly placed catalytic subunits. Once released, the CTP is equal to the expected CTP for catalytic subunits with access to the entire compartment that it is located in. Even for the very small volume of our simulation space, the CTPs for catalytic release are much slower than the rates for all tether models with the WT length (min 0.059s ±0.007 to max 0.087s ±0.011).

For some cell types, like the cardiac myocyte, AKAP directs phosphorylation to substrates that are distributed throughout the cytosol, thus the released catalytic subunit is not confined to a small compartment as in our LD simulations. In this case, the CTP for the substrate that the catalytic subunits were initially tethered to would decrease rapidly due to diffusion away from the initial location. Using our Michaelis-Menten analytical method, we predicted the change in the CTP over time as the catalytic subunits diffuse away from their initial position (Fig 4.4B). The change in concentration of catalytic subunit over

time was determined for a spherical volume with a radius equal to the mean squared displacement (MSD) of the catalytic subunit (Eq. 8).

$$(8)\ MSD = \sqrt{6Dt}$$

Once released, the catalytic subunit quickly diffuses away resulting in a drastic increase in the CTP (Fig 4.4B). The increase in CTP is such that after a few ms it would be unreasonable to expect that the catalytic subunit would return to its initial location and phosphorylate the AKAP bound substrate. Importantly, this demonstrates that outside of a small compartment like the dendrite of a neuron, release of the catalytic subunits from the AKAP-complex would be even less effective at achieving phosphorylation of complex bound substrates than for our small volume LD simulations.

Discussion

The importance of AKAPs in compartmentalization of cAMP-PKA signaling has been well demonstrated (*23*, *24*, *35*). It is now widely accepted that AKAPs not only tether PKA to a particular substrate, they also co-localize with other signal effectors like adenylate cyclase and phosphodiesterase, thereby acting to coordinate a signaling microdomain (*29*). Even though great progress has been made in our understanding of the spatial coordination of signaling components by AKAPs, how these AKAP complexes operate at the single molecule level remains poorly understood. While AKAPs are named for their ability to direct PKA phosphorylation to a particular substrate, we still do not have a molecular

mechanism to explain how this occurs. This phenomenon is further complicated by years of evidence suggesting that activation of PKA requires the release of a freely diffusible catalytic subunit. However, recent evidence suggests that in the cell, the catalytic subunit is capable of phosphorylating AKAP complex bound substrates without being released (*50*, *52*). It has been further demonstrated that structure of the PKA regulatory subunit tether is an important determinant of substrate phosphorylation.

We used Langevin Dynamic simulation of the AKAP-PKA complex to further explore the contribution of the structure of the PKA regulatory subunit tether to substrate phosphorylation with the hope of gaining additional mechanistic insight into the function of the AKAP-PKA complex. Our work first demonstrates that modulation of the tether length and flexibility changes the CTB between the catalytic subunit and substrate, with shorter and more flexible tethers tending to have faster CTBs (Fig 4.2A). The change in CTB, resulting only from alterations in tether structure, modulates the fraction of time that catalytic subunit and substrate spend in a bound state (Fig 4.2B). This translates into changes in the CTP, with models having higher FTBs showing decreased CTPs (Fig 4.3A). Since our primary interest is to understand how AKAPs direct PKA phosphorylation to AKAP bound substrates we also simulated how the release of the catalytic subunit from the complex affects phosphorylation. Positioning of the catalytic subunits within the space available to the WT tether length does not result in CTPs that are significantly different from those positioned randomly

throughout the simulation space, indicating that AKAPs do not effectively direct PKA phosphorylation to AKAP bound substrates if the catalytic subunits are released (Fig 4.4A). We further demonstrate that in a large compartment like the cytosol, release of the catalytic subunit from the AKAP complex would lead to its quick diffusion away from the anchored substrate without phosphorylation (Fig 4.4B). The results of our simulations suggest that in the cell the catalytic subunit is likely not released, as this would lead to a significant decrease in the efficiency of phosphorylation of AKAP complex bound substrates.

The decreased CTB and increased FTB for shorter tether lengths reflect an increased apparent forward rate of binding. Since the rate constants (k_f and k_r) remain the same for all model variations, the changes in the apparent forward rate indicate that the structure of the tether influences the probability of interaction of the catalytic subunit with its substrate. As the regulatory subunit tether is shortened, the space available to the catalytic subunit decreases, thereby increasing the probability that it will encounter and bind to the substrate as long as the substrate remains accessible. The increased probability of interaction has previously been interpreted as resulting from an increase in the local concentration of the catalytic subunit. While this interpretation allows us to easily predict the CTP via the Michaelis-Menten model, the changes in CTB, FTB, and CTP result from differences in structure, not concentration, and thus are more correctly thought of as changes in apparent forward rate constant. The flexibility of the tether likely modulates accessibility of the space within the

spherical volume defined by the tether length. For lengths that allow access to substrate in the most extended conformation, flexibility has little impact on CTB or FTB. With longer tethers that must deform in order to reach the substrate, changes in flexibility have much more impact on the CTB and FTB (Fig 4.2). Although differences in the regulatory subunit tether length are only expected with interspecies variation, positioning of substrates within the AKAP complex does vary and would affect rates of interaction similarly. One potential caveat to bear in mind is our inability to account for rotational conformation. In reality, phosphorylation of substrates by the catalytic subunit would require precise alignment of the catalytic cleft with the substrate. It may be possible that a certain degree of tether stiffness could actually facilitate phosphorylation by maintaining proper alignment of the catalytic subunit and substrate.

Changes in the CTP with tether length and flexibility are most likely driven by changes in the apparent forward rate of binding. Although the idea of a local concentration offers a simple method for analytical prediction of the CTP, the actual concentration of the catalytic subunit and substrate do not change. Considering the changes CTB and FTB as resulting from changes in apparent k_f rather than concentration offers interesting insight into the changes in CTP and, more generally, the function of AKAPs. Increasing the k_f of the binding reaction results in a decrease in the Michaelis constant (Methods Eq. 7), which translates into an increase in the velocity of the phosphorylation reaction according the Michaelis-Menten model (Methods Eq. 6). Interestingly, such change in the Km

also suggests that the efficiency of phosphorylation is improved according to the following equation (Eq. 9), where E is catalytic efficiency:

$$(9)\ E = \frac{k_{cat}}{Km}$$

This interpretation of the change in CTP resulting from changes in tether structure is a previously unconsidered, but incredibly important advancement in our understanding of the function of AKAPs. It suggests that AKAPs don't simply increase the speed or magnitude of phosphorylation by increasing local concentration of PKA, rather AKAPs increase the efficiency of phosphorylation of the AKAP complex bound substrate.

The increase in efficiency of phosphorylation of AKAP bound substrates is best illustrated by comparing the CTPs of tether models with those from our models of catalytic release. For models involving catalytic release, the CTP is at minimum 2.5-fold slower than the slowest tether model. Given the small size of our simulation space and our evidence that the rate of substrate phosphorylation depends on the size of the compartment for free catalytic subunit, the increase CTP is likely to be much more dramatic for most AKAP-PKA signaling systems in the cell.

Our new hypothesis regarding the function of AKAPs also offers some interesting interpretations of old data. While the definition of local concentration of PKA in the previous hypothesis is somewhat ambiguous, we will define it as concentration of PKA within the compartment of the AKAP-PKA complex.

Experiments in which AKAP-substrate binding has been disrupted demonstrate a reduction in phosphorylation of the intended substrates (*24*, *27*). While this was attributed to de-localization of PKA and hence, a decrease in local concentration, our evidence indicates that such delocalization would also occur upon activation of PKA if the catalytic subunit is released from the complex in order for phosphorylation to occur. The effect of tethering the catalytic subunit to its target is even better demonstrated through the use of the FRET sensor AKAR (A Kinase Activity Reporter 2), which measures PKA phosphorylation real time in cells (*25*). Addition of the PKA binding site to the AKAR2 construct resulted in FRET signal changes following stimulation that were both faster and of higher magnitude when compared to AKAR2 alone (*26*). Since AKAR2 with or without the addition of the PKA binding site is localized only to the cytosol, it is not reasonable to assert that there is difference in the local concentration of PKA. The sensor is located in the same compartment in both cases and we are not forcing redistribution of PKA to a larger space by preventing AKAP localization to a particular substrate. Our hypothesis that AKAPs increase the efficiency of AKAP complex bound substrate phosphorylation fits very well with this data. Our simulation data suggests that the increased rate of phosphorylation, and likely the increased magnitude, is what should be expected. Interestingly, we find that the kinetics of phosphorylation for released catalytic subunit are too slow to mediate some signal processes known to require PKA. The time scale of PKA mediated effects on Na^{2+} channels occur on the order of milliseconds, which

according to our LD simulations occurs too quickly to be mediated by the catalytic subunit if released from the complex (*36*).

Computational analysis of the AKAP-PKA complex using our novel software, *Langdyn,* has led to numerous exciting findings. First, we offer a mechanism for the changes in phosphorylation rate seen with alteration in the structure in regulatory subunit tether. Second, we present evidence that release of the catalytic subunit would likely abrogate the effect of tethering PKA to a particular substrate. This evidence suggests that for efficient substrate phosphorylation to occur, the catalytic subunit cannot be released. This change in the mechanism of phosphorylation also provides us with a partial molecular mechanism that explains how AKAPs might direct PKA phosphorylation to AKAP complex bound substrates. Finally, we propose an improvement to the hypothesis that AKAPs increase the speed and magnitude of substrate phosphorylation by increasing local concentration. We hypothesize that AKAPs act to increase the efficiency of PKA phosphorylation and suggest that local concentration should be thought of as the amount of enzyme and substrate within a volume defined by the length of the regulatory subunit tether, rather than within a local region or compartment within the cell. This revision of the AKAP hypothesis represents a critically important step forward in our understanding of PKA signaling.

Chapter 5

Conclusions

Since its discovery in 1958 by Sutherland and Rall, much progress has been made in our understanding of cAMP signaling. We know that cAMP is produced by adenylate cyclase (AC) following activation of G-protein coupled receptors (GPCRs) at the cell surface, that the rise in cAMP concentration activates signal effector proteins like PKA, exchange protein directly activated by cAMP (Epac), and cyclic nucleotide-gated channels, and that this signal is terminated by phosphodiesterases (PDEs) that degrade cAMP. It is understood that although many different GPCRs use cAMP and PKA to convey their signals, this signaling system is compartmentalized primarily through the ability of A-kinase anchoring proteins (AKAPs) to tether PKA to a particular substrate, thus directing its phosphorylation to the intended downstream target (*106*). We have also discovered that many AKAPs are capable of binding to AC, PDE, and other signal effectors, thereby allowing AKAPs to coordinate a cAMP-PKA signaling microdomain in which all of the necessary components are co-localized (29). Much of the work that has been done up to this point has focused upon identifying components of the AKAP complex and examining changes in physiology when specific components are inhibited or prevented from associating with the complex. This has lead us to think of the AKAP complex as a static entity in which all of the components necessary for signaling are always present in the complex, or at least in a vaguely defined compartment of the target substrate.

The work presented here forces us to think of the AKAP complex in new ways that represent an evolution in our understanding of the function of the

AKAP complex. In chapter two, I demonstrated that AKAP7γ is able to bind to itself, forming a dimer that has the potential to augment PKA phosphorylation. This indicates that in addition to other complex components being present or not, the stoichiometry of the AKAP complex is important and impacts the function of the complex. In chapter 3, I showed that AKAP7γ binding to PLB is phosphorylation-state dependent and that this state dependent mode of binding allows small quantities of the AKAP complex to control phosphorylation of large quantities of substrate. This work indicates that the AKAP complex is likely not a static entity in which AKAP binds to the necessary signal components, recruits them to a particular substrate, and remains in a stable complex. The AKAP complex is more likely a dynamic structure that may change composition continually due to binding and unbinding of components, or may change as a result of certain signaling events as we see with the AKAP-PLB interaction. Finally, in chapter 4, I added to the accumulating evidence that suggests the PKA catalytic subunit does not dissociate from the AKAP complex to phosphorylate its substrates. This work also demonstrates the importance of the structure or topology of the AKAP complex. While I demonstrated that the structure of the PKA regulatory subunit tether alters rates of phosphorylation, AKAPs themselves are also flexible structures that may allow for positional variation in phosphorylation rates of some AKAP complex components. Overall, this work is an important step forward towards understanding how AKAP complexes function.

In the following sections I present some final commentary on each of the chapters and discuss the potential for future work.

AKAP7γ Oligomerization augments PKA signaling

This chapter represents my earliest work and deserves some re-interpretation in light of the results presented in chapter 4. While I remain convinced of the ability of AKAP7γ to form dimers, and potentially higher order oligomers that were undetectable by PCH, I no longer believe that release of the catalytic subunit is necessary for PKA to phosphorylate its AKAP bound substrates. The mechanism of the feed-forward loop that defines activation and release of the catalytic subunit was partly a mechanism for dealing with the reported high cellular concentration of cAMP (1μM) and very high affinity of the regulatory subunit for cAMP. In my initial attempts to model the AKAP complex, controlling the activation and release of PKA was problematic. This was primarily due to the fact that the published kinetics defining activation and release led either to very high baseline activity of PKA, or conversely, made it very difficult to get an appropriate response to stimulation of β-adrenergic activity. Evidence presented by Martin et al suggested that auto-phosphorylation of the regulatory subunit was necessary for the release of catalytic, which provided us with a potential way to deal with the problematic activation/release kinetics (*51*). With the kinetics that required higher levels of cAMP for activation of PKA, requiring auto-phosphorylation of the regulatory subunit for release of the catalytic subunit

generated a feed-forward loop that gave an appropriate response to stimulation, and also demonstrated that oligomerization of AKAP7γ could potentiate increases in substrate phosphorylation. This hypothesis is still valid if one does not accept the emerging evidence that the catalytic subunit is not released from the AKAP complex in the cell.

Alternatively, if the catalytic subunit is not released from the oligomeric AKAP complex, the accelerated kinetics and increased magnitude of phosphorylation would depend on the topology of the complex and accessibility of each of the catalytic subunits to the complex bound substrate(s). Since PKA is also known to alter the activity of other potential components of the complex including AC, PDE, and PP1, the presence of multiple catalytic subunits in an oligomeric complex could also impact phosphorylation via regulation of cAMP production and degradation, or alteration in substrate dephosphorylation kinetics. We did not find this to be the case with our current version of the AKAP7γ oligomer model. However, a thorough investigation of the impact of oligomerization for an AKAP complex in which the catalytic subunit is not released would require construction of an entirely different model.

To continue this work, the effect of oligomerization of AKAP7γ on substrate phosphorylation in live cells needs to be demonstrated. The most direct way to assess this is to disrupt oligomerization in the cell and examine the levels of substrate phosphorylation pre and post β-adrenergic stimulation. While this could be done easily by generating a deletion mutant lacking the self-association sites,

these sites overlap with regions that would impact binding of other AKAP complex components, including PKA. Though difficult, it may also be possible to design reagents that could disrupt oligomerization. Similar to the design of Ht31, which dissociates PKA from AKAPs (*19*), short peptides mimicking the self-association sites may have a higher affinity for AKAP7γ than itself, resulting in the disruption of oligomerization. Alternatively, the impact of having multiple PKA molecules in the same complex could be assessed by creating a series of AKAR sensors linked to varying numbers of PKA binding sites.

Phosphorylation-state dependent interaction between AKAP7δ/γ and phospholamban increases phospholamban phosphorylation

This work provides an answer to a long standing and important question in the field of AKAP and cardiac biology: how does a protein like AKAP7γ, which is present in the cell at low concentration, control phosphorylation of a high concentration, widely dispersed protein like PLB or troponin. Additionally, this work also revives the importance of the AKAP7γ-PLB interaction, which has not been published on since 2012 when Jones et al suggested that it does not regulate PLB phosphorylation (*90*). While the computational model presents compelling data demonstrating that phosphorylation-state dependent binding of AKAP7γ with PLB greatly increases the magnitude of phosphorylation by AKAP7γ bound PKA, the next logical step for this work is to demonstrate this phenomenon experimentally. The phosphorylation state dependence of AKAP7γ

binding to PLB suggests that the complex should be highly mobile in response β-adrenergic stimulation. This mobility should be demonstrable via fluorescence resonance after photobleaching (FRAP). Comparison of the mobility of a GFP tagged AKAP7γ could be made a series of cell systems containing either a non-phosphorylatable PLB (S16A), WT PLB or a phospho-mimetic PLB (S16D). In this comparison, it would be expected that AKAP7γ has the lowest mobility in the PLB(S16A) system, an intermediate mobility in the WT PLB system, and the highest mobility in the PLB(S16D) system. This phenomenon could be further explored by examining the mobility of AKAP7γ-GFP in rat neonatal cardiac myocytes, which express endogenous PLB, pre and post β-adrenergic stimulation.

The phosphorylation state dependence of AKAP7γ-PLB binding also highlights the possibility that other AKAP binding partners also have state dependencies. Though controversial, evidence does exist that the affinity of RIIα for the PKA binding domains of AKAP7, mAKAP, and AKAP-Lbc is altered by RIIα phosphorylation (*107*). Similar changes in affinity following phosphorylation may exist for other AKAPs and their substrates, as well as for other binding partners like AC, PDE, etc. Such findings would be a clear indication that AKAP complexes are highly dynamic structures.

Langevin Dynamic Simulation of AKAP-PKA Complex: Re-envisioning the local concentration mechanism for directing PKA phosphorylation

The work presented in chapter 4 is certainly the most controversial, but also has the most exciting implications. The ability of the AKAP-PKA complex to retain the catalytic subunit following stimulation of cAMP production provides a very clear molecular mechanism that explains not only how AKAPs are able to compartmentalize cAMP-PKA signaling, but also indicates that the purpose of AKAPs is likely to enhance the efficiency of phosphorylation specific PKA. As is the case with most scientific progress, this work leads us to ask nearly as many questions as it answers. If the catalytic subunit retains its activity while still bound to the PKA regulatory subunit, how does PKA respond to increases in cAMP? How can the catalytic subunit phosphorylate substrates if the regulatory subunit is bound via the catalytic cleft? Are there specific conditions that determine whether or not the catalytic subunit is released? Unfortunately many of these questions are unlikely to be answered soon, and will need to wait for advances in technology that have not yet occurred. The structure of the entire PKA complex has yet to be solved due to the high degree of flexibility of the tether region. To capture the conformational changes in the catalytic subunit during a signaling event, within the AKAP complex, and in the cell would be an incredibly difficult task.

The most important follow up on this work is to demonstrate in a live cell whether or not the catalytic subunit is released in response to β-adrenergic

stimulation. This can be accomplished via total internal reflectance fluorescence-single particle tracking microscopy (TIRF-SPT). By tagging the catalytic subunit with a photo-switchable fluorophore like mEOS, we can image the population of mEOS-catalytic that is recruited to the cell membrane by AKAP and track the number of catalytic subunits at the membrane over time, in the presence and absence of β-adrenergic stimulation. I have conducted preliminary experiments with AKAP79 demonstrating that these experiments are possible. Unfortunately, AKAP79 does not stably associate with the membrane, making interpretation of catalytic release extremely difficult. This work would be better conducted using AKAP7α, which associates with the plasma membrane via post-translational lipid modification that allows for insertion into the plasma membrane. AKAP7α should form a stable association with the plasma membrane allowing for easier tracking of mEOS-catalytic. AKAP7α also offers the additional advantage of not associating with any signal components other than PKA and the ion channels that are its target substrates, making interpretation of the data much easier. Since our preliminary experiments seem to indicate that the catalytic subunit is released in response to high concentrations (10μM) of the β-adrenergic agonist, isoproterenol, and the direct activator of adenylate cyclase, forskolin, it is important to explore the response of the catalytic subunit to lower, more physiologically relevant drug concentrations.

Concluding Remarks

Overall, this work offers a number of novel and important ideas regarding the function of AKAP complexes. I have demonstrated the importance of both stoichiometry and structure of AKAP complex components, and have shown that AKAP complexes are likely to be more dynamic than previous thought. While this work goes a long way towards answering some major questions in the field of AKAP biology, it also provides avenues for important future work.

References

1. E. W. SUTHERLAND, T. W. RALL, Fractionation and characterization of a cyclic adenine ribonucleotide formed by tissue particles. *Journal of Biological Chemistry*. **232**, 1077–1091 (1958).

2. T. W. RALL, E. W. SUTHERLAND, Formation of a cyclic adenine ribonucleotide by tissue particles. *Journal of Biological Chemistry*. **232**, 1065–1076 (1958).

3. J. F. Kuo, P. Greengard, Cyclic nucleotide-dependent protein kinases. IV. Widespread occurrence of adenosine 3“,5-”monophosphate-dependent protein kinase in various tissues and phyla of the animal kingdom. *Proc. Natl. Acad. Sci. U.S.A.* **64**, 1349–1355 (1969).

4. T. W. RALL, Introduction. **5**, 1–2 (1975).

5. T. Hamaguchi *et al.*, In vivo Screening for Substrates of Protein Kinase A Using a Combination of Proteomic Approaches and Pharmacological Modulation of Kinase Activity. *Cell Struct. Funct.* **40**, 1–12 (2015).

6. S. L. Keely, Activation of cAMP-dependent protein kinase without a corresponding increase in phosphorylase activity. *Res. Commun. Chem. Pathol. Pharmacol.* **18**, 283–290 (1977).

7. T. W. Honeyman, L. K. Levy, H. M. Goodman, Independent regulation of phosphorylase and lipolysis in adipose tissue. *Am. J. Physiol.* **237**, E11–7 (1979).

8. J. S. Hayes, L. L. Brunton, J. H. Brown, J. B. Reese, S. E. Mayer, Hormonally specific expression of cardiac protein kinase activity. *Proc. Natl. Acad. Sci. U.S.A.* **76**, 1570–1574 (1979).

9. J. D. Corbin, P. H. Sugden, T. M. Lincoln, S. L. Keely, Compartmentalization of adenosine 3':5'-monophosphate and adenosine 3“:5-”monophosphate-dependent protein kinase in heart tissue. *Journal of Biological Chemistry*. **252**, 3854–3861 (1977).

10. S. H. Francis, J. D. Corbin, Structure and function of cyclic nucleotide-dependent protein kinases. *Annu. Rev. Physiol.* **56**, 237–272 (1994).

11. R. Fredriksson, M. C. Lagerström, L.-G. Lundin, H. B. Schiöth, The G-Protein-Coupled Receptors in the Human Genome Form Five Main Families. Phylogenetic Analysis, Paralogon Groups, and Fingerprints. *Molecular pharmacology*. **63**, 1256–1272 (2003).

12. D. Sarkar, J. Erlichman, C. S. Rubin, Identification of a calmodulin-binding protein that co-purifies with the regulatory subunit of brain protein kinase II. *Journal of Biological Chemistry*. **259**, 9840–9846 (1984).

13. K. L. Dodge-Kafka, L. Langeberg, J. D. Scott, Compartmentation of cyclic nucleotide signaling in the heart: the role of A-kinase anchoring proteins. *Circulation Research*. **98**, 993–1001 (2006).

14. E. J. Welch, B. W. Jones, J. D. Scott, Networking with AKAPs: context-dependent regulation of anchored enzymes. *Mol. Interv.* **10**, 86–97 (2010).

15. N. M. Alto *et al.*, Bioinformatic design of A-kinase anchoring protein-in silico: a potent and selective peptide antagonist of type II protein kinase A anchoring. *Proc. Natl. Acad. Sci. U.S.A.* **100**, 4445–4450 (2003).

16. F. W. Herberg, A. Maleszka, T. Eide, L. Vossebein, K. TASKEN, Analysis of A-kinase anchoring protein (AKAP) interaction with protein kinase A (PKA) regulatory subunits: PKA isoform specificity in AKAP binding. *Journal of Molecular Biology*. **298**, 329–339 (2000).

17. D. W. Carr *et al.*, Interaction of the regulatory subunit (RII) of cAMP-dependent protein kinase with RII-anchoring proteins occurs through an amphipathic helix binding motif. *Journal of Biological Chemistry*. **266**, 14188–14192 (1991).

18. D. W. Carr, R. E. Stofko-Hahn, I. D. Fraser, R. D. Cone, J. D. Scott, Localization of the cAMP-dependent protein kinase to the postsynaptic densities by A-kinase anchoring proteins. Characterization of AKAP 79. *Journal of Biological Chemistry*. **267**, 16816–16823 (1992).

19. D. W. Carr, Z. E. Hausken, I. D. Fraser, R. E. Stofko-Hahn, J. D. Scott, Association of the type II cAMP-dependent protein kinase with a human thyroid RII-anchoring protein. Cloning and characterization of the RII-binding domain. *Journal of Biological Chemistry*. **267**, 13376–13382 (1992).

20. C. Rosenmund *et al.*, Anchoring of protein kinase A is required for modulation of AMPA/kainate receptors on hippocampal neurons. *Nature*. **368**, 853–856 (1994).

21. L. B. Lester, L. K. Langeberg, J. D. Scott, Anchoring of protein kinase A facilitates hormone-mediated insulin secretion. *Proc. Natl. Acad. Sci. U.S.A.* **94**, 14942–14947 (1997).

22. S. Vijayaraghavan, S. A. Goueli, M. P. Davey, D. W. Carr, Protein kinase A-anchoring inhibitor peptides arrest mammalian sperm motility. *Journal*

of Biological Chemistry. **272**, 4747–4752 (1997).

23. M. A. Fink *et al.*, AKAP-mediated targeting of protein kinase a regulates contractility in cardiac myocytes. *Circulation Research*. **88**, 291–297 (2001).

24. B. K. McConnell *et al.*, Disruption of Protein Kinase A Interaction with A-kinase-anchoring Proteins in the Heart in Vivo: EFFECTS ON CARDIAC CONTRACTILITY, PROTEIN KINASE A PHOSPHORYLATION, AND TROPONIN I PROTEOLYSIS. *Journal of Biological Chemistry*. **284**, 1583–1592 (2008).

25. J. Zhang, C. J. Hupfeld, S. S. Taylor, J. M. Olefsky, R. Y. Tsien, Insulin disrupts beta-adrenergic signalling to protein kinase A in adipocytes. *Nature*. **437**, 569–573 (2005).

26. K. L. Dodge-Kafka *et al.*, The protein kinase A anchoring protein mAKAP coordinates two integrated cAMP effector pathways. *Nature*. **437**, 574–578 (2005).

27. B. Lygren *et al.*, AKAP complex regulates Ca2+ re-uptake into heart sarcoplasmic reticulum. *EMBO Rep.* **8**, 1061–1067 (2007).

28. V. M. Coghlan *et al.*, Association of protein kinase A and protein phosphatase 2B with a common anchoring protein. *Science*. **267**, 108–111 (1995).

29. M. S. Kapiloff, M. Rigatti, K. L. Dodge-Kafka, Architectural and functional roles of A kinase-anchoring proteins in cAMP microdomains. *J. Gen. Physiol.* **143**, 9–15 (2014).

30. P. C. Gray, V. C. Tibbs, W. A. Catterall, B. J. Murphy, Identification of a 15-kDa cAMP-dependent Protein Kinase-anchoring Protein Associated with Skeletal Muscle L-type Calcium Channels. *Journal of Biological Chemistry*. **272**, 6297–6302 (1997).

31. I. D. Fraser *et al.*, A novel lipid-anchored A-kinase Anchoring Protein facilitates cAMP-responsive membrane events. *EMBO J.* **17**, 2261–2272 (1998).

32. K. W. Trotter *et al.*, Alternative splicing regulates the subcellular localization of A-kinase anchoring protein 18 isoforms. *J. Cell Biol.* **147**, 1481–1492 (1999).

33. V. Henn *et al.*, Identification of a Novel A-kinase Anchoring Protein 18 Isoform and Evidence for Its Role in the Vasopressin-induced Aquaporin-

2 Shuttle in Renal Principal Cells. *Journal of Biological Chemistry*. **279**, 26654–26665 (2004).

34. J. T. Hulme, M. Ahn, S. D. Hauschka, T. Scheuer, W. A. Catterall, A Novel Leucine Zipper Targets AKAP15 and Cyclic AMP-dependent Protein Kinase to the C Terminus of the Skeletal Muscle Ca2+ Channel and Modulates Its Function. *Journal of Biological Chemistry*. **277**, 4079–4087 (2002).

35. F. Potet, J. D. Scott, R. Mohammad-Panah, D. Escande, I. Baró, AKAP proteins anchor cAMP-dependent protein kinase to KvLQT1/IsK channel complex. *Am. J. Physiol. Heart Circ. Physiol.* **280**, H2038–H2045 (2001).

36. V. C. Tibbs, P. C. Gray, W. A. Catterall, B. J. Murphy, AKAP15 anchors cAMP-dependent protein kinase to brain sodium channels. *Journal of Biological Chemistry*. **273**, 25783–25788 (1998).

37. A. R. Cantrell, V. C. Tibbs, R. E. Westenbroek, T. Scheuer, W. A. Catterall, Dopaminergic modulation of voltage-gated Na+ current in rat hippocampal neurons requires anchoring of cAMP-dependent protein kinase. *J. Neurosci.* **19**, RC21 (1999).

38. W. P. Few, T. Scheuer, W. A. Catterall, Dopamine modulation of neuronal Na(+) channels requires binding of A kinase-anchoring protein 15 and PKA by a modified leucine zipper motif. *Proc. Natl. Acad. Sci. U.S.A.* **104**, 5187–5192 (2007).

39. J. T. Hulme, T. W. C. Lin, R. E. Westenbroek, T. Scheuer, W. A. Catterall, β-Adrenergic regulation requires direct anchoring of PKA to cardiac CaV1.2 channels via a leucine zipper interaction with A kinase-anchoring protein 15. *Proc. Natl. Acad. Sci. U.S.A.* **100**, 13093–13098 (2003).

40. Y. Fu *et al.*, Deletion of the distal C terminus of CaV1.2 channels leads to loss of beta-adrenergic regulation and heart failure in vivo. *J. Biol. Chem.* **286**, 12617–12626 (2011).

41. B. J. Murphy, S. Rossie, K. S. De Jongh, W. A. Catterall, Identification of the sites of selective phosphorylation and dephosphorylation of the rat brain Na+ channel alpha subunit by cAMP-dependent protein kinase and phosphoprotein phosphatases. *Journal of Biological Chemistry*. **268**, 27355–27362 (1993).

42. E. Klussmann, W. Rosenthal, Role and identification of protein kinase A anchoring proteins in vasopressin-mediated aquaporin-2 translocation. *Kidney Int.* **60**, 446–449 (2001).

43. D. H. MacLennan, E. G. Kranias, Calcium: Phospholamban: a crucial regulator of cardiac contractility. *Nat Rev Mol Cell Biol*. **4**, 566–577 (2003).

44. K. R. Johnson, J. Nicodemus-Johnson, G. K. Carnegie, R. S. Danziger, Molecular evolution of A-kinase anchoring protein (AKAP)-7: implications in comparative PKA compartmentalization. *BMC Evol. Biol.* **12**, 125 (2012).

45. R. L. Brown, S. L. August, C. J. Williams, S. B. Moss, AKAP7gamma is a nuclear RI-binding AKAP. *Biochem. Biophys. Res. Commun.* **306**, 394–401 (2003).

46. A. Bengrine, J. Li, M. S. Awayda, The A-kinase anchoring protein 15 regulates feedback inhibition of the epithelial Na+ channel. *FASEB J*. **21**, 1189–1201 (2007).

47. J. M. Redden *et al.*, Spatiotemporal regulation of PKC via interactions with AKAP7 isoforms. *Biochem. J.* **446**, 301–309 (2012).

48. E. C. Greenwald, J. M. Redden, K. L. Dodge-Kafka, J. J. Saucerman, Scaffold state switching amplifies, accelerates, and insulates protein kinase C signaling. *J. Biol. Chem.* **289**, 2353–2360 (2014).

49. A. Singh, J. M. Redden, M. S. Kapiloff, K. L. Dodge-Kafka, The large isoforms of A-kinase anchoring protein 18 mediate the phosphorylation of inhibitor-1 by protein kinase A and the inhibition of protein phosphatase 1 activity. *Molecular pharmacology*. **79**, 533–540 (2011).

50. S. Yang, W. H. Fletcher, D. A. Johnson, Regulation of cAMP-dependent protein kinase: Enzyme activation without dissociation. *Biochemistry*. **34**, 6267–6271 (1995).

51. B. R. Martin, T. J. Deerinck, M. H. Ellisman, S. S. Taylor, R. Y. Tsien, Isoform-Specific PKA Dynamics Revealed by Dye-Triggered Aggregation and DAKAP1α-Mediated Localization in Living Cells. *Chemistry & Biology*. **14**, 1031–1042 (2007).

52. F. D. Smith *et al.*, Intrinsic disorder within an AKAP-protein kinase A complex guides local substrate phosphorylation. *Elife*. **2**, e01319 (2013).

53. J. D. Scott, T. Pawson, Cell signaling in space and time: where proteins come together and when they're apart. *Science*. **326**, 1220–1224 (2009).

54. J. S. Logue, J. D. Scott, Organizing signal transduction through A-kinase anchoring proteins (AKAPs). *FEBS J.* **277**, 4370–4375 (2010).

55. M. H. Ali, B. Imperiali, Protein oligomerization: how and why. *Bioorg. Med. Chem.* **13**, 5013–5020 (2005).

56. N. J. Marianayagam, M. Sunde, J. M. Matthews, The power of two: protein dimerization in biology. *Trends Biochem. Sci.* **29**, 618–625 (2004).

57. S. Ferré *et al.*, G protein-coupled receptor oligomerization revisited: functional and pharmacological perspectives. *Pharmacol. Rev.* **66**, 413–434 (2014).

58. D. Yablonski, I. Marbach, A. Levitzki, Dimerization of Ste5, a mitogen-activated protein kinase cascade scaffold protein, is required for signal transduction. *Proc. Natl. Acad. Sci. U.S.A.* **93**, 13864–13869 (1996).

59. H. Storez *et al.*, Homo- and hetero-oligomerization of beta-arrestins in living cells. *Journal of Biological Chemistry*. **280**, 40210–40215 (2005).

60. K. L. Dodge *et al.*, mAKAP assembles a protein kinase A/PDE4 phosphodiesterase cAMP signaling module. *EMBO J.* **20**, 1921–1930 (2001).

61. C. W. Dessauer, Adenylyl cyclase--A-kinase anchoring protein complexes: the next dimension in cAMP signaling. *Molecular pharmacology*. **76**, 935–941 (2009).

62. A. L. Bauman, J. D. Scott, Kinase- and phosphatase-anchoring proteins: harnessing the dynamic duo. *Nat. Cell Biol.* **4**, E203–6 (2002).

63. P. C. Gray *et al.*, Primary structure and function of an A kinase anchoring protein associated with calcium channels. *Neuron*. **20**, 1017–1026 (1998).

64. A. Zelada, R. Castilla, S. Passeron, L. Giasson, M. L. Cantore, Interactions between regulatory and catalytic subunits of the Candida albicans cAMP-dependent protein kinase are modulated by autophosphorylation of the regulatory subunit. *Biochim. Biophys. Acta*. **1542**, 73–81 (2002).

65. C. T. Pawson, J. D. Scott, Signal integration through blending, bolstering and bifurcating of intracellular information. *Nat. Struct. Mol. Biol.* **17**, 653–658 (2010).

66. K. Herrick-Davis, E. Grinde, A. Cowan, J. E. Mazurkiewicz, Fluorescence correlation spectroscopy analysis of serotonin, adrenergic, muscarinic, and dopamine receptor dimerization: the oligomer number puzzle. *Molecular pharmacology*. **84**, 630–642 (2013).

67. Y. Wang, E. A. Elion, Nuclear export and plasma membrane recruitment of the Ste5 scaffold are coordinated with oligomerization and association with signal transduction components. *Mol. Biol. Cell*. **14**, 2543–2558 (2003).

68. M. K. Hayashi, H. M. Ames, Y. Hayashi, Tetrameric hub structure of postsynaptic scaffolding protein homer. *J. Neurosci.* **26**, 8492–8501 (2006).

69. M. G. Gold *et al.*, Architecture and dynamics of an A-kinase anchoring protein 79 (AKAP79) signaling complex. *Proc. Natl. Acad. Sci. U.S.A.* **108**, 6426–6431 (2011).

70. S. Gao, H.-Y. Wang, C. C. Malbon, AKAP5 and AKAP12 Form Homo-oligomers. *J Mol Signal*. **6**, 3 (2011).

71. L. Baisamy, N. Jurisch, D. Diviani, Leucine zipper-mediated homo-oligomerization regulates the Rho-GEF activity of AKAP-Lbc. *Journal of Biological Chemistry*. **280**, 15405–15412 (2005).

72. M. G. Gold, F. D. Smith, J. D. Scott, D. Barford, AKAP18 contains a phosphoesterase domain that binds AMP. *Journal of Molecular Biology*. **375**, 1329–1343 (2008).

73. J. M. Mason, K. M. Arndt, Coiled coil domains: stability, specificity, and biological implications. *Chembiochem*. **5**, 170–176 (2004).

74. H. Nishi, K. Hashimoto, A. R. Panchenko, Phosphorylation in protein-protein binding: effect on stability and function. *Structure*. **19**, 1807–1815 (2011).

75. K. Hashimoto, H. Nishi, S. Bryant, A. R. Panchenko, Caught in self-interaction: evolutionary and functional mechanisms of protein homooligomerization. *Phys Biol*. **8**, 035007 (2011).

76. A. W. Burgess, EGFR family: structure physiology signalling and therapeutic targets. *Growth Factors*. **26**, 263–274 (2008).

77. P. De Meyts, The insulin receptor: a prototype for dimeric, allosteric membrane receptors? *Trends Biochem. Sci.* **33**, 376–384 (2008).

78. H. Li *et al.*, Balanced interactions of calcineurin with AKAP79 regulate Ca2+-calcineurin-NFAT signaling. *Nat. Struct. Mol. Biol.* **19**, 337–345 (2012).

79. D. Diviani, J. Soderling, J. D. Scott, AKAP-Lbc anchors protein kinase A

and nucleates Galpha 12-selective Rho-mediated stress fiber formation. *Journal of Biological Chemistry*. **276**, 44247–44257 (2001).

80. G. K. Carnegie, C. K. Means, J. D. Scott, A-kinase anchoring proteins: from protein complexes to physiology and disease. *IUBMB Life*. **61**, 394–406 (2009).

81. H. H. Patel *et al.*, Disruption of Protein Kinase A Localization Using a Trans-activator of Transcription (TAT)-conjugated A-kinase-anchoring Peptide Reduces Cardiac Function. *Journal of Biological Chemistry*. **285**, 27632–27640 (2010).

82. M. D. Kritzer, J. Li, K. Dodge-Kafka, M. S. Kapiloff, AKAPs: the architectural underpinnings of local cAMP signaling. *Journal of Molecular and Cellular Cardiology*. **52**, 351–358 (2012).

83. B. Lygren, K. Taskén, The potential use of AKAP18δ as a drug target in heart failure patients. *Expert Opin. Biol. Ther.* **8**, 1099–1108 (2008).

84. A. R. Cantrell *et al.*, Molecular mechanism of convergent regulation of brain Na(+) channels by protein kinase C and protein kinase A anchored to AKAP-15. *Mol. Cell. Neurosci.* **21**, 63–80 (2002).

85. F. Ahmad *et al.*, Regulation of sarcoplasmic reticulum Ca2+ ATPase 2 (SERCA2) activity by phosphodiesterase 3A (PDE3A) in human myocardium: phosphorylation-dependent interaction of PDE3A1 with SERCA2. *J. Biol. Chem.* **290**, 6763–6776 (2015).

86. D. M. Bers, Cardiac excitation-contraction coupling. *Nature*. **415**, 198–205 (2002).

87. J. J. Saucerman, A. D. McCulloch, Mechanistic systems models of cell signaling networks: a case study of myocyte adrenergic regulation. *Prog. Biophys. Mol. Biol.* **85**, 261–278 (2004).

88. J. J. Saucerman, L. L. Brunton, A. P. Michailova, A. D. McCulloch, Modeling beta-adrenergic control of cardiac myocyte contractility in silico. *Journal of Biological Chemistry*. **278**, 47997–48003 (2003).

89. A. Scholten, T. A. B. van Veen, M. A. Vos, A. J. R. Heck, Diversity of cAMP-dependent protein kinase isoforms and their anchoring proteins in mouse ventricular tissue. *J. Proteome Res.* **6**, 1705–1717 (2007).

90. B. W. Jones *et al.*, Cardiomyocytes from AKAP7 knockout mice respond normally to adrenergic stimulation. *Proc. Natl. Acad. Sci. U.S.A.* **109**, 17099–17104 (2012).

91. M. S. Kapiloff, R. V. Schillace, A. M. Westphal, J. D. Scott, mAKAP: an A-kinase anchoring protein targeted to the nuclear membrane of differentiated myocytes. *J Cell Sci*. **112**, 2725–2736 (1999).

92. J. P. Schmitt *et al.*, Dilated cardiomyopathy and heart failure caused by a mutation in phospholamban. *Science*. **299**, 1410–1413 (2003).

93. K. Haghighi *et al.*, Human phospholamban null results in lethal dilated cardiomyopathy revealing a critical difference between mouse and human. *J. Clin. Invest.* **111**, 869–876 (2003).

94. M. Weisenhaus *et al.*, Mutations in AKAP5 disrupt dendritic signaling complexes and lead to electrophysiological and behavioral phenotypes in mice. *PLoS ONE*. **5**, e10325 (2010).

95. E. G. Kranias, Regulation of calcium transport by protein phosphatase activity associated with cardiac sarcoplasmic reticulum. *Journal of Biological Chemistry*. **260**, 11006–11010 (1985).

96. P. Nicolaou *et al.*, Inducible expression of active protein phosphatase-1 inhibitor-1 enhances basal cardiac function and protects against ischemia/reperfusion injury. *Circulation Research*. **104**, 1012–1020 (2009).

97. A. Pathak *et al.*, Enhancement of cardiac function and suppression of heart failure progression by inhibition of protein phosphatase 1. *Circulation Research*. **96**, 756–766 (2005).

98. J. A. Beavo, L. L. Brunton, Cyclic nucleotide research -- still expanding after half a century. *Nat Rev Mol Cell Biol*. **3**, 710–718 (2002).

99. I. Snook, The Langevin and Generalised Langevin Approach to the Dynamics of Atomic, Polymeric and Colloidal Systems (2006).

100. S. S. Andrews, D. Bray, Stochastic simulation of chemical reactions with spatial resolution and single molecule detail. *Phys Biol*. **1**, 137–151 (2004).

101. R. Erban, S. J. Chapman, Stochastic modelling of reaction-diffusion processes: algorithms for bimolecular reactions. *Phys Biol*. **6**, 046001 (2009).

102. B. P. English *et al.*, Ever-fluctuating single enzyme molecules: Michaelis-Menten equation revisited. *Nat. Chem. Biol.* **2**, 87–94 (2006).

103. S. C. Kou, B. J. Cherayil, W. Min, B. P. English, X. S. Xie, Single-

molecule Michaelis-Menten equations. *J Phys Chem B*. **109**, 19068–19081 (2005).

104. R. Swaminathan, C. P. Hoang, A. S. Verkman, Photobleaching recovery and anisotropy decay of green fluorescent protein GFP-S65T in solution and cells: cytoplasmic viscosity probed by green fluorescent protein translational and rotational diffusion. *Biophysj*. **72**, 1900–1907 (1997).

105. P. C. Sims *et al.*, Electronic measurements of single-molecule catalysis by cAMP-dependent protein kinase A. *J. Am. Chem. Soc.* **135**, 7861–7868 (2013).

106. M. Colledge, J. D. Scott, AKAPs: from structure to function. *Trends in Cell Biology*. **9**, 216–221 (1999).

107. S. Manni, J. H. Mauban, C. W. Ward, M. Bond, Phosphorylation of the cAMP-dependent Protein Kinase (PKA) Regulatory Subunit Modulates PKA-AKAP Interaction, Substrate Phosphorylation, and Calcium Signaling in Cardiac Cells. *Journal of Biological Chemistry*. **283**, 24145–24154 (2008).